

МІНІСТЕРСТВО ОСВІТИ І НАУКИ УКРАЇНИ
НАЦІОНАЛЬНИЙ АВІАЦІЙНИЙ УНІВЕРСИТЕТ
КАФЕДРА АВІАЦІЙНИХ ДВИГУНІВ

**ДОПУСТИТИ ДО
ЗАХИСТУ**

Завідувач кафедри
д-р техн. наук, проф.

_____ Ю.М. Терещенко
« ____ » _____ 2020 р.

ДИПЛОМНА РОБОТА

(ПОЯСНЮВАЛЬНА ЗАПИСКА)

ЗДОБУВАЧА ОСВІТНЬОГО СТУПЕНЯ

«МАГІСТР»

ЗА ОСВІТНЬО-ПРОФЕСІЙНОЮ ПРОГРАМОЮ

«ТЕХНІЧНЕ ОБСЛУГОВУВАННЯ ТА РЕМОНТ ПОВІТРЯНИХ СУДЕН ТА
АВІАДВИГУНІВ»

**Тема: “Дослідження методів удосконалення охолодження
конструктивних елементів турбін газотурбінного двигуна для середньо-
магістральних літаків”**

Виконав: _____ **Бакало Є.М.**

Керівник: к.т.н., доцент _____ **Гвоздецький І.І.**

Консультанти з окремих розділів

пояснювальної записки:

Охорона праці:

Канд. тех. наук, доц. _____ **Коновалова О.В.**

Охорона навколишнього

Середовища

Канд. біол. наук, доц _____ **Радомська М.М.**

Нормоконтролер: _____

Київ 2020

MINISTRY OF EDUCATION AND SCIENCE OF UKRAINE
NATIONAL AVIATION UNIVERSITY
DEPARTMENT OF AVIATION ENGINES

AGREED

Head of the department
 doctor of science, professor

_____ Y. M. Tereschenko
 « ____ » _____ 2020 year

DIPLOMA WORK

(EXPLANATORY NOTE)

GRADUATE EDUCATIONAL DEGREE MASTER

FOR EDUCATIONAL-PROFESSIONAL PROGRAM
 «MAINTENANCE AND REPAIR OF AIRCRAFT AND AVIATION ENGINES»

**Theme: “Investigation of measures improvement of turbine
 constructive element gas turbine engine cooling for middle range
 aircrafts”**

Performed by: _____ **Bakalo E.M.**

Supervisor: Ph.D., Assoc. Professor _____ **Gvozdetskyi I.I**

Consultants in separate sections of the explanatory note:

Labour precaution:

Candidate of science, assoc. prof _____ **Konovalova O.V**

Environmental protection:

Candidate of science, assoc. prof _____ **Radomska M.M.**

Standard controller: _____

Kyiv 2020

NATIONAL AVIATION UNIVERSITY

Faculty: Aerospace Faculty

Department: Aeroengine Department

Educational degree: Master

The specialty: 272 «Aviation Transport»

Educational Professional Program: «Maintenance and Repair of Aircraft and Aero-Engines»

APPROVED BY

Head of the department

doctor of science, professor

_____ Y. M. Tereschenko

«_____» _____ 2020 year

THESIS ASSIGNMENT

Student`s name: Bakalo Evhenii Mykolayovich

1 . Theme: “Investigation of measures improvement of turbine constructive element gas turbine engine cooling for middle range aircrafts”

Approved by the Rector’s order of ._08.10_2020 , № 1950 /CT,,

2. The paper to be performed from 05 october 2020 up to 27 December 2020p.

3. Initial data for the paper (thesis): TFE should be analyzed at start initial data
V=0; H=0; IST;

4. The object of the study is the first stage gas turbine blade. Subject of research - the effect of improvement of turbine constructive element gas turbine engine cooling.

5. The content of the explanatory note (the list of problems to be considered):

Introduction; The brief description problem of gas turbine engine cooling elements and propositions for it improvement; Selection of the initial parameters of the working process and thermo-gas dynamic calculation of the engine; Calculations for the strength of the main engine parts; Development of functional engine systems. General conclusion on the work

5. The list of mandatory graphic materials: Engine general views; Turbine designed scheme and graphics for scientific part of the diploma work.

6. Time and Work Schedule

#	<i>Stages of Graduation Paper Completion</i>	<i>Stage Completion Dates</i>	<i>Remarks</i>
1	Analysis of the current state of the cooling problem of gas turbines	5.10.20 – 12.10.20	
2	Patent search on the topic	12.10.20 – 17.10.20	
3	Development of ways to solve the problem of cooling	18.10.20 – 25.10.20	
4	Thermodynamic and gas-dynamic calculation of TFE	26.10.20 – 31.10.20	
5	Development of a drawing of the constructive-power scheme of TFE	01.11. 20-10.11. 20	
6	Development of improvement of design elements of the turbine unit	11.11.20 – 14.11.20	
7	Development of a cooling system with advanced elements	14.11.20 – 17.11.20	
8	Selection of the latest materials and systems for their implementation in GTE. Comparative analysis of innovations.	18.11.20 – 21.11.20	
9	Labor protection	22.11.20 – 23.11.20	
10	Environmental protection	24.11.20 – 27.11.20	
11	Calculations of cooling efficiency of GTE turbine elements due to the proposed solutions	28.11.20 – 30.11.20	
12	Execution of an explanatory note and its submission for plagiarism	01.12.20 – 10.12.20	
13	Registration of drawings	11.12.20-15.12.20	

7. Advisers on individual sections of the work (Thesis)

Section	Adviser	Date, Signature	
		Assignment Delivered	Assignment Accepted
<i>Labour precaution</i>	Konovalova O.V.		
<i>Environmental protection</i>	Radomska M.M		

8. Assignment issue date 05th of October, 2020 year

Thesis Supervisor: _____ Gvozdetskyi I.I.
(signature)

Assignment is accepted for performing: _____ Bakalo E.M
(signature)

ABSTRACT

Explanatory note to the diploma work: “Investigation of measures improvement of turbine constructive element gas turbine engine cooling for middle range aircrafts” consist of:

97 pages. 24 drawings, 2 table, 1 appendixes

The object of the diploma work is GTE turbine unit and it`s cooling elements .

The subject of the diploma work is the effect of a new methods for the operational characteristics of the gas turbine engine.

The purpose of the diploma work is the development of recommendations aimed at improving the cooling system of the turbine elements and improving their service life.

The research methods is a calculation method based on statistic information on overheating and failure of turbine elements in operation.

The practical significance of the results of diploma work is determined by the increased efficiency of the technical operation of the object of research at high temperatures. The ability to accept larger loads and increased operational durability of object .

Materials of the diploma work are recommended to be used in the educational process and practical work of specialists of design bureaus.

GTE DURABILITY, COMPLEX THERMOMECHANICAL LOADING, NON-DESTRUCTIVE CONTROL, ENGINE RESIDUAL LIFE, CYCLING LOAD, HEAT-RESISTANT ALLOYS, GAS TURBINE DIAGNOSTICS, GAS TURBINE BLADE, COOLING PROCESS, HIGH TEMPERATURE ALLOYS.

Contents

LIST OF ABBREVIATIONS AND EXPLANATION OF TERMS	8
INTRODUCTION.....	9
1. Analysis of the current state of problem of gas turbine elements cooling	11
1.1 General description	12
1.2 Structural components.....	13
1.3 Engine Oil System	20
1.4 Fuel and Power Control System	21
1.5 Starting the Engine	21
1.6 General characteristics of the blade apparatus of the turbine	23
1.7 Working Rotating turbine blades	24
1.8 Materials used for the manufacture of turbine blades of the GTE	25
1.9 Information and analytical research of problem ("weak") places, which manifest themselves in the operation of aircraft GTE	26
1.10 Ways of cooling turbine elements.....	28
1.11 Five main elements	28
Conclusions.....	34
2. Development of ways to solve the problem of cooling	35
2.1 Development of a method for monitoring system elements cooling turbine blade	36
2.2 Microcircuit cooling for a turbine blade tip	38
2.3 Types of technology used for turbofan engine cooling system.....	43
2.4 Cooling system Technology	45
Conclusions	48
3. Selection of the latest materials and systems for their implementation in a gas turbine engine. Comparative analysis of innovation.....	49
3.1 Results of Patent analyses of modern states of problem cooling	49
3.2 Active control clearance between the tips of the rotor blades	52
3.3 Turbine Disk with impellers for cooling the turbine blades attached to the said disk, and corresponding cooling method of turbine blades.....	53
3.4 Modern vane's cooling system of high loaded as turbines.....	58
Conclusions	59
4. Environmental protection	60
4.1 Harmful factors that occur during the operation of the GTE.....	60
4.2 Water pollution	61

4.3 Noise pollution	63
4.4 Emission of aircraft engines.....	63
4.5 ICAO CO ₂ certification requirement	67
4.6 Emissions trading system.....	70
Conclusions	72
5. Labor Protection	73
5.1 Analysis of harmful and dangerous production factors	73
5.2 Development of measures for safety.....	77
5.3 Fire Safety	81
5.4 Typical calculation or safety issue detail	82
5.5 The main requirements for compliance with the rules of labor protection during operation of the designed engine	90
Conclusions	91
GENERAL CONCLUSIONS	93
REFERENCES	94

LIST OF ABBREVIATIONS AND EXPLANATION OF TERMS

GT – gas turbine
CA – civil aviation
CC – combustion chamber
ERE – early removal of the engine
ERU – early removal of unit
FFE – fractional factorial experiment
FFO – failures, which could be fixed in operation
FLM – fuel and lubricating materials
FOD – foreign object damage
GTE – gas turbine engine
HPC – high pressure compressor
HPR – high pressure rotor
HPT – high pressure turbine
ISA – International standard atmosphere
LPC – low pressure compressor
LPT – low pressure turbine
SFC – specific fuel consumption
TVE – two-variable experiment
SPD – surface plastic deformation
MBS – Micro-balls strengthening
HTT – high-temperature treatment
HTVT – high-temperature vacuum treatment
FCC – face-centered cubic
VPTHE – vacuum plasma technology high energy
ECT – equivalent-cyclic test
HSDC – high speed directed crystallization

INTRODUCTION

Advanced heat transfer and cooling techniques form one of the major pillars supporting the continuing development of high efficiency, high power output gas turbine engines. Conventional gas turbine thermal management technology is composed of five main elements including internal convective cooling, external surface film cooling, materials selection, thermal-mechanical design at the component and system levels, and selection and/or pre-treatment of the coolant fluid.

The technology of cooling gas turbine components, primarily via internal convective flows of single-phase gases and external surface film cooling with air, has developed over the years into very complex geometries involving many differing surfaces, architectures, and fluid-surface interactions. The fundamental aim of this technology area is to obtain the highest overall cooling effectiveness with the lowest possible penalty on the thermodynamic cycle performance. As a thermodynamic Brayton cycle, the efficiency of the gas turbine engine can be raised substantially by increasing the firing temperature of the turbine. Modern gas turbine systems are fired at temperatures far in excess of the material melting temperature limits. [1]

This is made possible by the aggressive cooling of the hot gas path components using a portion of the compressor discharge air, as depicted in (Fig. 1.) The use of 15–25% of this compressed air to cool the high-pressure portions of the turbine presents a severe penalty on the thermodynamic efficiency unless the firing temperature is sufficiently high for the gains to outweigh the losses. [2] In all properly operating cooled turbine systems, the efficiency gain is significant enough to justify the added complexity and cost of the cooling technologies employed. Actively or passively cooled regions in power generating gas turbines include the stationary vanes or nozzles and the rotating blades or buckets of the high-pressure stages, the shrouds bounding the rotating blades, and the combustor liners and flame holding segments (fuel nozzles, splash plates).

All such engines additionally cool the interfaces and secondary flow regions around the immediate hot gas path.

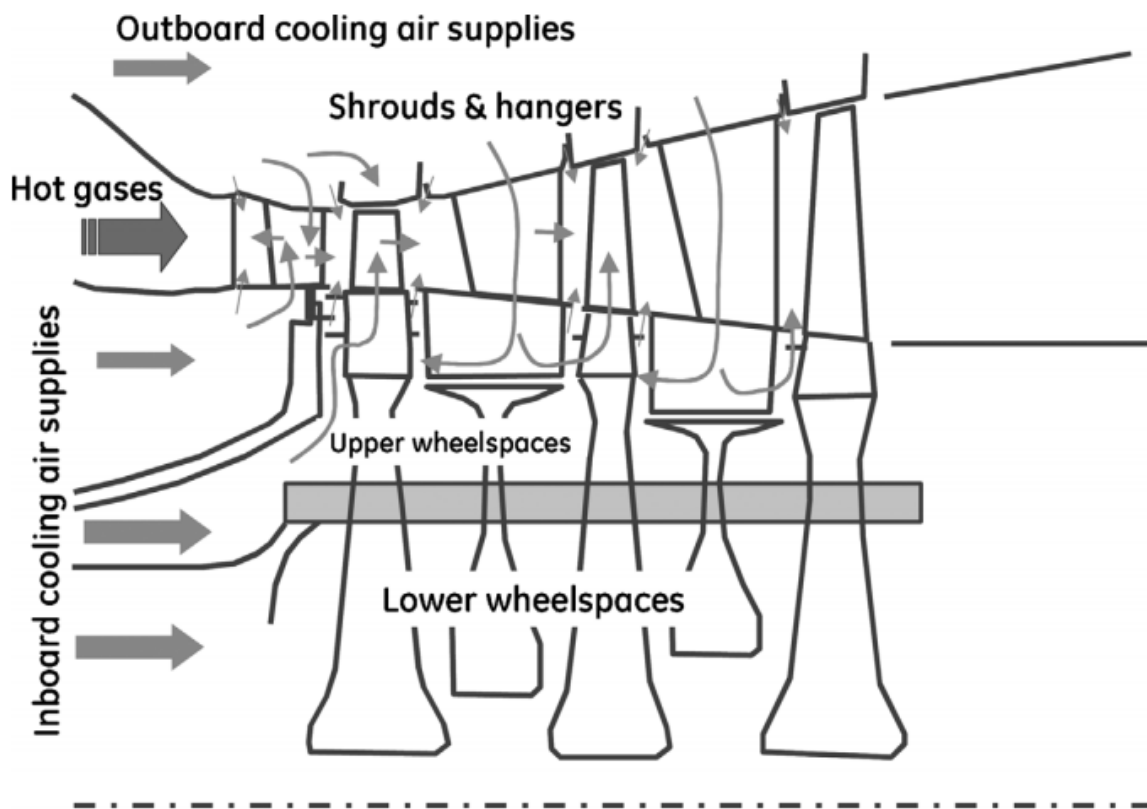


Figure 1 - Schematic of turbine with cooling flows.

1 Analysis of the current state of problem of gas turbine elements cooling

To date, the main areas of gas temperature increase are the use of heat-resistant alloys, ceramic materials and cooling systems of open and closed type. But the use of only heat-resistant alloys can not yet meet the required temperature level. Therefore, today, in parallel with the use of new materials, a promising direction for raising gas temperatures is the development and improvement of gas turbine (GT) cooling systems. The modeling of the cooling system is based on the network method, which is a branched hydraulic system and has a large number of channels of different geometries, which regulate the flow of the cooler and thus affect the efficiency of the gas turbine unit (GTU). Also in some important cases, such as in the current in the atrial cavity or in the cavities between two disks, at critical and supercritical values of pressure in the channels the nature of the flow becomes extremely difficult, and the inclusion in the hydraulic network of bearing cooling, where oil is used as a coolant complicates the modeling process. other physical properties. Therefore, the process of modeling such channels and including them in the overall hydraulic scheme is a difficult task. And the accuracy with which the cost characteristics of the circuit elements are, is a decisive factor that determines the reliability of the modeling of the cooling system as a whole. Thus, the issues of further improvement of cooling systems with different types of rotating elements of gas turbines, the study of the structure and properties of the flow, obtaining dependences describing this flow are relevant for turbine construction.[3]

The object of the study is a blade of the first stage of the turbine GTE.

The subject of the study is the effect of a new heat-resistant material on the operational characteristics of the gas turbine engine.

The list of tasks that the author solves in the submitted diploma work:

- Consider the working principle of the Continuous turbofan engine by prototype D 436.
- to consider methods of protecting the turbine blades of the GTE during operation, as well as methods for improving their durability and economy
 - Weak" places of the shoulder blade and forces that affect it;
- consider the ways of ensuring the performance of the turbine blade at temperatures between 1500 and 1600 ° C;
- to evaluate the introduction of new heat-resistant alloys in the GTE (according to information sources), to choose alternative solutions;
 - to use Microcircuit cooling for a turbine blade tip
- analyze the advantages of introducing a new alloy into a gas turbine engine.

1.1 General description of three-shaft turbofan engine

Three-shaft turbofan engine is designed for short-haul passenger aircrafts.

This three-shaft scheme engine consists of a 15-stage axial compressor, intermediate casing, annular combustion chamber, five-stage turbine, thrust reverser with rotating cascade in the secondary flow and a separate unregulated output nozzles for secondary and primary flows. The feature of three-shaft scheme is that the compressor rotor consists of three independent rotors, each of which is rotated by its turbine. [4]

Its rotors have different optimal speeds and are linked only by gas-dynamic coupling.

The rotor has six supports and each of the three rotors are mounted on two supports.

The three-shaft engine design scheme has the following advantages:

- To use the compressor stage with high efficiency;
- To provide the necessary compressor gas-dynamic stability;
- To use the low power starting arrangement, as at start, the starter turns only one high pressure rotor to start the engine.

The engine bypass ratio at takeoff is 5.

A high engine bypass ratio and thermodynamic cycle parameters ensure high efficiency of the engine.

The engine consists of fourteen modules and one sub-module, one of which is a complete design and technology unit and perhaps beyond the main (fourteenth) module removed and replaced without disassembling the engine's neighboring modules in aviation and technical bases.

Modular design provides the ability to restore its serviceability by replacement of modules in operation. High testability and controllability-transition is from a planned preventive maintenance to the operation of the technical condition.

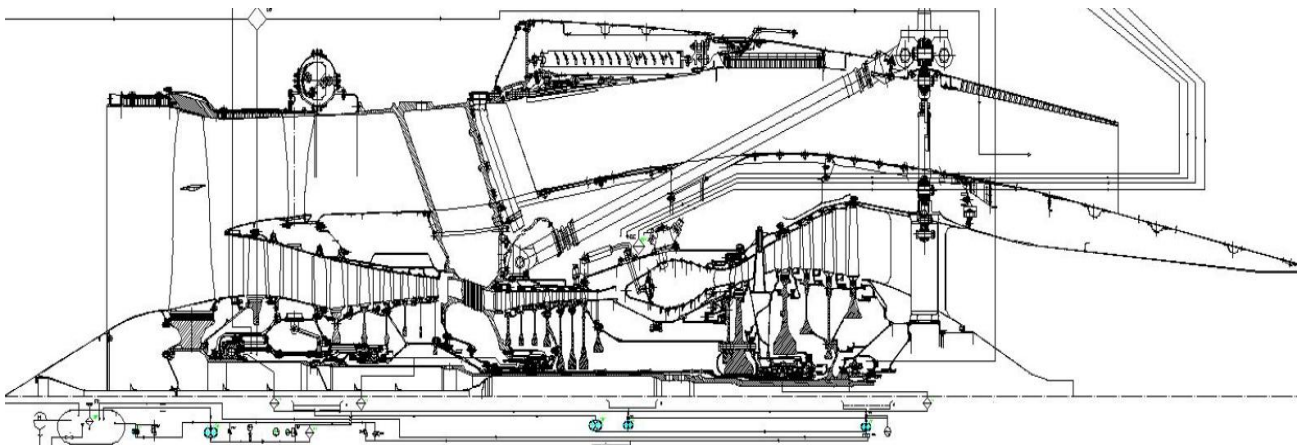


Figure 1.1 – Three-shaft turbofan engine

1.2 Structural components of gas turbine engine

Compressor – The compressor is an axial, three-spool compressor consisting of a transonic fan stage, subsonic intermediate pressure compressor and high pressure compressor. The single fan does not have inlet guide vanes and consists of a rotor, stator with directing vanes in the secondary flow and the guide vanes in the primary flow where the shaft bearing units, tapered spinner rotates and continuously heats air. Connections of drive the fan rotor wheel with the shaft and spinner is made with the help of bolts and blades attached to a disc by "Fir tree" type roots. Fan

rotor blades have anti-vibration shrouds, arranged in the flow part of the secondary flow. Directing unit (of the fan) has a collapsible design. The inner surface of the outer ring of the directing device has an acoustic panel. To the front flange casing of the fan, an air-intake is attached via retainers. The guide vanes of the fan are installed at the entrance of the primary flow by booster rotor wheel stage form. Fan shaft is connected to the shaft of the fan turbine by splines. The fan and fan turbine turbofan rotor is mounted on two bearings. Both bearing units have oil dampers. Odd stage rotor wheel is connected to the fan rotor wheel by bolts at the junction of its flange and fan shaft. The odd stage guide device is structurally part of the Intermediate Pressure Compressor stator (IPC).

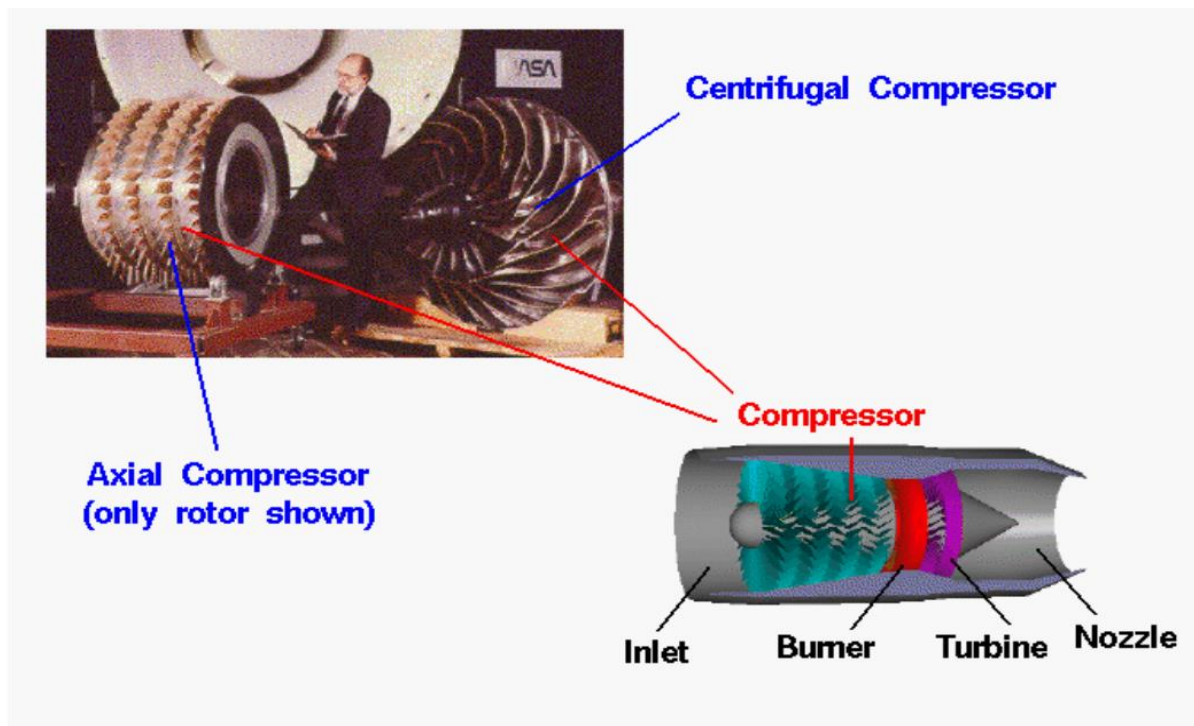


Figure 1.2 – Structural component of Three-shaft turbofan engine, Compressor [6]

Intermediate Pressure Compressor is a six-stage compressor and consists of a stator and rotor. Stator fairing separates airflow behind the fan rotor wheel from the primary and secondary flows.

The IPC stator includes:

Intermediate Pressure Compressor vanes front casing with guide vanes of odd stage, IPC invariable inlet guide vanes, and units of the front supports of fan and IPC rotors.

Intermediate Pressure Compressor casing with IPC guide vanes, working rings and air bypass valves behind the IPC third stage for stable operation of the compressor at low ratings.

Compressor rotor is of a drum-disc design. Discs of first, second and third stages and welded drum of fourth, fifth and sixth stages are connected to each other and to the front and rear shafts by bolts. Rotor blades of the first stage connected with the disc by "Fir tree" type roots and blades from second to sixth stages by "dovetail" type of roots. IPC rotor is connected with the Intermediate Pressure Turbine (IPT) rotor through the splines and form an intermediate pressure rotor.

Rotor is mounted on two bearing unit with oil dampers. The front ball bearing is mounted on an elastic support of "squirrel cage" with sag limiter.[7]

High pressure compressor is a seven-stages compressor and consists of variable inlet guide vanes, rotor, stator and Air Bleed Valve (ABV) behind the fourth stage. High pressure compressor rotor has a drum-disk structure. Welded Drum from first to fourth stages, and discs till the last stages. Front and rear shafts are interconnected by bolts. First stage blades and discs are connected by "dovetail" type roots through the longitudinal grooves in the disc. Blades with discs from the second to the seventh stages are interconnected by "dovetail" type roots with circular grooves in the discs.[8]

HPC rotor is connected to the high pressure turbine rotor by bolts to form a high pressure rotor, mounted on two supports.

Front ball bearing is mounted on an elastic support of "squirrel cage" type with limiter of sag, mounted in the intermediate case. Rear roller bearing is mounted on an oil damper as in the case of turbine supports.

HPC Variable Inlet Guide Vanes (VIGV) allow you to make engine adjustments at bench trials. After setting the Inlet Guide Vanes (IGV), they are fixed in the selected position.

The intermediate casing is used for the formation of the transition channel from IPC to HPC air channel of the secondary flow, allocation of aggregate units and their drives, the HPC front rotor support as well as units of front engine mount.

Annular shells of intermediate casing, forming the air-gas channel of the primary and secondary flows are interconnected by eight hollow racks, within which the communications of the engine systems are located.

Intermediate casing consists of the intermediate casing, the central drive, the gear box and intermediate drive. All driven aggregates are mounted on the gear box and get rotation from the rotor by means of gears, drives, splines and springs. To the rear flange of the outer shell of the intermediate casing, the design elements of the reverse device are mounted and the intermediate casing is attached to the front flange.

The combustion chamber consists of a casing, an input diffuser with the HPC seventh stage, directing vanes, flame tube, fuel manifold, fuel nozzles and pilot burners.[4]

Flame tube is of annular type, with twelve fuel nozzles and has a welded structure, consisting of individual welded rings having a number of holes for the passage of the secondary air.

Fuel nozzles are of centrifugal-type, double-channel. Four of them are air nozzles to ensure stable combustion at leaning of fuel-air mixture.

Fuel manifold and tubes of fuel supply to nozzles have the protective housing preventing fuel hit on hot casing details in case of infringement of leakproofness of

a manifold and tubes. On the combustion chamber casing two pilot burners of torch type with spark plugs are installed.

In the front of the combustion chamber casing two bleed valves behind the HPC at start are installed. On one of valves the connecting pipe for an air bleeding behind the HPC for needs of the airplane is installed.

The turbine is three-spool and consists of five-stages. It consists one-stage high pressure turbines (HPT), one-stage Intermediate Pressure Turbine (IPT) and three-stages of Low Pressure Turbine (LPT). [3]

Each of turbines turns a matching rotor of the compressor: HPT - the HPC rotor, IPT – rotor of IPC, LPT - LPC rotor.

The High Pressure Turbine consists of a nozzle diaphragm (ND) and a rotor. ND is made from ten separate sectors. Three of them are (in one sector two) vanes connected among themselves with the help brazing. Nozzle diaphragm vanes are hollow and are cooled by air bled behind the HPC. They have deflectors for tightening cooling air to go inside walls of the blade aerofoil part and system punches in walls of aerofoil and a platform through which cooling air escapes on an external surface of the airfoil and protects it from hot gases.[5]

HPT rotor consists of rotor wheel (disc with blades), labyrinth disc and HPT shaft. Rotor blades are cooled and consists of a root, legs, shank, aerofoil part and shroud cap. Cooling air is supplied to the shank passes through the radial channels in the body of the blade and out through holes in the front and back of the blade in the gas flow. Two blades are set in each disc groove. Rotor blades are connected by roots of "fir tree" type. Labyrinth disc and HPT are cooled by air bleeding behind the HPC. [38]

Intermediate pressure turbine consists of a rotor and the casing of the turbines' supports with the IPT ND.

Rotor IPT consists of the rotor wheel (disc with blades) and IPT shaft connected by bolts.

Rotor blades of IPT are uncooled, connected with disc by roots of "fir tree"-type. Discs cooled by air bled behind HPC.

In the casing of turbine supports outer and inner shells are connected by racks located inside the hollow nozzle diaphragm vanes of the second stage turbine. Through vanes the pipes of oil and air communications are also passed. In the casing of turbine supports, there are bearings of units of Intermediate and high pressure rotors supports are present.

Nozzle vanes are casted in the form of sectors; three vanes each. They are cooled by air bled behind the HPC fourth stage.

The Low Pressure Turbine (LPT) consists of a rotor and stator. The stator consists of a turbine casing and three nozzle diaphragms, including separate casted sectors with five blades each.

Turbine rotor is disc-drum design. Discs are interconnected between themselves and turbine shaft are connected by bolts. Blades and vanes are uncooled. Discs are cooled by air that bleeds behind the HPC. Rotor blades of the stages are shrouded and connected to discs by "fir tree"-type roots.

The Exhaust Arrangement consists of a turbine rear support casing, jet nozzle of primary flow and fairing.

On the casing of rear turbine support, the attachment fittings of the rear engine mount to the aircraft is located.

Rear engine attachment fittings are installed on the power ring as part of the outer shell of the rear support casing. Inside the casing, the LPC rotor bearing assembly is located. In the racks, connecting the inner and outer shells of the casing, the communications of rear support are located.

Thrust Reverse is used to create the reverse (negative) engine thrust to reduce the landing distance of the aircraft during landing or when the takeoff is interrupted.

Thrust reverser is of clamshell-type, ring-type with fixed cascade vanes and twelve blocker doors that block off the secondary flow nozzle at reversing thrust. At the

mode of direct thrust, the blocker doors are in the mobile casing of the reverser flush with its inner surface that forms the secondary flow channel in the area between the outer shell of the intermediate channel and jet nozzle secondary flow.

Reverser is mounted on the rear flange of the intermediate casing and includes, besides the reverser, the kinematic unit of the control mechanism, a feedback mechanism, locking mechanism, an alarm system. Reverser Control system is of hydraulic type, using hydraulic fluid from the hydraulic system of the aircraft. The system includes: hydraulic motor, control valve, divider thermal valve, check valves and fine filter. For the control of the reverser, the reverser lever is located in the cockpit.[8]

The nozzle secondary flow jet of the engine is mounted to the rear flange of the reverser fixed casing. The nozzle is a part of the output exhaust arrangement, which also includes cowls, forming with the nozzle the secondary flow channel behind the intermediate casing.

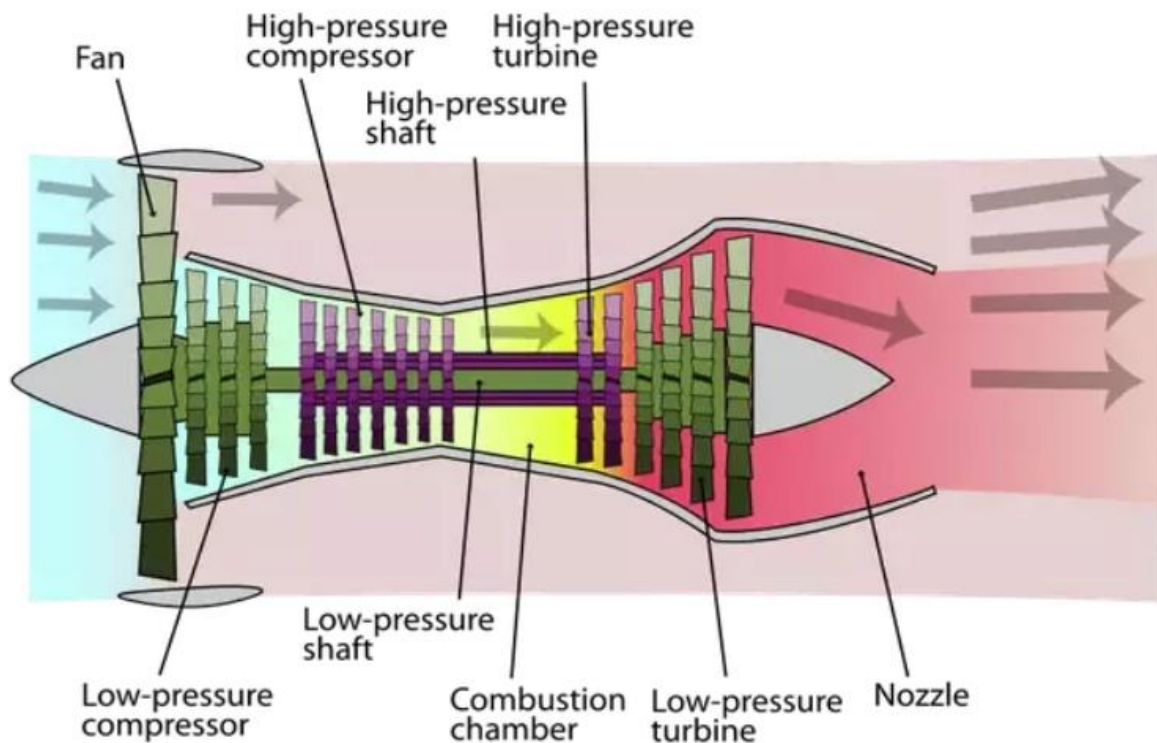


Figure 1.2 –Working of Three-shaft turbofan engine [7]

1.3 Engine Oil System is autonomous, circulating under pressure. Supply of lubricating oil to the oil tank by supply stage of oil pump block. Three suckedscavenge stage oil pump block scavenge oil from oil support cavities of engine rotors to the cavity of gear box, from which fourth scavenge stage pumps oil to the oil tank through centrifugal de-aerator and fuel oil cooler. Cooling oil is in palyvnomaslyanomu unit, installed in the fuel line low pressure between the fuel pump low and high pressure fuel pump unit.

Breathing of turbine support oil cavities is implemented through separating cavity (vertical rack of intermediate casing), by means of the separation of oil from oil-air mixture (emulsion). Then theemulsion of compressed flow into the turbine support emulsion and the mix goes into the centrifugal breather, where purified air is released outside the nacelle through active ejector, and oil discharged into the cavity of an intermediate drive. Air chamber of oil tank is breathed through the gear box which is turn let to the atmosphere through the centrifugal prompter.[38]

1.4 Fuel and Power Control System (hydromechanical) provides the fuel supply to the engine in an amount determined by the position of the engine Power Control Lever (PCL) and flight conditions. It includes the following main units:

power pumps

fuel regulator

fuel oil unit.

Fuel system aggregates carry out:

- Automatic fuel closing at startup, acceleration and operation at steady state rating;
- Maintaining the invariability of a given position of PCL at changing flight conditions (altitude, speed, ambient temperature).[39]

Electronic control system provides all range limiting according to set law for a given gas temperature at IPT discharge and limiting the high pressure and low pressure rotor speed. Shut down of the engine is implemented by an

electromagnetic valve, with the help of the engine shut-off lever on the electrical signal.

1.5 Starting the Engine

Starting the Engine is automatic. HPT rotor motoring is implemented by air starter set on the gear box. As a source of compressed air for the air starter an auxiliary gas turbine engine, mounted on aircraft or ground source with the same parameters of the air and the engine running are used. The starting program is carried out automatically by aggregates of the starting system and the fuel automatic control system.[14]

The compressor control system includes an automatic control of IPC ABV and HPC ABV which at the specified routines control the opening and closing of IPC ABV and HPC ABV.

Aggregates of aircraft power supply system, that is, starter-generator, air-oil heat exchanger and oil filter in the oil system of the starter-generator are located on the engine. On the gear box there are two drives for hydraulic pumps that are installed when installing the engine on the plane. When mounting the engine such components of airborne fire control system: signaling devices, manifolds of fire extinguishing fluid supply and electric

1.6 General characteristics of the blade apparatus of the turbine

Next, a specific object of this thesis will be considered, namely, the blade apparatus of the turbine. The blade apparatus of the GTE turbine is a set of static nozzle and working blades. The nozzle and working blades are the hottest parts of the turbine. Working blades, however, are prone to high static tensile and bending stresses as well as dynamic stresses. In the cooled vanes at the transitional operating modes of the turbine there are thermal stresses. [38; 39]

The socket and working blades work in a high-temperature gas environment, containing, in addition to oxygen, other aggressively active substances, including

particularly dangerous ones - vanadium and sulfur. These substances contribute to the development of gas corrosion, which destroys the blades.

Therefore, the materials of nozzle and working blades should be not only heat-resistant, but also heat-resistant, that is resistant to corrosion in atmospheric conditions and in a gas environment at working temperature. In addition to the heat resistance and heat resistance material blades of gas turbines should have a low sensitivity to stress concentration, to withstand heat fatigue, to be treated satisfactorily, to have an acceptable cost.

Nickel alloys ЖС-6К, ЖС-6Ф, ЖС-6УВІ are used in the USSR for the casting of nozzle and working blades since the 1960's. It is recommended to use these alloys to a temperature of 1050 ... 1100 K. Huge progress in turbine parameters and durability of nozzle and working blades has been achieved with the introduction into practice of alloys with directional crystallization and monocrystalline alloys. The main idea of an alloy with directed crystallization is to eliminate the boundaries between the grains perpendicular to the direction of the centrifugal forces, that is, the exclusion of the possibilities for creeping and breaking down the grain boundaries. The monocrystalline part has no grain boundaries at all, so it has optimum strength characteristics.[16]

Blades, obtained by the directional crystallization, have a 2.5 times increased durability, increased by 6 times the resistance to thermal obturation and increased in 2 times the oxidation and corrosion resistance. For a single crystal shovel, the strength and resistance to thermal resistance improve 9 times, respectively, and resistance to oxidation and corrosion - by 3.5 times.

1.7 Working Rotating turbine blades

Work blades - complex and expensive parts of the turbine. Just like nozzle blades, they are under the influence of a high-temperature gas stream. In addition, unlike nozzle blades, the working blades are subjected to the influence of centrifugal forces, rotating with a frequency of up to 20,000 rpm and a circumferential speed

up to 600 m / s. The stresses from the centrifugal forces make the work shafts more sensitive to vibrational loads. The need to withstand all of this load determines the design of the working blades.

The shovel consists of a profile part, a lock, a lower and an upper (tangent) shelves, and also legs, connecting a profile part and a lower shelf with a lock. The main and obligatory parts of the work shovel are the profile part, the lock and the lower shelf. The profile part of the work shovel during the installation of blades in the disk forms a blade crown, which provides the necessary rotation and expansion of the flow of the working body with minimal losses - that is, the execution of the main task of the shoulder blade.[18]

The lock of the workbench provides the fastening of the blade in the disk - in the grooves between the projections on the rim of the disc. Connection of a blade with a disk is made by means of a locks connection of the so-called "Christmas tree" type. The number of teeth in a "Christmas tree" castle can range from 1 to 2 (for blades working with small voltages from centrifugal forces) to 5 - for blades with high voltage. The stress level depends on the circumferential speed (rotor speed and the diameter of the flowing part) and the mass of the blade itself. In the aviation tweaks, the speed of the rotation is of primary importance

(up to 20,000 rpm), for the last stages of the turbines of stationary engines of high power of 200 ... 400mW) the voltage (at a rotational speed of 3000 ... 3600 rpm) is determined mainly by the mass of blades.

The direction of the groove in the rim of the disc may not correspond to the turbine rotation axis. This angle is determined when designing the root section of the shoulder blade. If the root section does not fit into the rectangle (which is the lower shelf with a straight groove), the lateral faces of the lower shelf are tilted at the desired angle to the turbine rotation axis. At the same angle to the rotation axis, the castle groove in the rim of the disk is also cut. This is a slightly better (rather than a straight groove on the disk) option, but sometimes it is inevitable. If the design

allows, it is possible to allow some difference between the angle of installation of the lock and the lower shelf of the shoulder blade (up to 15 °), while retaining the straight groove in the disc.

1.7.1 Turbine disks

The place of installation of working blades - there is a turbine disk. The disk is used to install working torques that create torque, and to transfer this torque from the blades to the shaft.

Connection of working blades with a disk - a tense and responsible place in the design of the turbine. At present, the mounting of the working blades in the turbine disk is carried out in the form of the so-called "Christmas tree" castle.

1.7.2 Manufacturing of blades of modern turbines

Shovels of modern turbines are almost exclusively cast on smelted models. Tin blades can be made by special technology of pouring and cooling - with the obtaining of casting with directional crystallization or single crystal. In the castings of working blades, machining only exposed to the surface of the "Christmas tree" locking compound, which is connected to the surface of the rack shelf and (in the blades with film cooling) openings of perforation.

When designing blades special attention should be paid to production possibilities. This applies to the choice of profile thickness in each section, the diameter of the input and especially the output edges. For the cooled blades, the minimum wall thickness and the ability to make the cooling channels of the inner cavity and the output edges are important. Only such an economically justifiable percentage of the yield of a suitable cast can be provided.

1.8 Materials used for the manufacture of turbine blades of the GTE manufacturing

The feature of the blade apparatus of the turbine is that the conditions for its operation are almost always close to the critical ones.

In modern engines, the temperature of the gas (after the torch) at the exit from the combustion chamber can reach 1650 ° C (with a tendency to increase), so for the normal operation of the turbine under such large thermal loads, it is necessary to take special precautions:

1. Use of heat-resistant and heat-resistant materials, as metal alloys, and (in the long run) of special composite and ceramic materials, which are used for manufacturing the most loaded parts of the turbine - nozzle and working blades, as well as disks. The most loaded ones are work shovels.

Heat-resistant alloys can be on aluminum, titanium, iron, copper, cobalt and nickel bases. The most widely used in aviation engines were nickel-based heat-resistant alloys, of which manufactured working and nozzle blades, turbine rotor discs, combustion chamber parts, etc. Depending on the manufacturing technology, nickel heat-resistant alloys can be foundry, deformed and powdered. The most heat-resistant are foundry hard-alloy alloys on a nickel base, capable to work up to temperatures of 1050-1100 ° C for hundreds and thousands of hours at high static and dynamic loads.[19]

In today's heat-resistant and heat-resistant alloys to obtain maximum high-temperature characteristics add up to 16 names of various alloying elements.

Among them, for example, chrome, manganese, cobalt, tungsten, aluminum, titanium, tantalum, bismuth and even rhenium, or ruthenium and others in its place. Particularly promising in this regard, the rhenium (Re - Rhenium, used in Russia), which is used now instead of carbides, but it is extremely expensive and its reserves are small. Also promising is the use of niobium silicide.

2. Use of a heat shield on the shoulder blades. The thermal protection layer (thermal-barrier coating) significantly reduces the amount of heat flow into the shoulder body (thermal barrier function) and protects it from gas corrosion (heat-resistant functions).

1.9 Information and analytical research of problem ("weak") places, which manifest themselves in the operation of aircraft GTE

On modern civilian TRDD high traction the temperature of gas before the turbine practically equaled with the temperature level before the turbine of the military TRDD.

The maximum temperature of gas in front of the TDD rotor reaches 1700 ... 1850K. The engines for short-range airplanes (CFM56, V2500) have a significantly lower temperature. The working and nozzle blades of the turbine operate in direct contact with the high-temperature gas, with the allowable temperature of the blade alloys below the operating temperatures of gas before each crown at 200 ... 500 ° C. The greatest difficulty is the reliability of the working blades, especially in the turbine of high pressure. They, along with nozzle blades, are subject to thermal fatigue, vibration, gas corrosion and erosion, and the effects of gas loads. In addition, the working blades are subjected to the action of centrifugal forces. Taking into account all this for reliable operation, the average temperature of metal blades should not exceed 900 ... 1000 ° C, and the maximum level - 1100 ° C. The level of permissible operating temperatures depends directly on the characteristics of the material used for blades.

Some of the rotor and stator parts of the turbine are also directly influenced by gas: the body, part of the wheel rim, labyrinths and other, less loaded parts. To ensure their reliable operation within the given resource, the following applies: special heat-resistant, heat-resistant and corrosion-resistant alloys, capable of resisting sulfide-oxide corrosion;

- manufacture of blades by the direction of crystallization or from a single crystal;
- coatings to increase the heat resistance of the material (for example, from aluminum oxide);

- metal multicomponent coatings to increase the corrosion resistance of the material, for example, a coating of four components (nickel - chrome - aluminum - yttrium);
- heat-shielding coatings made of ceramic materials with low thermal conductivity - to reduce the heat flow to the metal blades;
- Different schemes of air (for industrial turbines, sometimes even steam) cooling.

The optimum in terms of the cost of the engine life cycle, the design of the turbine implies the optimal combination of all of the above basic methods of ensuring efficiency. The use of expensive high-temperature alloys increases the cost of the material, but reduces the need for cooling. The use of a more complex and efficient cooling system for a turbine blade increases its cost, but allows the use of less expensive materials.

Designing an optimal cooling system involves the consistent finding of a reasonable compromise at all stages of the project implementation.

1.9.1 Characteristics of turbine elements defects

Modern engines are operated on a technical condition up to the exhaustion of their operational reserve or to any malfunction.

During stand tests and in operation, faults in the turbine can be detected by means of diagnostics of the engine (for example, raising the temperature behind the turbine) or during maintenance, using special means and control methods. Such means are optical endoscopes (for review of parts of the flowing part), devices for ultrasonic and current control of deflectors and disks. To facilitate diagnostics in turbine cases, hatches provide access to controls.

The turbine, as the most heat-stressed engine node, is also the most frequent source of malfunctions, which results in the sending of repairs and limits the resource. For example, with an intermediate repair time of 11,000 hours in two out of every three cases of sending to the repair of engines family RFU4000 (all models) the cause is a problem (burns and cracks).

1.10 Ways (Methods) of cooling turbine elements

1.10.1 Air cooling

The amount of thrust an engine produces is limited by the amount of heat that the turbine can withstand. One method of increasing this capability is by cooling the hot surfaces. The goal is to provide the maximum amount of cooling using a minimum amount of coolant. Lewis investigated three types of convective cooling of turbine blades: removal of heat at the blade root, air flow through hollow blades and liquid coolant flow through hollow blades. The lab was also studying different heat resistant materials, but cooling was a more cost-effective tactic. Air cooling, which diverts excess air flow from the compressor into hollow turbine blades to carry away the heat, is the least expensive type of cooling.

In 1945, Lewis researchers began studying the flow of air through hollow turbine blades. They determined that the efficiency of this system improved when fins were placed in the passages. They also experimented with modified leading or trailing edges. During 1948 and 1949, Lewis developed a method of fabricating these finned blades and established methods for predicting engine performance relative to turbine cooling. Much of this initial research was performed on test rigs with just the turbine. By 1950, these experimental turbines were tested on full-scale engines, including the General Electric I-40 in Cells 3 and 4 of the JPSL.

An analytical study predicted that applying cooling to engines operating at contemporary temperatures would likely result in better performance than cooling higher temperature engines. The goal was to reduce the amount of critical and costly materials needed. In 1953, researchers tested this theory on a Westinghouse TG-190 in Cell 6 of the JPSL. A compressor supplied cooling air to the iron turbine blades, which included corrugated inserts, to increase heat transfer. At a constant

speed, the thrust increased proportionally to the level of cooling air. The findings verified the theoretical predictions.

As engines increase speed, the inlet air temperature rises, which diminishes the effectiveness of air cooling. Nonetheless, internal convective air cooling was the primary engine cooling method in the 1960s and 1970s. Since the 1970s, it has been used in conjunction with external film cooling and impingement. Film cooling ejects cooling air from holes in the blade, resulting in a thin layer of cool air on the blade surface. Impingement systems shoot cooling air against the inside of the blade walls to facilitate the heat transfer. Cooling has allowed engines to operate at temperatures above the temperature limits of their materials, thus producing more thrust.

1.10.2 Liquid cooling

Liquid-cooling systems provide the best method of moderating turbine blade temperatures, but they require additional components and add weight to the engine. There are different liquid-cooling approaches, including film cooling and blades with cooling passages. The earliest method of cooling with liquids, however, involved spraying water into the airflow ahead of the turbine. The water strikes the hot blades and evaporates, carrying away the heat as it exits the tailpipe. Early spray-cooling systems were tested on jet engines in Great Britain. Although the cooling proved to be uneven, it was sufficient to warrant further research.

Spray cooling requires large quantities of water. Therefore, it would not be practical for normal flight, but NACA engineers hoped it could be used to reduce turbine temperatures during takeoff and afterburning situations. Researchers installed a spray system in a General Electric I-40 engine and tested it in the Torque Stand in 1950 and 1951. The water cooled the blades, but resulting temperature variations caused some of the blades to fail. The system was modified and retested at the JPSL during the summer of 1952. The I-40's thrust increased, but thermal

shock and inadequate cooling of the blade tips and edges resulted in blade failures. Further tests using blades cast from different alloys produced similar results. Spray cooling was thus shelved.

The NACA liquid-cooled turbine experiments, and those by manufacturers such as General Electric, were designed without grasping the complexities of engine heat distribution. NASA and industry continue to explore the concept as newer, more powerful engines emerge, but to date, there is no liquid cooling for turbine technology that has been proven flight-worthy. This is due to the complexities, poor heat transfer and lack of coolant flow data in liquid-cooled systems

1.10.3 Metal cooling

Liquid fusible alloys can be used as coolants in applications where high temperature stability is required, e.g. some fast breeder nuclear reactors. Sodium (in or sodium potassium alloy NaK are frequently used; in special cases lithium can be employed. Another liquid metal used as a coolant is lead, in e.g. lead cooled fast reactors, or a lead-bismuth alloy. Some early fast neutron reactors used mercury.

For certain applications the stems of automotive poppet valves may be hollow and filled with sodium to improve heat transport and transfer.

For very high temperature applications, e.g. molten salt reactors or very high temperature reactors, molten salts can be used as coolants. One of the possible combinations is the mix of sodium fluoride and sodium tetra fluoroborate (NaF-NaBF₄). Other choices are FLiBe and FLiNaK.

Also, A gas turbine engine with a closed-loop liquid metal cooling fluid system for cooling stator vanes within the turbine, in which the stator vanes are made of a metallic material that will not react with the liquid metal cooling fluid. The stator vane may be made from a typical metal material such as 7 ferrous metal alloys, nickel alloys or cobalt (Co) alloys, and an insert or liner made of

molybdenum or tantalum may be placed in side to protect the outer vane material from reacting with a liquid metal such as bismuth, lead (Pb), indium, or alloy mixtures of thereof. In the case where the liquid coolant is bismuth, the liquid bismuth may be purged from the cooling system before the fluid cools and solidifies so the solidified bismuth does not expand and break the vanes.

1.11 Five main elements of Cooling technology

Cooling technology, as applied to gas turbine components is composed of five main elements, (1) internal convective cooling, (2) external surface film cooling, (3) materials selection, (4) thermal-mechanical design, and (5) selection and/or conditioning of the coolant fluid. Cooled turbine components are merely highly specialized and complex heat exchangers that release the cold side fluid in a controlled fashion to maximize work extraction. The enhancement of internal convective flow surfaces for the augmentation of heat transfer was initially improved some 25–30 years ago through the introduction of rib-rougheners or turbulators, and also pin-banks or pin-fins. Figure 1.1 shows an example schematic of a blade cooling circuit that utilizes many turbulated passages, a pin bank in the trailing edge, and impingement in the leading edge (coolant is released via film holes, tip holes, and trailing edge). These surface enhancement methods continue to play a large role in today's turbine cooling designs. Film cooling is the practice of bleeding internal cooling flows onto the exterior skin of the components to provide a heat flux reducing cooling layer, as shown by the many holes placed over the airfoil in Fig. 1.2. Film cooling is intimately tied to the internal cooling technique used in that the local internal flow details will influence the flow characteristics of the film jets injected on the surface.

Several characteristics of gas turbine cooling are worth noting prior to describing any specific technologies. Almost all highly cooled regions of the high-pressure turbine components involve the use of turbulent convective flows and heat

transfer. Very few, if any, cooling flows within the primary hot section are laminar or transitional. Moreover, the typical range of Reynolds numbers for cooling techniques, using traditional characteristic lengths and velocities, is from 10,000 to 60,000. This is true of both stationary and rotating components. The enhancement of heat transfer coefficients for turbine cooling makes full use of the turbulent flow nature by seeking to generate mixing mechanisms in the coolant flows that actively exchange cooler fluid for the heated fluid near the walls. These mechanisms include shear layers, boundary layer disruption, and vortex generation. In a marked difference from conventional heat exchangers, most turbine cooling means do not rely on an increase in cooling surface area, since the available surface area to volume ratios are very small. Surface area increases are beneficial, but are not the primary objective of enhancements. The use of various enhancement techniques typically results in at least 50% and as much as 300% increase in local heat transfer coefficients over that associated with fully developed turbulent flow in a smooth duct.

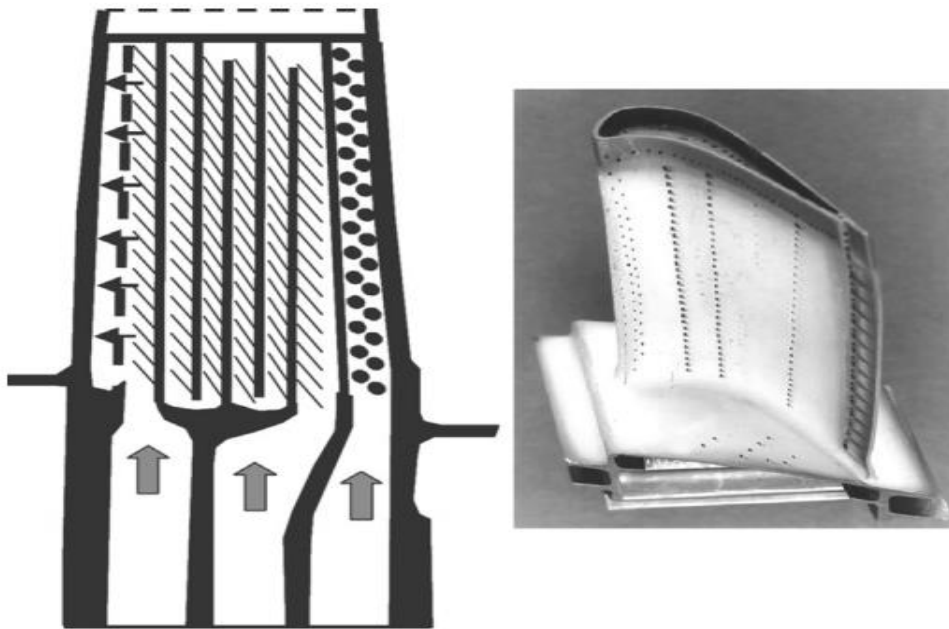


Figure 1.3 – Schematic of a blade cooling circuit.

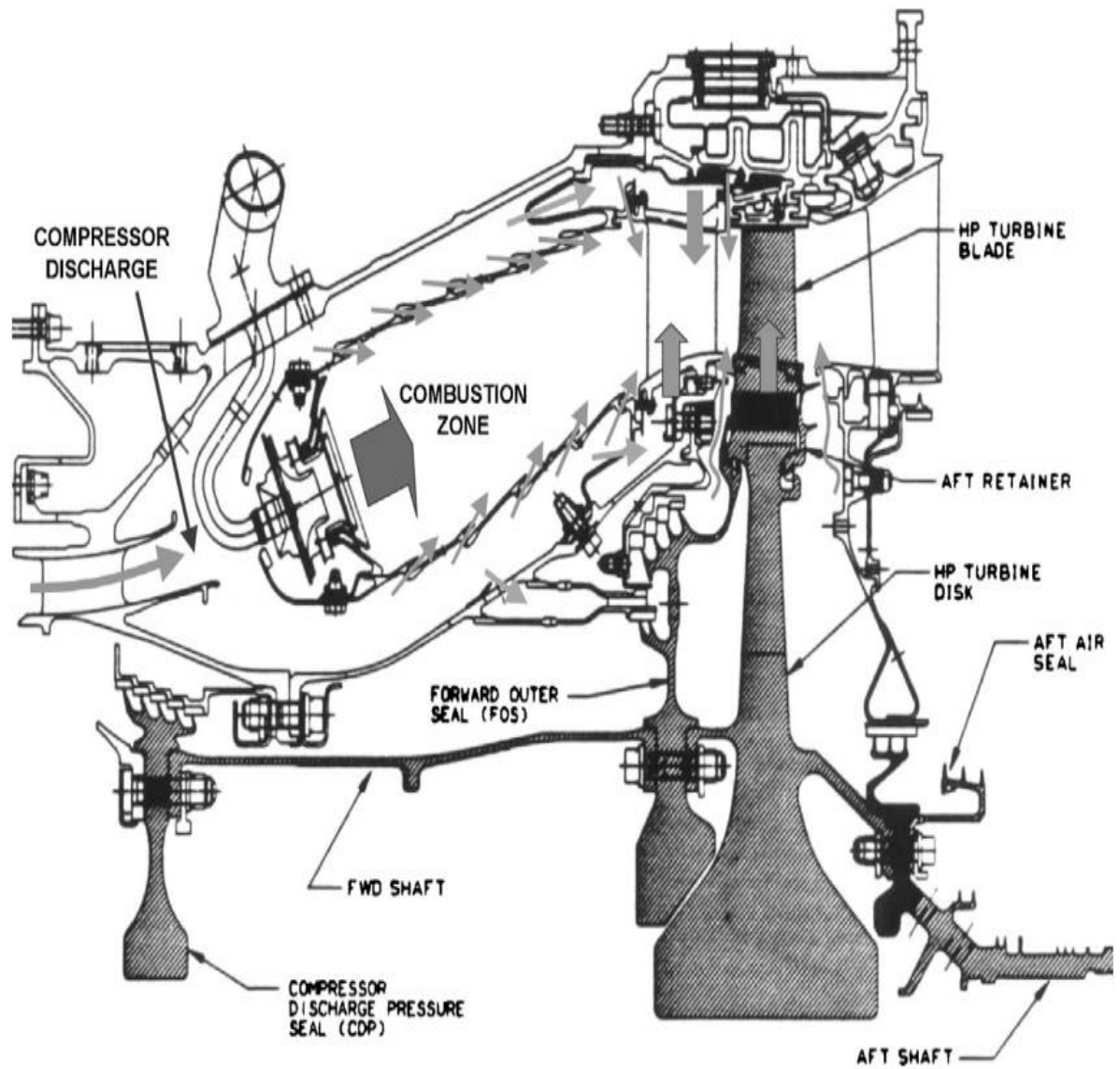


Figure 1.4 – Cooling flows for a combustor and high-pressure turbine.

Conclusion for analytical part

As part of the work, I would push off from the topic of the thesis, and submit information directly of turbine constructive element gas turbine engine cooling for middle range aircrafts. In this part, I have said about important of the topic. Advanced heat transfer and cooling techniques form one of the major pillars supporting the continuing development of high efficiency, high power output gas turbine engines. Conventional gas turbine thermal management technology is composed of five main elements including internal convective cooling, external surface film cooling, materials selection, thermal-mechanical design at the component and system levels, and selection and/or pre-treatment of the coolant fluid. The present summary will examine specific cooling technologies representing cutting edge, innovative methods expected to further enhance the aero-thermal-mechanical performance of turbine engines. The techniques discussed will include forced convective cooling with unconventional turbulators and concavity surface arrays, swirl-cooling chambers, latticework cooling networks, augmentations of impingement heat transfer, synergistic approaches using mesh networks, and film cooling.

2 Development of ways to solve the problem of cooling

The cooling system is now an integral part of the design any modern turbine. In high pressure turbines (HPT) all are cooled blades, rotors, housings. Low pressure turbines (LPT) have rotors, housings and quite often - the scapulae of the first stages. Continuous improvement and the complexity of cooling technologies is a prerequisite for implementation competitive turbine design - a design in which the magnification temperature in front of the turbine, the air flow for cooling does not overlap gain in specific parameters of the engine, and the resource of details of the turbine corresponds customer requirements.

The modeling of the cooling system is based on the network method, which is a branched hydraulic system and has a large number of channels of different geometries, which regulate the flow of the cooler and thus affect the efficiency of the gas turbine unit (GTU). Also in some important cases, for example, at a current in a near-disk cavity or in cavities between two disks, at critical and supercritical values of pressure in channels the character of a stream becomes extremely difficult, and the inclusion in the hydraulic network of the bearing cooling, where oil is used as a coolant complicates the modeling process, as the air suction we have an environment with completely different physical properties. Therefore, the process of modeling such channels and including them in the overall hydraulic scheme is a difficult task. And the accuracy with which the cost characteristics of the circuit elements are, is a decisive factor that determines the reliability of the modeling of the cooling system as a whole. Thus, the issues of further improvement of cooling systems with different types of rotating elements of gas turbines, the study of the structure and properties of the flow, obtaining dependences describing this flow are relevant for turbine construction.

2.1 Development of a method for monitoring system elements cooling turbine blades

The main criteria for developing a control method are:

- high accuracy (measurement error no more than 5%);
- speed of the process (70 blades per shift);
- compactness and ease of management and handling;
- safe working conditions.

These criteria are met by a method for monitoring the cooling system of GTE turbine blades based on laser interferometry (optical Doppler effect) [9, 10]. Laser interferometry is based on the phenomenon of light interference [11]. The incoming beam from a coherent light source is split into two identical beams using an interferometer. Each of these beams travels a different path, called a trajectory, and they are brought together before entering the detector. The difference in the distance traveled by each ray creates a phase difference between them. It is the introduced phase difference that creates an interference pattern between initially identical waves (Fig. 2.1), which is determined on the detector.

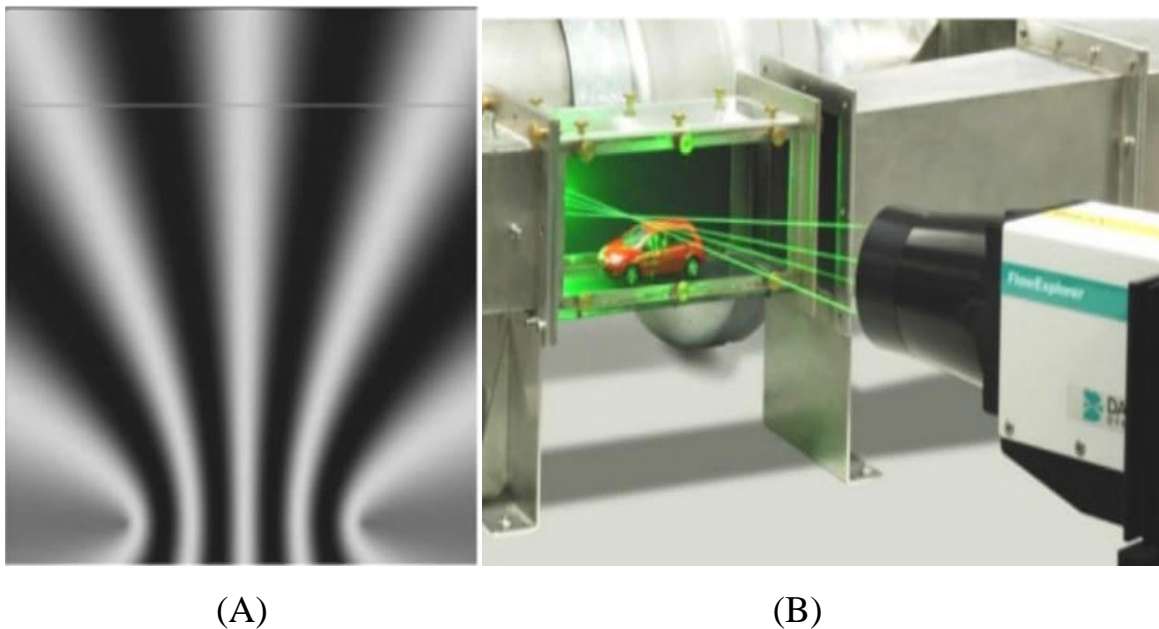


Figure 2.1– Interference pattern (A); example of laser interferometry application (B)

The principle of interferometry is used in a Laser Doppler anemometer (LDA) [12, 13].

Advantages of the method:

- high spatial and temporal resolution, providing minimum error (up to 5%);
- applicable for complex surfaces;
- no need for calibration;
- the ability to work in environments with a contaminated environment;
- compactness of the equipment used;
- safety of equipment operation;
- high speed of measurement.

The method presented in this article is based on measuring the flow rate of particles from the holes in the perforation of the blade. The measurement of the speed of particles flying through the measuring area is performed using an LDA (Fig. 2.2). The readings are taken along the equidistant to the blade profile.

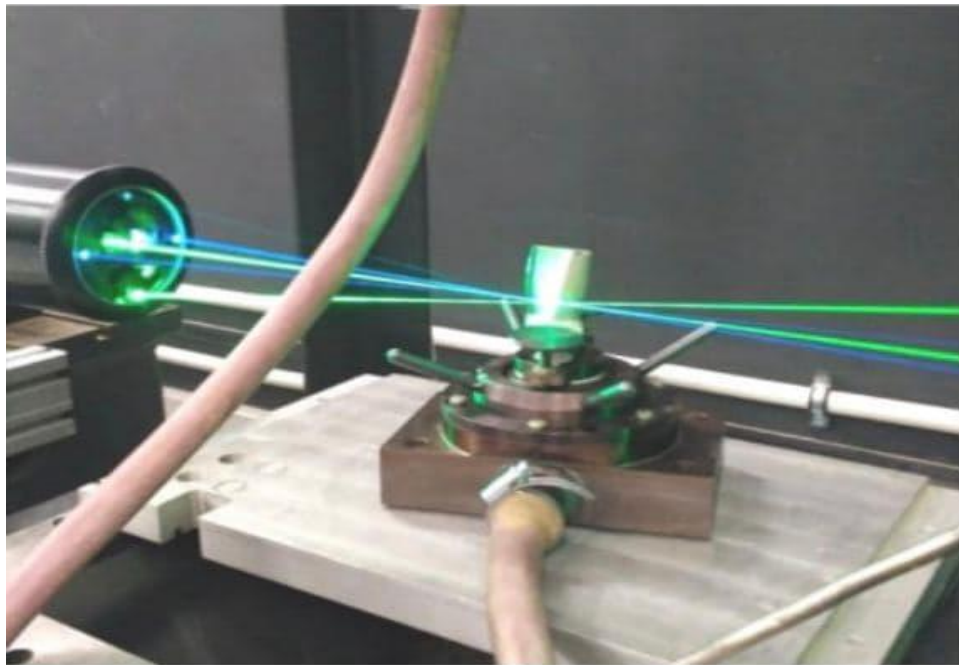


Figure 2.2 – Speed measurement process with LDA

2.2 Microcircuit cooling for a turbine blade tip

An improved cooling design and method for cooling airfoils within a gas turbine engine is provided which includes an embedded microcircuit that traverses a tip between a suction sidewall and a pressure sidewall of the airfoil. The micro circuit includes at least one inlet disposed proximate to the tip and one of the sidewalls for receiving cooling air from an internal cooling cavity of the airfoil and at least one outlet disposed proximate to the tip through which the cooling air is exhausted into a region outside the airfoil.

This invention relates to coolable airfoils of the type used in high temperature rotary machines such as gas turbines and, more particularly, to an improved tip cooling scheme for airfoils.

Efficiency is a primary concern in the design of any gas turbine engine. Historically, one of the principle techniques for increasing efficiency has been to increase the gas path temperatures within the engine. Using internally cooled components made from high temperature capacity alloys has accommodated the increased temperatures. Turbine stator vanes and blades, for example, are typically cooled using compressor air worked to a higher pressure, but still at a lower temperature than that of the core gas flow passing by the blade or the vane. It will be understood that compressor bleed air for such cooling will be unavailable to support combustion in the combustor. The higher pressure provides the energy necessary to push the air through the component. A significant percentage of the work imparted to the air bled from the compressor, however, is lost during the cooling process. The lost work does not add to the thrust of the engine and negatively affects the overall efficiency of the engine. [41]

A person of skill in the art will recognize therefore, that there is a tension between the efficiency gained from higher core gas path temperatures and the concomitant need to cool turbine components and the efficiency lost from bleeding air to perform

that cooling. There is, accordingly, great value in maximizing the cooling efficiency of whatever cooling air is used.

Film cooling has been shown to be very effective but requires a great deal of fluid flow to be bled off the compressor for cooling. Further, film cooling is actively controlled in a complex and expensive manner. Also, the fabrication and machining of an airfoil with film cooling holes adds a degree of complexity that is costly. It will also be appreciated that once the cooling air exits the internal cavity of the airfoil and mixes with the hot gases, a Severe performance penalty is incurred due to the mixing process and the different temperature levels of the mixing flows. Thus, film cooling requires a greater amount of cooling air with the possibility of inadequate cooling of the outer Surfaces of the airfoil.

Prior art coolable airfoils typically include a plurality of internal cavities (cooling circuit), which are Sup plied with cooling air. The cooling air passes through the wall of the airfoil (or the platform) and transfers thermal energy away from the airfoil in the process. Typically in the prior art, blade tip film cooling holes provide external film cooling issued on the blade tip preSSure Side in the radial and axial directions. Some designs use as many film holes as possible, in the limited Space available, in an effort to flood the pressure Side tip region with coolant. It is desired that this film cooling then carry over onto the outer tip Surface to provide cooling there and also over the Suction Side Surfaces of tip. Film holes are oriented in the radially outward direction because the prevailing mainstream gas flows tend to migrate in this manner in the tip region. In practice, it is still very difficult and very inconsistent to cool the blade tip in this manner due to the very complex nature of the cooling flow as it mixes with very dynamic hot gases of the mainstream flow.

In some prior art arrangements, cooling flow exits the film holes and is Swept by the hot combustion gases towards the trailing edge of the airfoil and away from tip cap. Typically, this results in a mixed effect, where Some of the cooling air is caught up and mixed with the hot gases and Some goes onto tip cap and Some goes

axially along the airfoil to trailing edge. This results in inadequate cooling of tip cap and eventual temperature inflicted degradation of tip Cap.

Turbine engine blade designers and engineers are constantly Striving to develop more efficient ways of cooling the tips of the turbine blades to prolong turbine blade life and reduce engine operating cost. Cooling air used to accom plish this is expensive in terms of overall fuel consumption. Thus, more effective and efficient use of available cooling air in carrying out cooling of turbine blade tips is desirable not only to prolong turbine blade life but also to improve the efficiency of the engine as well, thereby again lowering engine operating cost. Consequently, there is a continuing need for a cooling design that will make more effective and efficient use of available cooling air.

Thus, to minimize any sacrifice in engine performance due to unavailability of cooling airflow to Support combustion, any Scheme for cooling blades and Vanes must optimize the utilization of compressor bleed cooling air. Airfoil cooling is accomplished by external film cooling, internal air impingement and forced convection either separately or a combination of all cooling methods.

The above discussed and other drawbacks and defciencies are overcome or alleviated by the present invention. The present invention provides a microcircuit cooling system that employs a new and effective approach to convectively cool a tip of an airfoil in combination with film cooling. In particular, this combination provides an advantage over the prior art tip cooling schemes in that, to achieve the same metal temperature at the tip, less cool compressor air is required to cool the tip. Less compressor bleed flow results in the additional advantage of providing an increase in turbine efficiency. The cooling system of the present invention employs at least one plenum transversely disposed between the pressure and suction sidewalls of the airfoil. A plurality of inlets and a plurality of outlets are in How communication with the plenum. Cooling air, supplied from the cooling circuit of the airfoil, enters said inlets, transitions into said plenum and exits said outlets into

a region outside the airfoil. It is preferred that the plenum includes a plurality of micropassages through which the cooling air flows through.

As described above, the present invention can be implemented and utilized in connection with many alternative airfoil (blade and vane) configurations. The combination of a) effective convective cooling provided by the micropassages and b) effective thermal insulation on the tip surface due to film cooling provides a cooler tip, as compared to conventional and current designs. Thus, an airfoil tip employing the beneficial cooling design of the present invention will not only have a longer service life but also improve overall turbine efficiency. [40]

The present invention also contemplates a method for cooling a tip of a turbine blade suitable for use in gas turbine, comprising the steps of a) fabricating a microcircuit under a surface of the tip and b) providing cooling flow from a cooling flow source to flow into an inlet of the microcircuit, through a plurality of micropassages, and out of an outlet of the microcircuit to exit into the gas stream at the tip of the blade.[41]

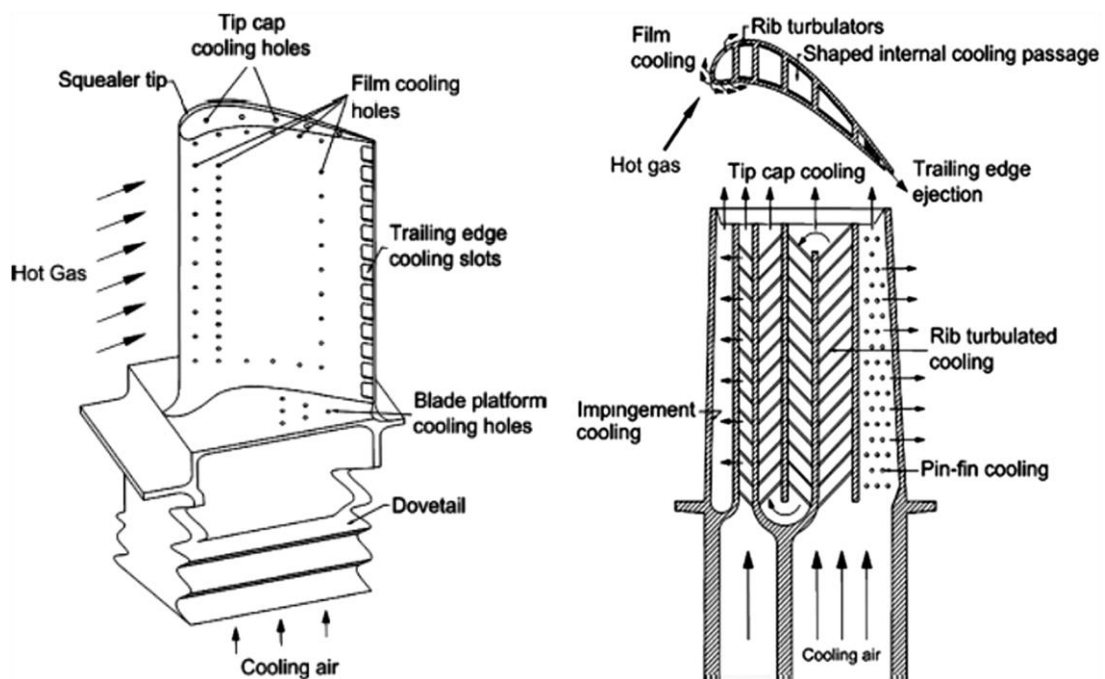


Figure 2.3 – microcircuit cooling scheme of blade [41]

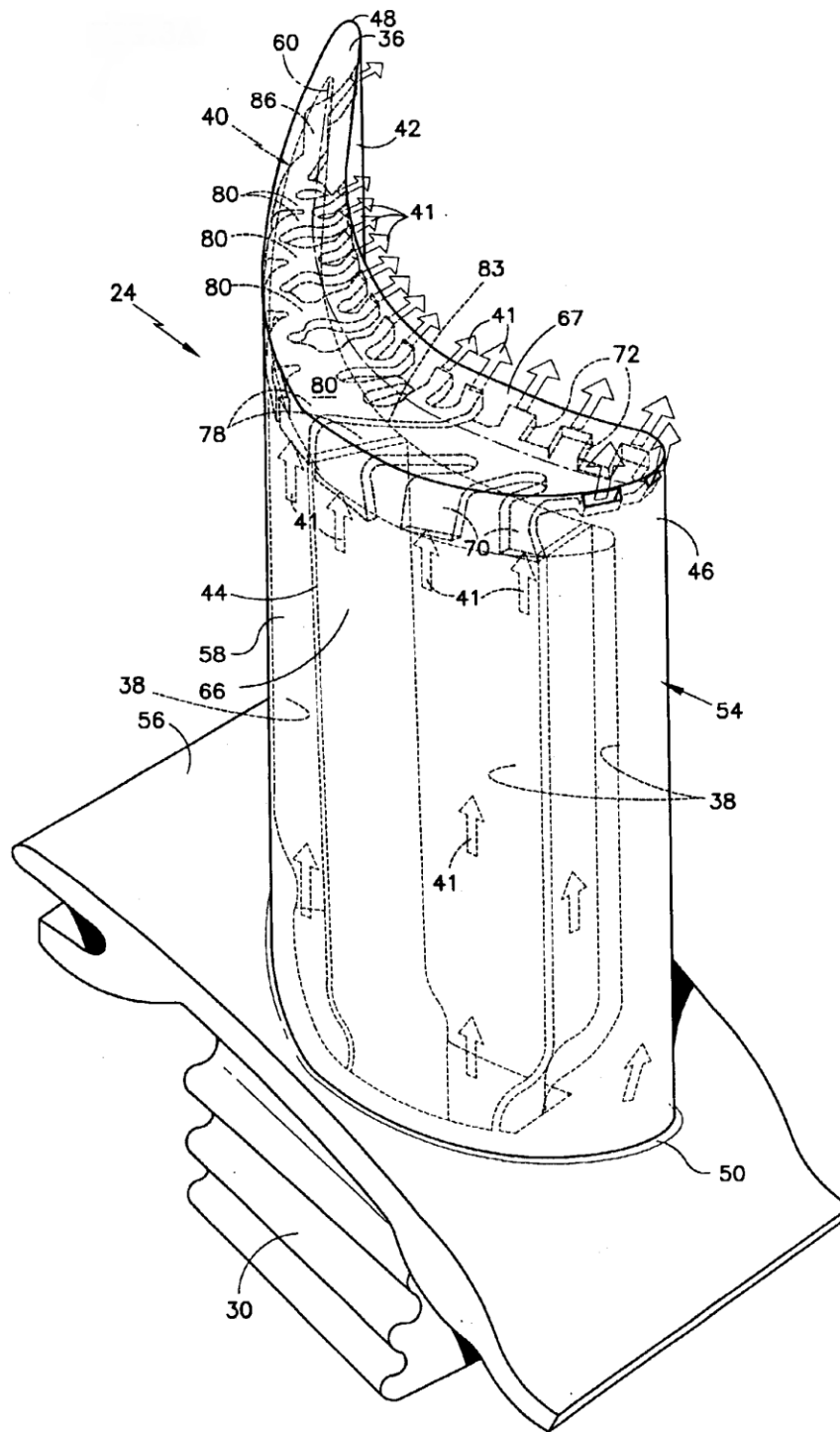


Figure 2.4 – Perspective view of an airfoil incorporating the microcircuit cooling scheme of the present invention [41]

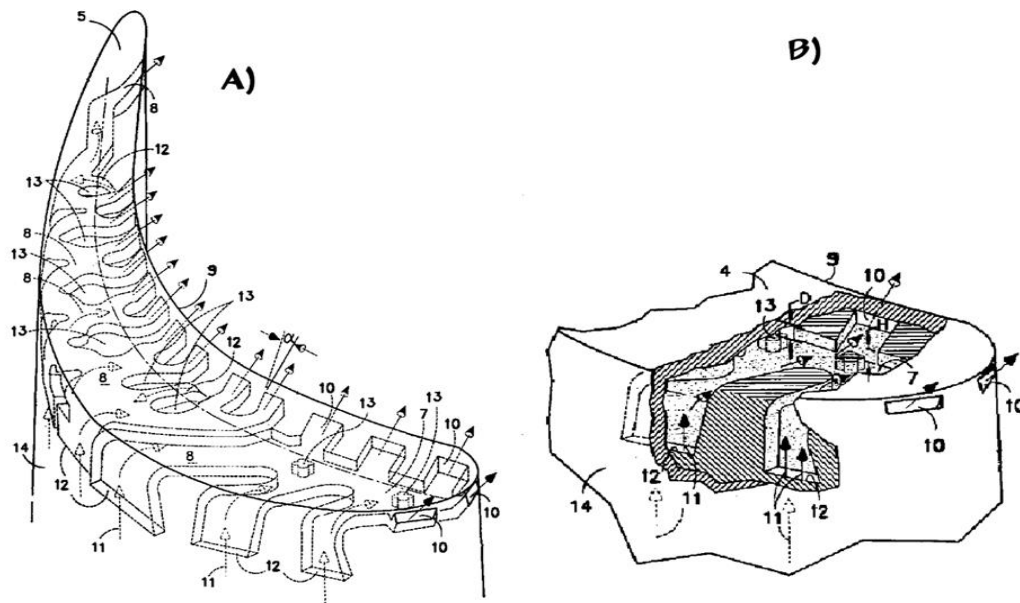


Figure 2.5 – A) partial perspective view of the tip of the airfoil B) enlarged partial perspective view showing the tip adjacent the leading edge of the airfoil of Figure A [41]

2.3 Types of technology used for turbofan engine cooling system

As explained in a previous section, the efficiency of the gas turbine cycle increases as the turbine inlet temperature (TIT) increases. Consequently, the hotter the combustion gases entering the first stage of the turbine, the more the specific power of the jet engine can produce. Of course, the TIT is limited by the metallurgical limits of the blade materials, in particular the blade root stress, the creep deformation and the melting point of the blade material. Centrifugal stresses at the root increase linearly with the density of the blade material and linearly with both the square of the speed of rotation and the square of the ratio of the radius from root to tip. Creep is the continuous and progressive extension of a material under a constant load over time.

In addition to distorting the physical dimensions and thereby reducing the performance of the motor, the induced creep stresses exacerbate the centrifugal

operating stresses and will therefore cause premature material failure. Typically, the life of the blade is halved (for a specific blade material and cooling technology) for every 10°C increase in metal temperature.

The TIT went from around 1050 K in 1944 to around 1750 in the Rolls-Royce Trent engine from 1994. This is partly due to the use of better materials such as Inconel and monocrystalline metals with better properties. creep and fatigue. However, this solution is linked to the fact that these nickel-based alloys are generally quite heavy, which causes an increase in centrifugal stresses at the root. Therefore, the technology of channeling cold air from the compressor to cool the turbine blades has been more important in this development. The use of these advanced cooling techniques allowed engineers to increase the TET beyond the melting point of the blade materials.

2.3.1 Methods of cooling turbine elements

In a modern engine a certain amount of the compressed air is bled off for cooling and sealing purposes for nozzle guide vanes and turbine blades. This internal air system illustrated in (Figure 2.6) is also used to prevent the any hot mainstream gases from flowing over the heavily stressed blade-attachment discs and control tip clearances between turbine blades and casing. The stators and outer wall of the turbine flow passage use cooling air traveling from the compressor between the combustor and outer engine casing. The turbine rotor blades, disks and inner walls of the turbine flow passage use air bled from the compressor through inner passageways. Since the stators (or nozzle guide vanes) appear before the first row of rotating blades, the first stage of stators are exposed to the highest temperatures, including local hot-spots from the combustor close by. The temperature at the first rotor stage is then somewhat decreased by dilution of the gases with cooling air, relative velocity effects and power extraction (by gas

expansion causing a drop in temperature) from the turbine. In this manner the temperature reduces through each blade row.

The laws of thermodynamics require that due to combustion inefficiencies there be a pressure loss within the combustor. This means that the mainstream pressure at the first row of stators in the turbine directly after the combustor be lower than at the exit of the final stage of the compressor. It is this pressure difference that we use to drive the cooling air through the internal passageways and into the stators and blades. In this respect improvements in combustor design over the last years has been both an advantage and a disadvantage for cooling engineers. Improvements in combustor design has led to lower pressure losses within the compressor such that more force is available to drive the bled air to the hotter parts of the engine. On the other hand, with increasing compression ratios the air within the compressor naturally reaches higher exit temperatures (today around 900 K prior to combustion) reducing the effect that the cooling air has on the turbine blades. Furthermore, the cooling air is expensive from an efficiency point of view since work has been done on the compressed fluid and we would ideally like to “waste” as little as possible for secondary cooling purposes. As in most case a compromise has to be struck between power output and turbine life.

2.4 Cooling system Technology

The technology of cooling gas turbine components, primarily via internal convective flows of single-phase gases and external surface film cooling with air, has developed over the years into very complex geometries involving many differing surfaces, architectures, and fluid-surface interactions. The fundamental aim of this technology area is to obtain the highest overall cooling effectiveness with the lowest possible penalty on the thermodynamic cycle performance. As a thermodynamic Brayton cycle, the efficiency of the gas turbine engine can be

raised substantially by increasing the firing temperature of the turbine. Modern gas turbine systems are fired at temperatures far in excess of the material melting temperature limits. This is made possible by the aggressive cooling of the hot gas path components using a portion of the compressor discharge air. The technologies below were extracted from the researches of “*GE Global Research Center, USA*” by R.S. Bunker entitled “*Innovative gas turbine cooling techniques*” chapter 7.[18]

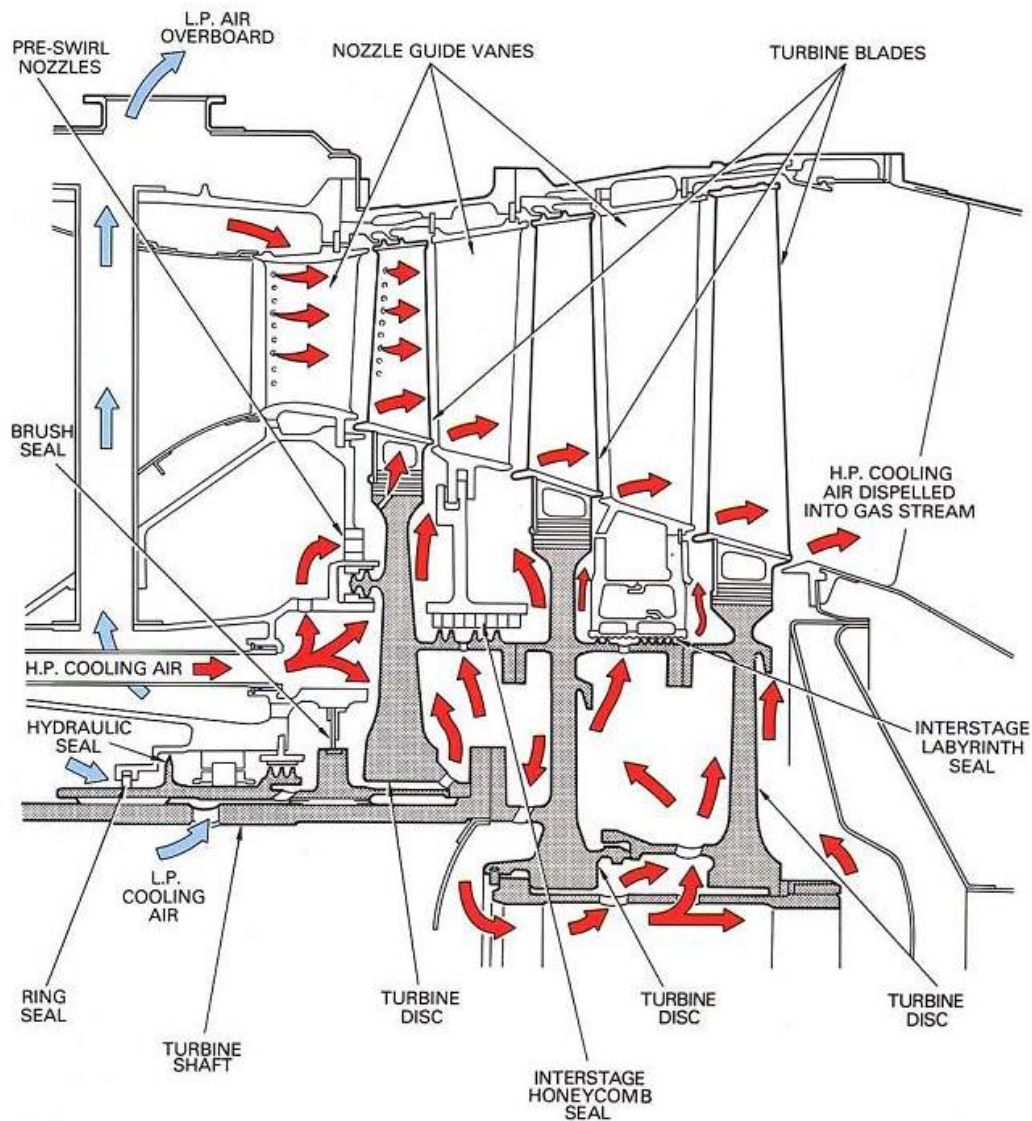


Figure 2.6 – Hypothetical turbine cooling and sealing arrangement

2.5 An example of a cooling circuit of a blade

When evaluating the efficiency of the cooling system, additional hydraulic losses on the shoulder blades are also taken into account as a result of changes in their shape during the release of cooling air. The efficiency of a real cooling turbine is about 3-4% lower than uncooled.

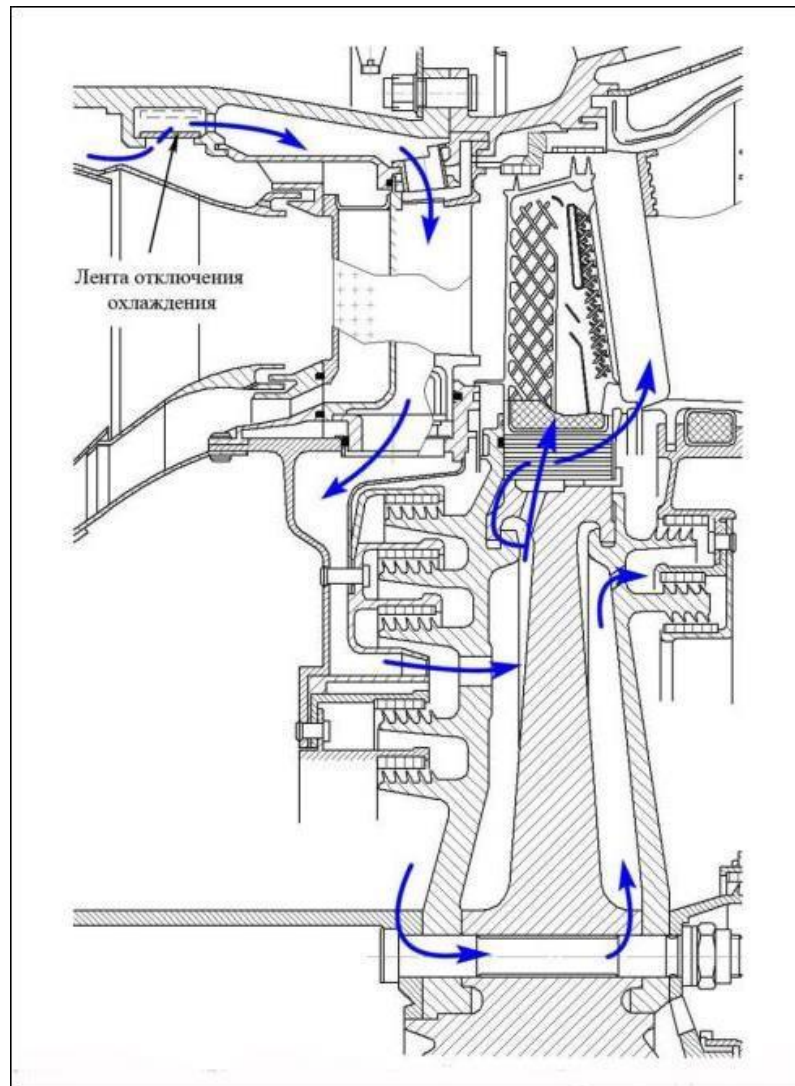


Figure 2.7 - Cooling scheme of the 1st stage of the turbine TRDD D436. Also shown are cellular seals and a disconnection cooling tape at reduced engine operating modes.

Conclusion for part number 2

In this part was considered recommends of Development of a method for monitoring system elements cooling turbine blades, with a dvantages of the method:

- high spatial and temporal resolution, providing minimumerror (up to 5%);
- applicable for complex surfaces;
- no need for calibration;
- the ability to work in environments with a contaminated environment;
- compactness of the equipment used;
- safety of equipment operation;
- high speed of measurement.

Also I have said about Mircocicuit cooling for a turbine blade tip. The present invention also contemplates a method for cooling a tip of a turbine blade Suitable for use in gas turbine, comprising the Steps of a) fabricating a microcircuit under a Surface of the tip and b) providing cooling flow from a cooling flow Source to flow into an inlet of the microcir cuit, through a plurality of micropassages, and out of an outlet of the microcircuit to exit into the gas Stream at the tip of the blade.

3 Selection of the latest materials and systems for their implementation in a gas turbine engine. Comparative analysis of innovations.

Turbofan turbine elements (blades, disks, vanes, etc.) are critical components in aircraft engine, which convert the linear motion of high temperature and high pressure steam flowing down a pressure gradient into a rotary motion of the turbine shaft. The low pressure turbine blades, designed to extract the final remnant of energy from the passing steam flow, are relatively large scale rotating airfoils due to the significant centrifugal forces experienced during normal operation. Statistics show that low-pressure (LP) turbine blades are generally more susceptible to failure than those of the high pressure (HP) and intermediate pressure (HP). Furthermore, almost 50% of the failures are related to fatigue, stress corrosion cracking, and corrosion fatigue which are majorly caused by heat.

Cooling is also needed because high temperatures damage engine materials and lubricants and becomes even more important in hot climates. The combustion chamber of turbofan engines burn fuel hotter than the melting temperature of engine materials, and hot enough to set fire to lubricants. Engine cooling removes energy fast enough to keep temperatures low so the engine can survive. A complex air system is built into most turbine-based jet engines, primarily to cool the turbine blades, vanes and discs and engine casing.

3.1 Active control clearance between the tips of the rotor blades.

In order to strengthen the argumentation of microcircuit cooling system improving control clearance control, we are referring to patent research:

Patent number: 8998563 [8]

Type: Grant

Filed: Jun 8, 2012

Date of Patent: Apr 7, 2015

Patent Publication Number: [20130330167](#)

Assignee: [United Technologies Corporation](#) (Hartford, CT)

Inventor: [Philip Robert Rioux](#) (North Berwick, ME)

An active backlash control system for a gas turbine engine includes a structural member which is configured to be disposed near a blade tip. A plenum includes first and second walls providing first and second cavities, respectively. The first wall has impact holes. The plenum is placed on the structural element. A source of fluid is fluidly connected to the second cavity to provide impact cooling flow from the second cavity through the impact holes to the first cavity on the structural member. A method includes the steps of providing conditioning fluid to an external cavity of a plenum providing an impact cooling flow through impact holes from an interior wall of the plenum to an interior cavity the impact cooling flow on a structural element and to condition a temperature of the structural element with the impact cooling flow to control the play of the blade end.

3.2.2 Description of the invention

In one exemplary embodiment, an active clearance control system for a gas turbine engine includes a structural member that is configured to be arranged near a blade tip. A plenum includes first and second walls respectively providing first and second cavities. The first wall includes impingement holes. The plenum is arranged over the structural member. A fluid source is fluidly connected to the second cavity and is configured to provide an impingement cooling flow from the second cavity through the impingement holes to the first cavity onto the structural member.

In a further embodiment of any of the above, the system includes a valve that is fluidly connected between the fluid source and the plenum and is configured to selectively provide fluid to the second cavity.

In a further embodiment of any of the above, the fluid source is fan air. In a further embodiment of any of the above, the fluid source is rear hub air. In a further embodiment of any of the above, the system includes a controller in

communication with the valve and is configured to provide a command to selectively provide fluid to the plenum.

In a further embodiment of any of the above, the system includes an algorithm and multiple sensors in communication with the controller and is configured to provide information relating to a clearance condition between the structural member and the blade tip. The controller commands the valve to selectively provide fluid to the plenum. In a further embodiment of any of the above, the system includes first and second structural members having flanges secured to one another by fasteners at a joint. The plenum is arranged over the joint. In a further embodiment of any of the above, at least one of the first and second structural members includes a blade outer air seal that is arranged adjacent to the blade tip. In a further embodiment of any of the above, the blade outer air seal is integral with the structural member.

In a further embodiment of any of the above, the system includes multiple joints. The plenum is arranged over the multiple joints. In a further embodiment of any of the above, the structural member includes a first interlocking position, and the plenum includes a second interlocking portion cooperating with the first interlocking portion to maintain the plenum relative to the structural member in a desired position. In a further embodiment of any of the above, the first and second walls are concentric C-shaped structures that are secured to one another to provide the first and second cavities.

In another exemplary embodiment, a plenum for a gas turbine engine clearance control system includes first and second walls spaced apart from one another with the first wall arranged interiorly of the second wall. The first wall includes multiple impingement holes, and an interlocking feature is provided on the plenum and configured to cooperate with the corresponding interlocking feature on a structural member to locate the plenum relative to the structural member in a desired position. In a further embodiment of any of the above, the first and second walls are concentric C-shaped structures that are secured to one another to provide the first and second cavities. In a further embodiment of any of the

above, the first and second walls provide a unitary structure. In a further embodiment of any of the above, the first and second walls are stamped sheet metal.

In another exemplary embodiment, a method of actively controlling a clearance in a gas turbine engine includes the steps of providing a conditioning fluid to an outer cavity of a plenum, providing an impingement cooling flow through impingement holes from an inner wall of the plenum to an inner cavity, directing the impingement cooling flow .

3.2 Turbine Disk with impellers for cooling the turbine blades attached to the said disk, and corresponding cooling method of turbine blades.

Patent number: EP 2 589 753 A3 [42]

Filed: 01.11.2012

Date of Patent: 08.05.2013

Patent Publication Number: 12190939.4

Assignee: United Technologies Corporation Farmington, CT 06032 (US)

Inventor: • Wu, Charles C. Glastonbury, CT Connecticut 06033 (US) • McCusker, Kevin N. West Hartford, CT Connecticut 06107 (US)

An apparatus for cooling a rotating part (50) having cooling channels (70) therein, the rotating part (50) attaching to a disk (75) rotating about an axis (12), the disk (75) having a conduit (100) for feeding a cooling fluid to the cooling channel (70). The apparatus has a first impeller (90) rotating with the disk (75) and in register with the conduit (100) and an outer periphery of the disk (75), the impeller (90) directing the cooling flow to the conduit (100). A corresponding method for cooling a turbine blade.

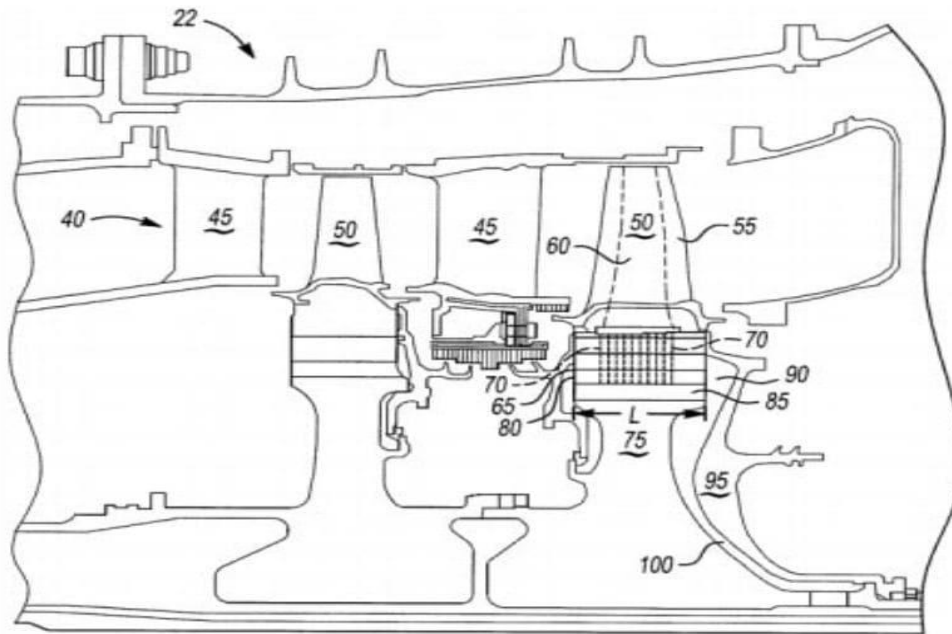


Figure 3.1 - Turbine Disk with impellers for cooling the turbine blades attached to the said disk

3.3 MODERN COOLING VANE'S SYSTEMS OF HIGH-LOADED GAS TURBINES

The nozzle blades are the most thermally loaded parts of the turbines of gas turbine engines (GTE). Taking into account the circumferential irregularity, the local gas temperature at the exit from the combustion chamber can reach values of the order of 2500 K [4]. Under these conditions, for promising gas turbine engines, the greatest problems are associated with reliable cooling of the nozzle blades in the area of the leading edge — due to the high curvature of the profile, low gas flow velocity in this place and the small pressure drop between the cooling air and gas; the back of the blade - due to high gas velocities, non-optimal blowing parameter in the last row of perforations along the back and the need to place it up to the throat of the nozzle apparatus. All these factors lead to the fact that for the leading edge the most important cooling methods are jet blowing and convective heat transfer in the perforation holes, and for the backrest - film cooling and backrest jet blowing from the inside in places below the last row of perforations downstream

[5]. During operation and long-term hot tests on the first stage nozzle blade tips of PS-90A, PS-90A2 engines and their modifications, damage was found: burnouts, cracks and irreversible deformations on the backs and entrance edges of the blades [6, 7] (Fig. 3.2)



Figure 3.2 – Burnout of nozzle blades after testing

As a result of the complex of computational and experimental work, it was possible to work out an effective method of designing nozzle blades, which makes it possible to carry out both quick approximate design calculations with the required accuracy and calculations, providing the ability to fine-tune the designed structure.

To solve the cooling problems, eliminate the above-described damage in operation and increase the blade life, based on the identified thermal models of the available blades, a three-cavity convection-film cooling scheme was developed and applied for the blades of PS-90A and PS-90A2 engines (Fig. 3,3; 3.4).

This scheme allows more efficient air distribution inside the blade and prevents irreversible deformation of the back due to the additional stiffening rib. Cooling air is supplied to the blade from above (through the outer ring) on the PS-90A engine. On the PS-90A2 engine, the front cavity is supplied from above, and into the middle and rear cavities from below (through the inner ring). The front cavity is made tapering from the outer ring to the inner one to ensure an even distribution of air pressure along the height of the blade. In addition, to ensure a guaranteed drop at the leading edge, the possibility of regulating the blowing parameters both on

the trough and on the back of the scapula, the anterior cavity of the scapula is additionally divided by vertical ribs into two more subcavities [11] (Fig. 3.5).

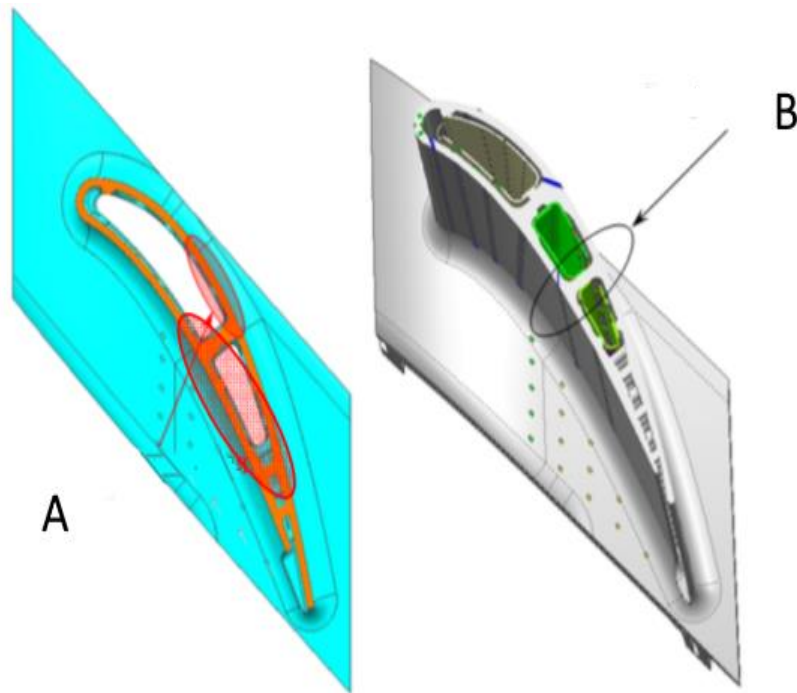


Figure 3.3 – Comparison of the blades of the original (left) and modified (right) designs of the PS-90A engine, where A (irreversible deformation of the backrest), and B (stiffener)

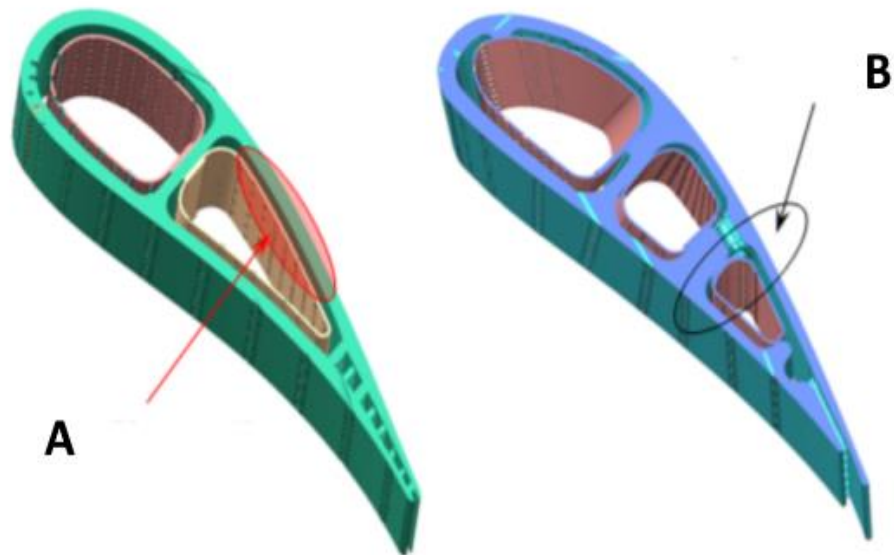


Figure 3.4 – Comparison of the blades of the original (left) and modified (right) designs of the PS-90A engine, where A (irreversible deformation of the backrest), and B (stiffener)

Mutual coordination of the efficiency of film and convective cooling and redistribution of the air flow rate over the subcavities are possible only by changing the holes in the deflector without altering the blade as a whole, which provides the flexibility of mutual coordination of convective and film cooling with minimal financial costs [12]

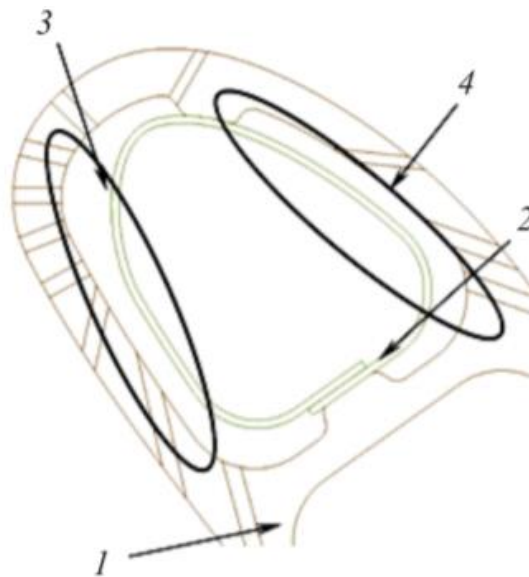


Figure 3.5 – The front cavity of the modified nozzle blade:

- 1 - body of the blade; 2 - deflector; 3 - high pressure cavity;
4- low pressure cavity

The use of a three-cavity scheme made it possible to reduce the consumption of cooling air into the blade by 0.5% of the GKVD for the PS90A engine and by 1% from the GKVD for the PS-90A2 engine and to reduce the temperature of the blade feathers by an average of 60–75 ° C, and at the site of damage by back - at 80–90 ° C, which is confirmed by calculations and tests. As a result, the efficiency of cooling the profile parts of the modified blades $\theta = 0.7 \dots 0.8$, which exceeds the level of most serial foreign developments (Fig. 3.6; 3.7).

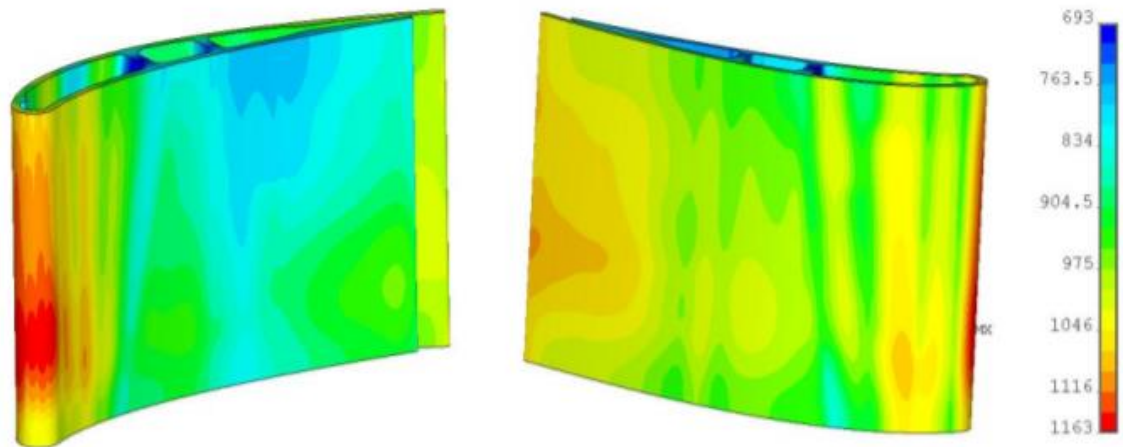


Figure 3.6 – Material temperature of the modified nozzle blade the of the first stage of the PS-90A engine for the Redline mode ($T_{\Gamma} = 2026\text{K}$, $T_{ca} = 1631\text{ K}$, $T_{K} = 871\text{ K}$, $GKVD = 77.654\text{ kg / s}$)

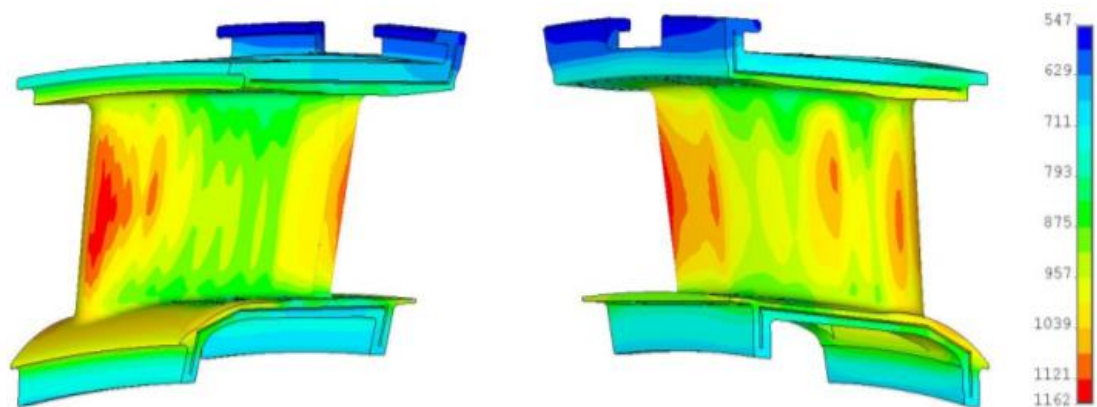


Figure 3.7 – Material temperature of the modified nozzle blade of the first stage of the PS-90A2 engine for the Redline mode ($T_{g} = 2317\text{ K}$, $T_{ca} = 1814\text{ K}$, $T_{K} = 916\text{ K}$, $GKVD = 83.93\text{ kg / s}$)

A promising nozzle blade was developed on the basis of the nozzle blades of the PS-90A and PS-90A2 engines (Fig. 3.8). The main differences from the previous blades are:

- additional division of the anterior cavity into three subcavities (high, medium and low pressure), which is due to a greater load on the stage, a large angle of flow rotation and a sharper change in the flow rate along the blade profile;
- the use of ovalized holes, shifted from the back of the scapula, to reduce the stress concentration (Fig. 3.9).

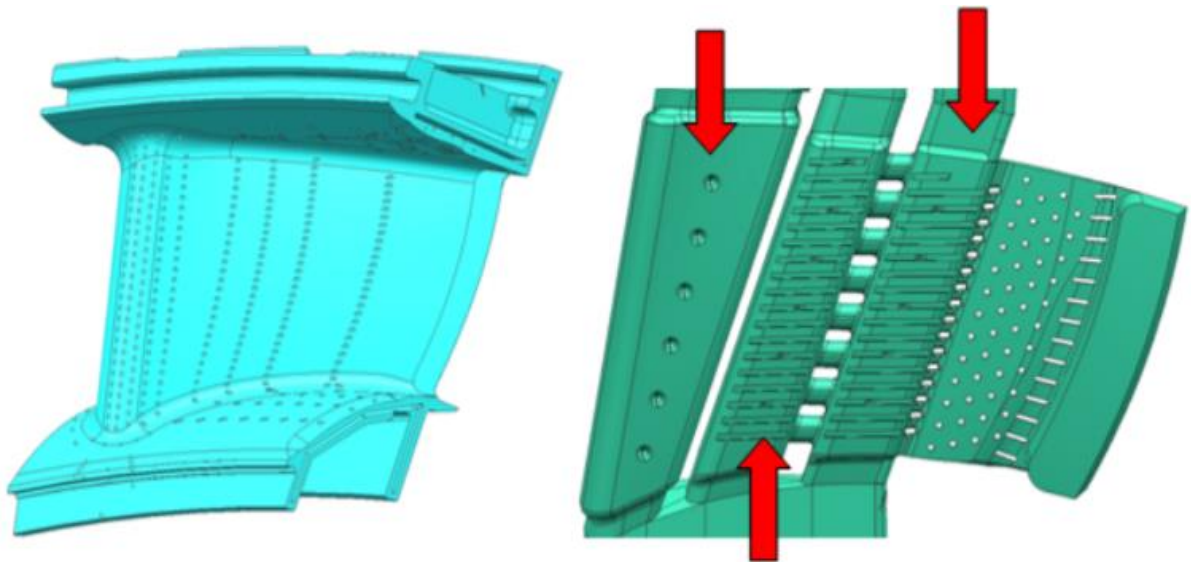


Figure 3.8 – General view of a perspective nozzle blade (left) and a rod (right).

Arrows indicate cooling air supply

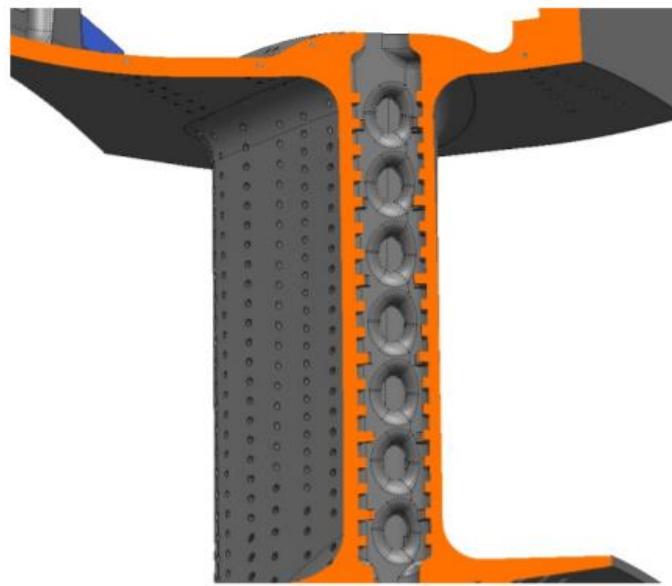


Figure 3.9 – Bypass holes between the middle and rear cavities

Conclusion for part number 3

Thus, in the process of working on a three-cavity cooling scheme, the following tasks were solved:

- ensuring the required flow rate and pressure drop in the last row on the back of the blade;
- determination of the place of the maximum efficiency of the film, determination of the ratio of the air consumption going to the film and for convective cooling of the back;
- ensuring a guaranteed drop at the leading edge at all engine operating modes;
- determination of the ratio of the pressure drops realized on the deflector and on the blade wall in order to obtain the most efficient cooling scheme of the leading edge;
- ensuring the permissible temperature on the trough of the blade at minimization of air consumption for cooling the trough (optimization of convective-film cooling of the trough by choosing the optimal pitches of holes in the rows of perforations);
- ensuring the rigidity of the back of the scapula by adding an additional bridge.

Currently, blades with a three-cavity cooling scheme are being run-in on ground gas turbine plants and on full-size aircraft engines in bench conditions

4 ENVIRONMENTAL PROTECTION

4.1 Harmful factors that occur during the operation of the GTE

According to the state standard, harmful and dangerous factors by action and nature of influence are divided into four classes: physical, chemical, biological and psychophysiological.

During the operation of the gas turbine engine, the possible negative impact on the environment above consists of several main factors: possible gas leakage and increased noise and vibration levels.

Noise and vibration are physical pollutants, and gas leaks are chemical pollutants. Noise is a set of sounds of different strength and frequency, which interfere with the perception of useful signals and adversely affect a person. The physical essence of sound is the oscillation of environmental particles that are perceived by human hearing as undesirable. During sound vibrations, areas of low and high pressure are formed, which act on the auditory analyzer (ear membrane). Vibration - the movement of a mechanical system, in which alternately increase and decrease over time the value of the quantity that characterizes this movement. Manifested in the form of mechanical oscillations of elastic bodies.

Harmful factors that adversely affect the environment above include:

- increased noise level during operation of the gas turbine;
- possible explosion of the gas-air mixture due to dangerous concentration (5 ÷ 15%) with air, formed due to gas leakage due to leakage in the joints, seals;
- chemical pollution associated with possible gas leakage due to leaks in joints, seals;
- vibration during operation of GTE.

4.2 Water pollution

Airports can generate significant water pollution due to their extensive use and handling of jet fuel, lubricants and other chemicals. Airports install spill

control structures and related equipment (e.g., vacuum trucks, portable berms, absorbents) to prevent chemical spills, and mitigate the impacts of spills that do occur. In cold climates, the use of deicing fluids can also cause water pollution, as most of the fluids applied to aircraft subsequently fall to the ground and can be carried via stormwater runoff to nearby streams, rivers or coastal waters.^{[123]:101} Airlines use deicing fluids based on ethylene glycol or propylene glycol as the active ingredient. Ethylene glycol and propylene glycol are known to exert high levels of biochemical oxygen demand (BOD) during degradation in surface waters. This process can adversely affect aquatic life by consuming oxygen needed by aquatic organisms for survival. Large quantities of dissolved oxygen (DO) in the water column are consumed when microbial populations decompose propylene glycol. Sufficient dissolved oxygen levels in surface waters are critical for the survival of fish, macroinvertebrates, and other aquatic organisms. If oxygen concentrations drop below a minimum level, organisms emigrate, if able and possible, to areas with higher oxygen levels or eventually die. This effect can drastically reduce the amount of usable aquatic habitat. Reductions in DO levels can reduce or eliminate bottom feeder populations, create conditions that favor a change in a community's species profile, or alter critical food-web interactions.

4.3 Noise pollution

One of the forms of physical pollution of the atmosphere is noise, adaptation of the organism to it is impossible. Noise is a set of sounds of different frequency and intensity that arise as a result of oscillating motion of particles in elastic media (solid, liquid, gaseous). Noise intensity of 30 ÷ 80 dB does not harm the human body. At the same time, noises of intensity of 85 dB and more lead to physiological and psychological negative consequences on the nervous system, sleep, emotions, and ability to work. Today, the problem of noise pollution is very relevant, as it grows over time. Usually noise is an unpleasant or unwanted sound or a set of sounds that interfere with the perception of useful sound signals, disturb the silence, have a harmful or irritating effect on the human body, reduce its

efficiency. Elevated noise has an adverse effect on the human body. The degree of this action depends on the characteristics of the noise and individual characteristics of the person. Noise affects not only the hearing organs, but also the nervous system, causes high blood pressure, decreased attention, leads to reduced productivity and increased injuries. Existing regulations provide for a maximum permissible sound level of 85 dB. Noise adversely affects various body systems: cardiovascular, nervous, disturbs sleep, attention, increases irritability, depression, anxiety, irritation, can affect the respiratory and digestive systems; hearing impairment with temporary or permanent hearing loss; impaired ability to transmit and perceive the sounds of speech; distraction from normal activities; changes in human physiological responses to stress signals; effects on mental and physical health; effect on labor activity and labor productivity. Studies show an adverse effect of noise on the central nervous, cardiovascular and digestive systems. At vibration of production mechanisms their fast oscillating and rotational movements are transferred to the objects contacting them including workers. The cause of vibration disturbances are unequal-weighted force effects arising during operation of machines: shock loads; reciprocating movements; imbalance. The reasons for the imbalance are: the heterogeneity of the material; discrepancy of centers of mass and axes of rotation; deformation. Vibration is a generally biologically harmful factor that leads to occupational diseases - vibration diseases, the treatment of which is possible only in the early stages. The disease is accompanied by persistent disorders in the human body. The person partially or completely loses his ability to work. According to the method of transmission to humans, vibration is divided into general and local. General – acts through the supporting surfaces of the feet on the whole body. Local - on certain parts of the body. Prolonged exposure to vibration causes an occupational disease - vibration disease.

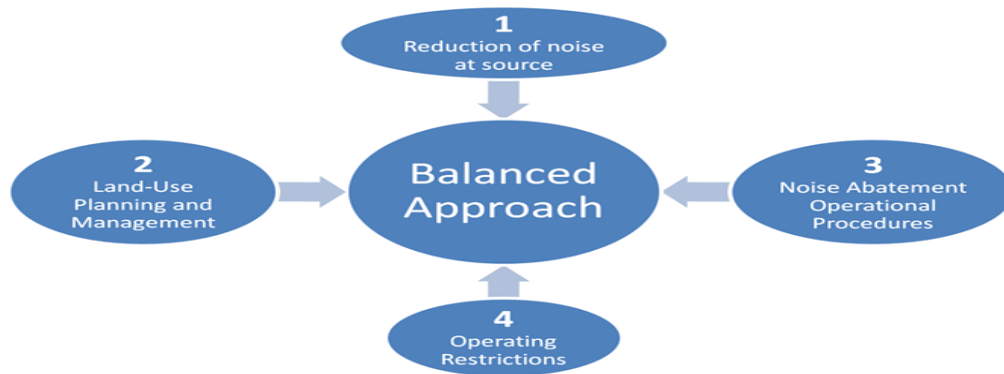


Figure 4.1 – The four principal elements of the Balanced Approach to Aircraft Noise

Additionally, noise technology goals have been developed, in a with the purpose of providing stretch yet reasonable targets for industry R&D to aim at, in cooperation with States.

4.4 Emission of aircraft engines

In modern internal combustion engines, two primary systems are responsible for the formation and reduction of pollutants:

- the combustion system
- the emission aftertreatment system.

The combustion system includes the combustion chamber, its shape and characteristics such as charge composition, charge motion, and fuel distribution. This is where pollutants such as NO_x, CO and PM are created as well as where incomplete oxidation of fuel occurs. What happens in the combustion system is greatly influenced by other engine systems such as the intake charge management system and the fuel injection system. In fact, the primary purpose of these secondary systems is to influence what happens during the combustion process. Numerous options are available to limit the formation of pollutants resulting from the combustion system. Once exhaust gas leaves the combustion system, its composition is essentially frozen until it reaches the emission aftertreatment

system (ATS, also abbreviated EAT or EATS) where further reductions in pollutants can be realized and also where secondary emissions such as N_2O , NO_2 and NH_3 can originate.[35]

The aftertreatment system consists of catalytic reactors that attempt to further lower pollutants. In some cases, such as stoichiometric spark ignition (SI) engines, a single three-way catalyst (TWC) is sufficient to achieve very significant reductions in pollutants. In other cases such as lean burn diesel engines, a number of catalytic devices are required. Secondary systems are required to ensure the ATS works as intended. These include: control of exhaust gas composition through control of exhaust stoichiometry or supply of additional reactants not normally found in exhaust gas or not present in sufficient quantity (e.g., urea, additional HCs, additional air or O_2), thermal management to ensure the catalysts operate within the required temperature window, systems to ensure contaminants and pollutants that might accumulate are removed (regeneration of filters, sulfur management, urea deposits,) and systems to minimize the formation of secondary pollutants such as the ammonia slip catalyst (ASC).

It would be a mistake to consider the combustion system and the ATS as separate systems. In order to maximize their effectiveness, a high degree of integration is required. A classic example is air-to-fuel ratio (AFR) in SI engines where a very high level of control precision is required to ensure the TWC performance is maximized. Thermal management of the ATS can be carried out by adjustments within the engine to affect the temperature of the exhaust gas leaving the cylinder. In some cases, additional fuel required by the ATS (e.g., for thermal management) can be supplied by the engine's fuel injectors.

It is important to realize that the objective of engine optimization is not to minimize the pollutant emissions from the combustion system or maximize the reduction of pollutants in the ATS. Rather the objective is to achieve a target level of emissions from the entire system. The target is generally sufficiently below the regulatory limit to allow for production variability. Doing so may require the emission of some pollutants from the combustion system to increase if ATS

performance is sufficiently high to still allow design target to be met. For example, NO_x emissions from engines equipped with a urea-SCR catalyst can be allowed to increase to minimize GHG emissions (due to the NO_x-BSFC trade-off) if high NO_x conversion in the SCR catalyst is achieved.

Fuels and lubricants are an important “partner” in the combined engine and aftertreatment system. Low emissions over the life of the engine would not be possible unless fuel contaminants such as sulfur and some inorganic minerals are controlled to very low levels.

The above technologies, discussed further in the following sections, are applicable to new (OEM) internal combustion engines. Some of these technologies may also be used to reduce emissions and/or improve efficiency of existing, in-use engines. There is also a group of technologies developed specifically for in-use applications, that are normally not used in new engines.

The content of CO and C_xH_y ingredients in the exhaust gases of aircraft engines is caused by incomplete combustion of fuel in the engine that depends on the characteristics of the combustion chamber of its combustion chamber (the value of the coefficient of completeness of combustion ξ) and the mode of operation of the engine. The maximum completeness of combustion in the engine takes place in the calculation mode - take-off (maximum thrust mode). In this mode, modern engines have $\xi = 0.97 \dots 0.99$. In all flight modes, the value is lower, i.e. the combustion completeness is less than $\xi = 0.75 \dots 0.85$, more products of incomplete combustion (CO and C_xH_y and others) are emitted into the atmosphere, and air pollution from extends. The content of the ingredient NO_x in the exhaust gases of the engine depends on the value of the mixture temperature in the combustion chamber (the higher the NO_x is formed), and the maximum (up to 2500 - 3000 K) on take-off, and the time of alternation of the mixture in the combustion chamber (than it the more NO_x is formed), and this occurs at low airspeeds. That is, the maximum output of NO_x takes place on the engine take-off mode and modes close to it, during the take-off of the aircraft and at climb. Obviously, in the area of the airport, the emission of an aircraft engine depends on

the mode of its operation and the duration of operation in this mode. Under the area of the airport we mean space limited by the height of 1000 m and the size of the airport. $R^* = R/R_0$, where R is the thrust of the engine at a given mode; R_0 - engine thrust on takeoff mode. The longest and most environmentally hazardous mode is the low gas mode. The total thrust in this mode for modern aircraft engines is 3 ... 9% from its maximum value R_0 . This mode is used for taxiing before take-off and after landing, as well as during engine warm-up during start-up. The duration of taxiing depends from the size of the airport, time of departure and arrival, intensity flights and meteo conditions. The ICAO Aircraft Engine Emissions Databank contains information on exhaust emissions of production aircraft engines, measured according to the procedures in ICAO Annex 16, Volume II, and where noted, certified by the States of Design of the engines according to their national regulations. The databank covers engine types which emissions are regulated, namely turbojet and turbofan engines with a static thrust greater than 26.7 kilonewtons. The information is provided by the engine manufacturers, who are solely responsible for its accuracy. The European Aviation Safety Agency (EASA) is hosting the databank on behalf of ICAO and is not responsible for the contents.[35]

Engine manufacturers submit their data to the primary certifying authority (CA) for approval as part of the certification process. Once the data has been approved by the primary CA, manufacturers can voluntarily submit it to EASA for inclusion in the ICAO Engine Emissions Databank. The data must be submitted in a predefined format (see Excel data template in below Downloads section). The primary CA verifies that the data submitted to the databank is in conformity with the approved data from certification. EASA then checks the data format and consistency before publishing it. The frequency of databank updates depends on the availability of new data but is aimed to be at least once a year.

4.5 ICAO CO₂ certification requirement

In February 2013, ICAO's environmental committee finalized a CO₂ certification requirement to serve as the basis for a global CO₂ (efficiency) standard for new aircraft. Under the requirement, the CO₂ intensity of new aircraft will be evaluated at three steady-state cruise test points, with aircraft required to meet efficiency targets set as a function of their maximum take-off mass (MTOM) after correcting for the floor area of the aircraft.

This approach is expected to rank the CO₂ intensity of new commercial aircraft in proportion to emissions per seat kilometer flown, can be used to set a standard via a single continuous line, and should be inexpensive for manufacturers to certify as it is patterned on existing data gathering practices. Disadvantages of the procedure include its failure to measure non-cruise fuel burn, the use of flight conditions unrepresentative of day-to-day operations, providing no direct crediting for lightweight materials, and uncertainty about whether some future technologies to reduce fuel burn will be accurately characterized under the procedure.

Following three years of work, the International Civil Aviation Organization's (ICAO) Committee for Environmental Protection (CAEP) finalized a carbon dioxide (CO₂) certification requirement, including metrics, fuel efficiency test points, and detailed certification procedures, to be added as a new volume to Annex 16 of ICAO's Convention on International Civil Aviation. The certification procedure describes how manufacturers should measure and report the CO₂ intensity of new aircraft to certifying authorities, and will serve as the basis for a global CO₂ (efficiency) standard for new aircraft when finalized. The bulk of work on the certification requirement was devoted to developing a suitable metric system for the standard.[35]

Salient features of that system include:

1. A metric of $1/[SAR]$, divided by a proxy of aircraft floor area raised to an exponent of 0.24, by which CO₂ emissions intensity will be reported.

2. A scaling factor of maximum take-off mass (MTOM) to assign regulatory targets to individual aircraft types.

3. Three equally weighted steady-state test points, representing high, medium, and low gross weights, at which the efficiency of each aircraft type will be evaluated. ICAO's CO₂ certification requirement has certain merits. As noted above, the metric system is capable of distinguishing different aircraft technology levels, and is expected to rank the efficiency of commercial aircraft, which are responsible for the vast majority of civil aviation fuel use and CO₂ emissions, in rough proportion to emissions per seat kilometer flown. This is important because the latter quantity is not certifiable since the number of seats on a given aircraft is determined by an airline, not the manufacturers.

The metric system can be used to set a CO₂ standard via a single continuous line, reducing the opportunity for gaming through means such as corner effects or reclassifying a given aircraft as a different type in order to gain access to a weaker standard. Finally, it should be inexpensive for manufacturers to certify their aircraft to the standard because the certification requirement is built upon industry practices already used by manufacturers to collect fuel burn data for airlines.

The metric system displays certain shortcomings, notably:

1. Failure to measure non-cruise fuel burn: since SAR does not directly measure fuel consumed in non-cruise flight segments – landing and take-off, taxi, climb and descent – technologies such as electric taxi or more efficient auxiliary power units that reduce fuel burn on those flight segments will not be promoted by the standard.

2. Unrepresentative of day-to-day operations: Aircraft are typically operated at off-optimal flight conditions, meaning that the fuel efficiency test points identified above are not representative of typical operations, particularly for service ceiling limited aircraft such as turboprops and some regional jets. This divergence of test conditions from real operations means that improvements measured on the metric may not necessarily translate to real emission reductions in-service.

3. No direct crediting of lightweight materials: since the empty weight of the aircraft is never defined in the certification requirement, ICAO’s CO2 standard will provide only limited, indirect incentives for technologies to reduce aircraft weight, notably lightweight composites.

4. Concerns about “futureproofing”: The RGF factor, which helps normalize efficiency scores across various aircraft types, was developed based upon empirical comparisons between today’s business jets, turboprops, and turbofan aircraft, not an assessment of future technologies. It unclear whether this metric system will be appropriate for future aircraft with radically different engine or airframe architectures, including open rotor engines and, more speculatively, blended wing body configurations.

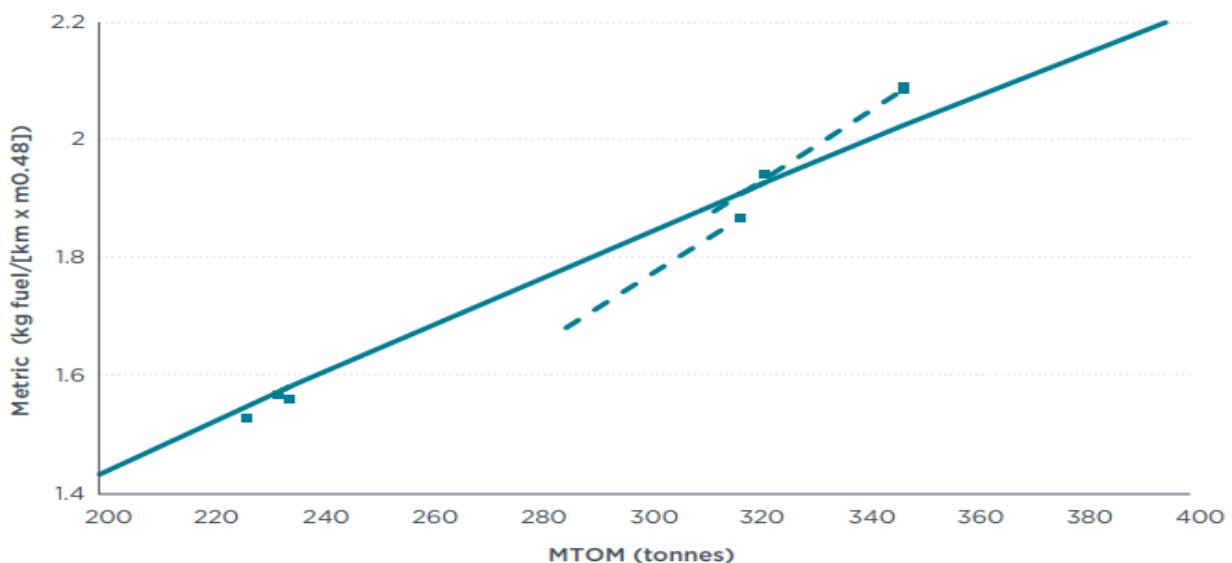


Figure 4.1 – MTOM “paper” changes under a CO2 standard

For this reason, it will be possible for manufacturers to make aircraft comply with the CO2 standard without incremental investments in fuel efficiency technology by lowering the range of MTOMs at which they are marketed. These lower paper MTOM variants, while nominally complying with the standard, will have identical emissions to higher, non-compliant MTOM variants when used in service. As a rule of thumb, a 5% paper MTOM reduction, which would have

marginal impacts on revenue and aircraft values, should provide an additional 1.5% margin to a standard.

4.6 Emissions trading system

Effectively addressing the impact of aviation on climate change may prove a major challenge for policymakers. The European Union Emissions Trading Scheme (EU ETS) is one of the main instruments used to reach the statutory reduction of greenhouse gas emissions. This paper examines policy issues regarding the implementation of the EU ETS in aviation. A two-round Delphi study was undertaken based on a sample of 31 experts from Airlines and the International Air Transport Association; Air Navigation Service Providers; Civil Aviation Authorities; Government Institutions; and informed individuals (consultants and academics). The different allocation methods of allowances; the linking of EU ETS to similar schemes in other countries/continents; and the interconnection of the scheme with related environmental policies in Europe are found to significantly affect the efficiency of the EU ETS. Simpler monitoring, reporting and verification processes; streamlining and increased transparency of the auctions and penalties revenue policy; and achievement of balance in the allowance market are recommended to rectify caveats of the EU ETS from a policy perspective. Aviation was brought into the EU's emission trading system (ETS) in 2012, covering all flights to and from EU airports. Following significant international and industry pressure, the scope was reduced to cover intra-EU flights only (known as "stop the clock"). This was ostensibly to give time for the UN agency which regulates aviation, ICAO, to agree a global measure. A second stop-the-clock regulation to extend the reduced scope was agreed in 2014 to afford ICAO more time. At its 2016 triennial assembly, ICAO adopted the outline of a global offsetting scheme known as Corsia. However the environmental integrity of that scheme remains unknown, and T&E is among those who have severe doubts as to its potential effectiveness. As a result, the exemption of flights to and from Europe was extended only until 2024, by which time regulators in Europe will

have a better understanding of how Corsia will operate. Each year, polluters have to surrender a number of permits equivalent to the amount of CO₂ they emitted in the preceding year. Polluters acquire permits through an annual allocation system and some are issued by member states for free. If polluters don't have enough allowances to acquit their previous year's emissions, they can buy additional permits at auction or from other companies having a surplus. The EU puts a maximum cap on the CO₂ emissions that can be emitted by restricting the number of permits available on the market. As issued permits become scarcer due to progressive reductions in the cap, the permit price goes up, providing emitters with an incentive to reduce their emissions where that is cheaper than buying permits.

Aviation was incorporated in the EU ETS, effective as of 1 January 2012, and required all airlines departing or arriving at an EU airport to surrender allowances covering the emissions of all EU flights they had operated in a given year. Following an international outcry orchestrated by US carriers against the inclusion of foreign carriers in the scheme, the European Commission limited the scheme's application to airlines operating flights in and between EU airports only ("stop-the-clock"). This was billed as a temporary measure to give ICAO time to agree a global measure. When minimal progress was made at ICAO's 38th assembly in October 2013, the clock was stopped again. After reviewing the 2016 ICAO outcome, when a global market-based measure was agreed, the Commission proposed to extend the exemption indefinitely pending a review of the effectiveness of the Corsia. The co-legislative process eventually settled on an extension to 2024, when further details about Corsia will be known. Not at present. Until recently the ETS suffered from a gross over-allocation of permits, causing the price of allowances to crash. This gave airlines effectively unlimited access to cheap ETS credits, the cost of which hardly impacted on growth in any way. However, reforms of the ETS in late 2017 resolved some of these issues, and saw prices almost treble in the space of a few months. They're still short of the price level needed to drive significant reductions, so further reforms are needed.

Conclusion to part 4

In this section of the master's thesis:

- reviewed regulatory documents that regulate environmental protection during aircraft operation;
- analysis of harmful factors during operation and maintenance of the aircraft engines;
- Measures have been developed to protect the environment during operation and maintenance of the aircraft engines thereby we took in consideration the materials that should be used to reduce excessive aircraft emissions.

5 LABOR PROTECTION

Transport category aircraft are used for transporting passengers and freight in the commercial airline/airfreight industry. Both the manufacturing and maintenance process involve operations that remove, fabricate, alter and/or install components all over the aircraft itself. These aircraft vary in size but some (e.g., Boeing 747, Airbus A340) are among the largest aircraft in the world. Due to the size of the aircraft, certain operations require personnel to work while elevated above the floor or ground surface. There are many potential fall situations within both aircraft manufacturing and maintenance operations throughout the air transport industry. While each situation is unique and may require a different solution for protection, the preferred method of fall protection is by preventing falls through an aggressive plan for hazard identification and control. Effective fall protection involves an institutional commitment addressing every aspect of hazard identification and control. Each operator must continually evaluate its operation for specific fall exposures and develop a protection plan comprehensive enough to address each exposure throughout their operation.[36]

5.1 Analysis of harmful and dangerous production factors

Dangerous factor of production — a factor of production, the action of which on the worker in certain conditions leads to injury or other sudden sharp deterioration of health. Harmful factor of production — a factor of production, the effect of which on the worker in certain conditions leads to disease or reduced efficiency. In accordance with ДНАОП .1.30-1.06-98 and ГОСТ 12.0.003-74 "Dangerous and harmful production factors" [36] at the facility, the following unsafe and harmful factors are possible:

- unprotected moving elements of GTE, lifting mechanisms and production equipment;
- vehicles for delivery of equipment units;
- increased slipperiness (due to ice, wetting and oiling of the installation surface);
- increased vibration level;

- increased level of infrared radiation from the heated parts of the drive
- increased noise level (reduces productivity, quickly causes fatigue, may be the result of occupational diseases);
- increased level of ultraviolet and thermal radiation;
 - increased dust and gassiness in the GTE area;
- increased or decreased surface temperature of GTE equipment and materials;
 - dangerous voltage level in the electrical network
 - physical overload (static and dynamic);
- neuropsychological (emotional).

Chemical hazardous and harmful production factors:

- by the nature of the action on the human body
 - general toxic and irritating;
- by penetration into the human body - penetrating through the respiratory system, gastrointestinal tract, skin and mucous membranes

5.1.1 Construction Materials

Aircraft engines are primarily constructed of metallic components, although recent years have seen the introduction of plastic composites for certain parts. Various aluminium and titanium alloys are used where strength and light weight are of primary importance (structural components, compressor sections, engine frames). Chromium, nickel and cobalt alloys are used where resistance to high temperature and corrosion are required (combustor and turbine sections). Numerous steel alloys are used in intermediate locations.

Since weight minimization on aircraft is a critical factor in reducing life-cycle costs (maximizing payload, minimizing fuel consumption), advanced composite materials have recently been introduced as light-weight replacements for aluminium, titanium and some steel alloys in structural parts and ductwork where high temperatures are not experienced. These composites consist primarily of polyimide, epoxy and other resin systems, reinforced with woven fibreglass or graphite fibers.

5.1.2 Manufacturing Operations

Virtually every common metalworking and machining operation is used in aircraft engine manufacture. This includes hot forging (airfoils, compressor disks), casting (structural components, engine frames), grinding, broaching, turning, drilling, milling, shearing, sawing, threading, welding, brazing and others. Associated processes involve metal finishing (anodizing, chromatin and so on), electroplating, heat-treating and thermal (plasma, flame) spraying. The high strength and hardness of the alloys used, combined with their complex shapes and precision tolerances; necessitate more challenging and rigorous machining requirements than other industries.

Some of the more unique metalworking processes include chemical and electrochemical milling, electro-discharge machining, laser drilling and electron-beam welding. Chemical and electrochemical milling involve the removal of metal from large surfaces in a manner, which retains or creates a contour. The parts, depending upon their specific alloy, are placed in a highly concentrated controlled acid, caustic or electrolyte bath. Metal is removed by the chemical or electrochemical action. Chemical milling is often used after forging of airfoils to bring wall thicknesses into specification while maintaining the contour.

Electro-discharge machining and laser drilling are typically used for making small-diameter holes and intricate contours in hard metals. Many such holes are required in combustor and turbine components for cooling purposes. Metal removal is accomplished by high-frequency thermo-mechanical action of electro-spark discharges. The process is carried out in a dielectric mineral oil bath. The electrode serves as the reverse image of the desired cut.

Electron-beam welding is used to join parts where deep weld penetration is required in hard-to-reach geometries. The weld is generated by a focused, accelerated beam of electrons within a vacuum chamber. The kinetic energy of the electrons striking the work-piece is transformed into heat for welding.

Labour safety as a branch of practical activity is aimed at creating safe and harmless working conditions. Providing safe and harmless conditions in the workplace requires considerable investments, implementation of knowledge and making scientific research in the field of labour precaution. Therefore, the role of knowledge on labour precaution for engineers and technical workers is of great importance.

Legislation of Ukraine on labour precaution is a system of interrelated normative legal acts regulating relations in the field of implementation of the state policy on measures and means to preserve the health and human efficiency in the workplace. It consists of the Law “On Protection of Labour”, Labour Code of Ukraine, Law “On compulsory state social insurance against accidents at work and occupational diseases that caused disability”, Law "On sanitary and epidemiological welfare", Code of Civil Protection of Ukraine, Law of Ukraine “Human protection against ionizing radiation”, Norms of Radiation Safety of Ukraine (OCHY-2005). As for aviation, it’s also necessary to consider Air Code of Ukraine and Labour safety rules for maintenance and operation repair of aviation equipment.

Ukrainian legislation on labour precaution is based on the constitutional right of all citizens of Ukraine to proper, safe and healthy working conditions, guaranteed by Article 43 of the Constitution of Ukraine. This article also establishes prohibition of employment of women and juveniles in hazardous works for their health. Art. 45 of the Constitution guarantees the right of all workers to a weekly rest and annual paid leave, as well as establishing shorter working day for certain professions and industries, and reduced working hours at night. According to Article 46 citizens have the right to social security, including the right to security in cases of complete, partial or temporary disability, widowhood, unemployment due to circumstances beyond their control, and in old age and in other cases stipulated by law.

The fundamental document in the field of labour precaution is Law of Ukraine "On Protection of Labour", which defines the basic provisions for the implementation of the constitutional right of workers to protection of their life and health in the workplace, to proper, safe and healthy working conditions, regulates with the participation of relevant state authorities relationship between employer and employee on issues of security, health and environment and establishes a uniform procedure of organizing labor precaution in Ukraine. Other regulations must conform not only to the Constitution and other laws of Ukraine, but, above all, this law.

5.2 Development of measures for safety

Health hazards associated with aircraft engine manufacture are primarily related to the toxicity of the materials used and their potential for exposure. Aluminium, titanium and iron are not considered significantly toxic, while chromium, nickel and cobalt are more problematic. Certain compounds and valence states of the latter three metals have indicated carcinogenic properties in humans and animals. Their metallic forms are generally not considered as toxic as their ionic forms, typically found in metal finishing baths and paint pigments.

In conventional machining, most operations are performed using coolants or cutting fluids which minimize the generation of airborne dust and fumes. With the exception of dry grinding, the metals usually do not present inhalation hazards, although there is concern about the inhalation of coolant mists. A fair amount of grinding is performed, particularly on jet engine parts, to blend contours and bring airfoils into their final dimensions. Small, hand-held grinders are typically used. Where such grinding is performed on chromium-, nickel- or cobalt-based alloys, local ventilation is required. This includes down-draft tables and self-ventilating grinders. Dermatitis and noise are additional health hazards associated with conventional machining. Employees will have varying degrees of skin contact with coolants and cutting fluids in the course of fixing, inspecting and removing parts. Repeated skin contact may manifest itself in various forms of dermatitis in some

employees. Generally, protective gloves, barrier creams and proper hygiene will minimize such cases. High noise levels are often present when machining thin-walled, high-strength alloys, due to tool chatter and part vibration. This can be controlled to an extent through more rigid tooling, dampening materials, modifying machining parameters and maintaining sharp tools. Otherwise, PPE (e.g., ear muffs, plugs) is required.

Safety hazards associated with conventional machining operations mainly involve potential for physical injuries due to the point-of-operation, fixing and power transmission drive movements. Control is accomplished through such methods as fixed guards, interlocked access doors, light curtains, pressure-sensitive mats and employee training and awareness. Eye protection should always be used around machining operations for protection from flying chips, particles and splashes of coolants and cleaning solvents.

Metal-finishing operations, chemical milling, electrochemical milling and electroplating involve open surface tank exposures to concentrated acids, bases and electrolytes. Most of the baths contain high concentrations of dissolved metals. Depending upon bath operating conditions and composition (concentration, temperature, agitation, size), most will require some form of local ventilation to control airborne levels of gases, vapours and mists. Various lateral, slot-type hood designs are commonly used for control. Ventilation designs and operating guidelines for different types of baths are available through technical organizations such as the American Conference of Governmental Industrial Hygienists (ACGIH) and the American National Standards Institute (ANSI). The corrosive nature of these baths dictates the use of eye and skin protection (splash goggles, face shields, gloves, aprons and so on) when working around these tanks. Emergency eyewashes and showers must also be available for immediate use.

Health hazards associated with test operations usually involve radiation (x or gamma rays) from radiographic inspection and noise from final product tests. Radiographic operations should include a comprehensive radiation safety programme, complete with training, badge monitoring and periodic surveys.

Radiographic inspection chambers should be designed with interlocked doors, operating lights, emergency shut-offs and proper shielding. Test areas or cells where assembled products are tested should be acoustically treated, particularly for jet engines. Noise levels at the control consoles should be controlled to below 85 dBA. Provisions should also be made to prevent any build-up of exhaust gases, fuel vapours or solvents in the test area.

The concentration and combinations of chemicals may also be complex and highly variable. Delayed work performed out of normal sequence may result in hazardous materials being used without proper engineering controls or adequate personal protective measures. The variations in work practices between individuals and the size and configuration of different airframes may have a significant impact on exposures. Variations in solvent exposures among individuals performing wing tank cleaning have exceeded two orders of magnitude, due in part to the effects of body size on the flow of dilution air in extremely confined areas.

Potential hazards should be identified and characterized, and necessary controls implemented, before materials or processes enter the workplace. Safe usage standards must also be developed, established and documented with mandatory compliance before work begins. Where information is incomplete, it is appropriate to assume the highest reasonably expected risk and to provide appropriate protective measures. Industrial hygiene surveys should be performed at regular and frequent intervals to ensure that controls are adequate and working reliably.

Table 5.1 - Technological development requirements for health, safety and environmental control for new processes and materials.

Parameter	Technological requirement
Airborne levels of contaminants	Analytical methods for chemical quantification Air monitoring techniques
Potential health impact	Acute and chronic toxicology studies
Environmental fate	Bioaccumulation and biodegradation studies
Waste characterization	Chemical compatibility test Bioassays

The difficulty of characterizing aerospace workplace exposures necessitates close cooperation between hygienists, clinicians, toxicologists and epidemiologists. The presence of a very well informed workforce and management cadre is also essential. Worker reporting of symptoms should be encouraged, and supervisors should be trained to be alert to signs and symptoms of exposure. Biological exposure monitoring may serve as an important supplement to air monitoring where exposures are highly variable or where dermal exposure may be significant. Biological monitoring can also be used to determine whether controls are effective in reducing employee uptake of contaminants. Analysis of medical data for patterns of signs, symptoms and complaints should be performed routinely.

Paint hangars, aircraft fuselages and fuel tanks may be served by very high volume exhaust systems during intensive painting, sealing and cleaning operations. Residual exposures and the inability of these systems to direct air flow away from workers usually require the supplemental use of respirators. Local exhaust ventilation is required for smaller painting, metal treating and solvent cleaning operations, for laboratory chemical work and for some plastics lay-up work. Dilution ventilation is usually adequate only in areas with minimal chemical usage or as a supplement to local exhaust ventilation. Significant air exchanges during winter can result in excessively dry interior air. Poorly designed exhaust systems which direct excessive cool air flow over workers' hands or backs in small parts assembly areas may worsen hand, arm and neck problems. In large, complex manufacturing areas, attention must be paid to properly locating ventilation exhaust and intake points to avoid re-entraining contaminants.

Precision manufacturing of aerospace products requires clear, organized and well controlled work environments. Containers, barrels and tanks containing chemicals must be labelled as to the potential hazards of the materials. First aid information must be readily available. Emergency response and spill control information also must be available on the MSDS or similar data sheet. Hazardous work areas must be placarded and access controlled and verified.

5.3 Fire safety

5.3.2 Engine Fire Detection

Detection is achieved by means of linear pneumatic sensing systems, often referred to as fire loops, which are gas filled pipes routed around potentially abnormal heat sources. If the temperature in the vicinity of the sensing element rises, the electrical resistance of the core material decreases and a warning indication can be triggered. They are duplicated to allow for continued detection if a single loop in the system becomes faulty. An open loop due to a short circuit fault will be detectable during daily pre flight testing or by annunciation of a fault in service. Physical damage to a loop such as a 'pinching' may lead to a false fire warning but would also produce an independent fault annunciation. The same principles apply to the protection of APUs.

5.3.3 Engine Fire Extinguishing

On modern commercial passenger jet aircraft, engine compartments are usually divided into two zones '1' and '2' for the purposes of fire protection. Two electrically operated extinguishers containing Halon 1301 or in newer aircraft, HFCs (Hydrofluorocompounds), are available to each engine.

These are sometimes installed in the nose cowling of each nacelle but may also be located within the fuselage and "shared" by the engines of a twin engine aircraft or be located in a dry bay in the wing and be "shared" by the engines on that wing of a multiengine aircraft. When activated, the contents of the extinguisher bottle are discharged into engine Zone 1, the engine fan assembly. Fires in Zone 2, the engine core, are extinguished by shutting down the engine. The flight crew engine fire drill includes shutting off the fuel and hydraulic fluid supplies to the engine concerned and the supply of oil, the other potentially readily-inflammable substance, is rapidly diminished since it is an isolated supply in each engine/APU.

Activation of engine fire bottles is normally also advised as a precautionary measure whenever an engine shutdown drill is carried out because of severe damage.

APU Fire extinguishers are activated by the flight crew in the same way as engine extinguishers - by manual selection upon receipt of a fire warning - when airborne, but automatically, and with accompanying automatic APU shutdown, in the case of fire detection during ground running.

If indications are available that an airborne engine or APU fire has been extinguished successfully, then the fire occurrence itself does not then influence the flight crew decision on how urgent it is to land the aircraft. However, in a twin engine aircraft, the shutdown of an engine will usually result in landing as soon as practical. Experience has shown that in certain circumstances, continued indications of engine fire may be presented after engine shutdown and the discharge of both bottles has resulted in the complete cessation of fire. If this occurs, then the flight crew cannot be absolutely sure that their action has fully extinguished the fire and are prudent to decide to 'land as soon as possible'.

5.4 Typical calculation or safety issue detail

Aircraft maintenance work includes inspection and repair of aircraft structures, coatings, and systems in hangars and on the air field. Good training and work practices ensure aircraft and worker safety.

Tall, heavy aircraft make it hard to see people on the ground when maneuvering in the hangar or maintenance area. Watch and communicate with the aircraft operator to avoid caught/crush accidents (getting run over by a tire or colliding with a wing or tail). Never enter the ramp or flightline without permission from the air field controller.

Work at a steady pace. Rushing your work increases aircraft turnaround and accidents. To avoid a fall, watch for ground lines to the aircraft. Well-lit work areas are safer. Watch sharp leading edges like wing tips and pointy antennas, probes, and "Remove Before Flight" flags that stick out from the aircraft. Colliding with hard, sharp surfaces or protrusions causes bumps, bruises, and cuts.

Stay inside painted hazard lines and keep clear of aircraft “prop arcs.” Contact with a propeller, rotor, or exposed rotating part can cause severe injuries. Keep hair tied back and avoid loose clothing and jewelry to prevent entanglement with moving parts. Don’t lean on or place your hands or feet near engine intake areas. Keep tools away and pick up debris near the engine. If an engine starts, you could be severely injured, or small items could be turned into projectiles.

Tall aircraft require ladders, platforms, and scaffolds to reach work areas. Follow ladder safety guidelines. Use a fall protection harness where required. You may need to work in cramped quarters while performing aircraft maintenance. Evaluate aircraft access areas and job tasks with limited egress and follow confined space procedures if needed.

Aircraft chemicals include lubricants, fuels, coating strippers, paints, and solvents. These can be concentrated and contain hazardous materials; use material safety data sheets (MSDS). MSDS explain how to handle chemicals, proper storage and disposal, and the required personal protective equipment (PPE) for safe work. Do not smoke around aircraft maintenance areas where chemicals and fuels are flammable.

Fabrication and repair work requires tools such as welding torches, drills, rivets, or grinders. Properly maintain your tools and follow safety procedures. When moving large, bulky aircraft parts and materials, use assistive devices or get help to make the lift safe. Use good ergonomic practices such as frequent 30-second micro-breaks and job task rotation to prevent fatigue and injury.

PPE varies with the job task. Bump caps protect you from an accidental collision with an aircraft part. Hard hats protect you from falling objects. Safety glasses, a face shield, and goggles protect your face and eyes, depending on the task and materials. Coveralls and rubber gloves and boots protect your hands and feet from chemicals. Sturdy work gloves protect your hands from cuts and scrapes while steel-toe work boots with non-slip soles protect your toes and decrease the chance of falls. Wear adequate hearing protection (ear plugs, muffs, etc.) to protect

you from aircraft noise. A respirator may be needed to control dusts from grinding and sanding operations.

5.4.1 Calculation of ventilation equipment for explosion hazard

An emergency ventilation system is provided in the production room, where a large amount of explosive substance may suddenly enter the air. This danger is posed by GPA in engine rooms. Table 5.2 shows the volume fractions of combustible components of natural gas.

The initial data for the calculation of emergency ventilation are:

Table 5.2 - Volume fractions of natural gas components

№	Component composition of gas	Volume fractions of components
1	CH ₄	95,26
2	C ₂ H ₄	1,123
3	C ₃ H ₈	0,986
4	C ₄ H ₁₀	0,121
5	C ₅ H ₁₂	0,017

Determine the lower explosive limit according to the shape of the Leshatelier volume composition of the gas:

$$L_{H.B} = \frac{100}{\sum_{i=1}^n \frac{r_i}{L_i^{H.B}}},$$

where n - number of components of natural gas;

r_i – volume fraction of the i-th component;

$L_i^{H.B}$ – the lower limit of explosiveness of the i-th component of the mixture with air.

$$L_{H.B} = \frac{100}{\frac{95,26}{5,3} + \frac{1,123}{3} + \frac{0,986}{2,2} + \frac{0,121}{1,9} + \frac{0,017}{1,3}} = 5,299 \text{ \%}.$$

Emergency ventilation is activated automatically when the concentration of explosive mixture in the room reaches 15% of the lower explosive limit, $5,299 \cdot 0,85 = 4,504$ %.

Based on the data obtained, choose the type of fan.

Fan performance can be calculated by the following formula:

$$L = n \cdot V_{np}, \text{ where:}$$

n – multiplicity of air exchange

V_{np} – volume of the room

The volume of the room is determined by the following formula:

$$V_{np} = (1 - 0,3) \cdot V_{ГМА}, \text{ where:}$$

$V_{ГМК}$ – volume of hole $543,9 \text{ m}^3$

$$V_{ГМК} = a \cdot b \cdot c$$

$$V_{ГМК} = 9,2 \cdot 8,1 \cdot 7,3 = 543,9 \text{ m}^3$$

$$V_{ПП} = (1 - 0,3) \cdot 543,9 = 380,8 \text{ m}^3$$

Determine the amount of gas emission into the room in the event of failure of one GTE.

The volume of the supercharger is equal $0,2237 \text{ m}^3$

Determine the volume of gas reduced to standard conditions, which is in the supercharger:

$$V = \frac{P_{BC}}{P_{CT}} \cdot \frac{T_{CT}}{T_{BC}} \cdot \frac{1}{z}$$

P_{BC} i T_{BC} – respectively, the pressure and temperature of the gas under suction conditions, for the worst conditions $P_{BC}=3,5 \text{ MPa}$, $T_{BC}=283^0\text{K}$

P_{CT} i T_{CT} respectively gas pressure and temperature under standard conditions: $P_{CT}=101325 \text{ Pa}$, $T_{CT}=293,15 \text{ K}$.

Then the coefficient of compressibility of the gas for suction conditions is equal to:

$$z = 1 - 5,5 \cdot 10^6 \cdot \frac{P_{BC} \cdot \Delta^{1,3}}{T_{BC}^{3,3}}$$

The mass of gas that will enter the room is determined by:

$$M = V \cdot \rho_{CT}$$

So:

$$z = 1 - 5,5 \cdot 10^6 \cdot \frac{3,5 \cdot 0,591^{1,3}}{283^{3,3}} = 0,921$$

$$V = \frac{3,5}{0,101325} \cdot \frac{293,15}{283} \cdot \frac{1}{0,921} = 38,831 \text{ m}^3$$

Check if an explosive mixture has formed:

$$\alpha = \frac{38,831}{380,8} = 10,19\%$$

Conclusion: the concentration of gas in the air exceeds the upper limit of the flash. This situation is dangerous and requires the creation of forced ventilation.

The permissible concentration of natural gas for this room is 5%, ie the allowable volume of gas in the room is:

$$V_{г.доп} = 380,8 \cdot 0,05 = 19,4, \text{ m}^3$$

Assuming that the gas from the GTE is emitted within two minutes, the gas consumption reduced to the flow rate for one hour is equal to:

$$G = \frac{38,831}{120} \cdot 3600 = 1164,9 \frac{\text{m}^3}{\text{ч}}$$

Then the multiplicity of air exchange is defined as:

$$n = \frac{1164,9}{38,831 - 19,4} = 38,59$$

The frequency of air exchange for emergency ventilation is in the range from 20 to 40, we accept n- accepted with a margin, if the time of sudden release is less than two minutes.

Then the required fan performance is determined by the formula:

$$L = 40 \cdot 380,8 = 15231,9 \frac{\text{m}^3}{\text{ч}}$$

According to this productivity we choose the centrifugal fan with productivity limits of $15 \div 23.3$ thousand m³ / hour, in number of 8 pieces.

5.5 The main requirements for compliance with the rules of labor protection during operation of the designed engine

Maintenance of the equipment, including its start, stop and regulatory issues, must be carried out in accordance with the requirements of the technical instructions of the manufacturer. Operation of GTE with the parameters having deviations from the values specified in the operation manual is not allowed.

After installation of the main and auxiliary equipment during commissioning, when the compressor station concentrates construction, installation, operation and commissioning equipment, special attention should be paid to compliance with safety rules. Before supplying gas to the compressor station, all personnel of construction, installation, commissioning and other organizations involved on the site must be instructed in safety, which must be documented.

At installation of GTE it is necessary to pay attention to the following:

- lifting the turbine unit should be performed using a special traverse;
- lifting of other units (suction chamber, oil cooler unit, exhaust device, muffler, etc.) must be performed in accordance with the insurance schemes and in accordance with the recommendations set out in the technical documentation at the GTE.

All leaks and crevices in the joints of the gas turbine units must be eliminated, the lids of the oil tanks must be installed tightly. On the non-functioning unit of the blinds of the air cleaning device, the air intake compartment of the engine must be closed, the inlet diffusers of the fans of the oil cooler unit are covered.

Operating personnel who have undergone special training, passed exams and are admitted to their maintenance and operation in accordance with the established procedure are allowed to operate and repair gas turbine units.

Before starting the gas turbine, it is necessary to make sure that the sound signal is triggered by pressing the "Start" button. Starting of the unit without

protections and covers on rotating details and on the knots which are at height no more than 2 m from floor level (fans of the block of cooling of oil, the coupling of starting pumps) or their removal during unit operation is not allowed.

During operation of GTE it is forbidden:

- enter the engine compartment when starting and running the engine;
- perform work on the engine when the gas turbine system is under current;
- perform work in the suction chamber and exhaust shaft of the unit during start-up or during engine operation;
- work with open doors of the engine compartment, supercharger and suction chamber.

The air in the oil tank should be checked daily for the content of flammable gases in it with an entry in the log. When the content of flammable gases in the oil tank of the unit is more than 1%, work is not allowed.

It is not allowed for the service personnel to be near the working unit without personal protective equipment against noise, for more than one hour during one work shift.

The permissible vibration level of the gas turbine, measured by standard equipment, should not exceed 30 mm / s.

Emergency shutdown of the unit must be performed in the following cases:

- when the safety of service personnel is threatened;
- at breakdown of the unit;
- with the appearance of metal knocks and shocks;
- severe oil or gas losses;
- ignition of oil or gas;
- surge phenomena in the unit.

All engine adjustment work can only be performed when unit stopped. Regular and repair work on the engine should be performed only after cooling of its external surfaces to a temperature of 45⁰C. During the assembly and

disassembly of the unit it is necessary to use serviceable special tools and devices that ensure safe work.

It is forbidden:

- use faulty lifting mechanisms and devices for lifting the engine, supercharger cover, rotor and other prefabricated units of the unit;
- leave the parts suspended on the lifting gear;
- operate lifting mechanisms at temperatures below - 20 °C.

Lifting mechanisms that work in pairs should be loaded evenly to avoid breakage and injury to personnel.

When decontaminating and washing parts, fire-safe technical detergents should be used.

It is forbidden to store kerosene, gasoline and other flammable materials in the shelters of the GTU or near them.

Operation of the fire extinguishing system is inadmissible if the service life of cylinders has expired, and also the defects excluding a guarantee of safe work of installation are revealed. It is forbidden to transport the installation in the presence of extinguishing agent in cylinders. It is allowed to enter the compartments of the engine and supercharger after the operation of the fire extinguishing system without a gas mask only after thorough ventilation and sampling of gassiness in the room.

To determine the content of harmful substances in the air of the working area should be performed control measurements by sampling at least once a year.

Conclusion to part 5

Maintenance hangars perform highly specialized, mission-critical functions, so fire detection and suppression technologies need to keep pace with MROs' constantly evolving protection needs. This includes enhancing heat and smoke detection systems with optical flame detection capabilities, using 3-D mapping and analysis to validate optical flame detector placement and positioning, and employing the most up-to-date commissioning tools such as jet fuel fire simulation for proving detector performance. Providing fire protection for MRO facilities is certainly a task for the industry's experts, but knowing what is available for aircraft hangar fire protection is a critical aspect of every MRO facility manager's job. The above evaluations and/or recommendations are for general guidance only and should not be relied upon for legal compliance purposes. They are based solely on the information provided to us and relate only to those conditions specifically discussed. We do not make any warranty, expressed or implied, that your workplace is safe or healthful or that it complies with all laws, regulations or standards.

General conclusions and recommendation

In this work the features of application of gas turbine engines, their "weak" places, prototype D 436, and also methods of increase of their durability and efficiency were considered. Actuality and perspectivity of the research related to the GTS are confirmed. . As a promising object, from the point of view of increasing the operation of the parameters, turbine blades were selected. Ways of protection of blades from high-temperature influence were considered. A similar goal can be achieved by using protective coatings or by using constructive measures aimed at increasing operational parameters, in particular durability.

A general static calculation of the blade of the GTE has been performed to analyze the "weak" places of the shoulder blade and the forces that affect it.

Thus, in the process of working on a three-cavity cooling scheme, the following tasks were solved:

- ensuring the required flow rate and pressure drop in the last row on the back of the blade;
- determination of the place of the maximum efficiency of the film, determination of the ratio of the air consumption going to the film and for convective cooling of the back;
- ensuring a guaranteed drop at the leading edge at all engine operating modes;
- determination of the ratio of the pressure drops realized on the deflector and on the blade wall in order to obtain the most efficient cooling scheme of the leading edge;
- ensuring the permissible temperature on the trough of the blade at minimization of air consumption for cooling the trough (optimization of convective-film cooling of the trough by choosing the optimal pitches of holes in the rows of perforations);
- ensuring the rigidity of the back of the scapula by adding an additional bridge.

Currently, blades with a three-cavity cooling scheme are being run-in on ground gas turbine plants and on full-size aircraft engines in bench conditions

REFERENCES

1. Sendyurev S.I., Tikhonov A.S., KHayrulin V.T., Samokhvalov N.Yu. *Sovremennyye sistemy okhlazhdeniya soplovykh lopatok vysokonagruzhennykh gazovykh turbin* [Present-day Systems of High Load Gas Turbine Vanes Cooling]. PNRPU Aerospace Engineering Bulletin, 2015, № 42.
2. Inozemtsev A.A., Nikhamkin M.A., Sandratskiy V.L. *Osnovy konstruirovaniya aviatsionnykh dvigateley i energeticheskikh ustanovok* [Fundamentals of Aircraft Engines and Power Generation Gas Turbines Design: handbook]. Moscow, Mashinostroenie, 2008, Vol. 2, 368 p.
3. Уланов, А. М. Динамика и прочность авиационных двигателей и энергетических установок. [Электронный ресурс] : электрон, учеб. пособие / А. М. Уланов; Минобрнауки России, Самар. гос. аэрокосм, ун-т им. С. П. Королева (Нац. исслед. ун-т). – Электрон
4. Бондалетова Л.И. Полимерные композиционные материалы (часть 1): учебное пособие / Л.И. Бондалетова, В.Г. Бондалетов. – Томск: Изд-во Томского политехнического университета, 2013. – 118 с.
5. Неметаллические композиционные материалы в элементах конструкций и производства газотурбинных двигателей: Учеб. пособие для вузов / Ю.С. Елисеев, В.В. Крымов, С.А. Колесников, Ю.Н. Васильев. – М.: Изд-во МГТУ им. Н.Э. Батмана. 2007. – 368 с.
6. Ceramic Matrix Composites: Fibre Reinforced Ceramics and their Applications. Walter Krenkel (Editor). ISBN: 978-3-527-62240-5 September 2008 440 Pages
7. Zoli, L.; Sciti, D. (2017). "Efficacy of a ZrB_2 –SiC matrix in protecting C fibres from oxidation in novel UHTCMC materials". *Materials & Design*. 113: 207–213. doi:10.1016/j.matdes.2016.09.104.
8. <https://www.grc.nasa.gov/WWW/K-12/airplane/compress.html>
9. Galizia, Pietro; Failla, Simone; Zoli, Luca; Sciti, Diletta (2018). "Tough salami-inspired Cf/ZrB_2 UHTCMCs produced by electrophoretic deposition".

Journal of the European Ceramic Society. 38 (2): 403–409. doi:10.1016/j.jeurceramsoc.2017.09.047.

10. Vinci, Antonio; Zoli, Luca; Sciti, Diletta; Melandri, Cesare; Guicciardi, Stefano (2018). "Understanding the mechanical properties of novel UHTCMCs through random forest and regression tree analysis". *Materials & Design*. 145: 97–107. doi:10.1016/j.matdes.2018.02.061.

11. T. R. Cooke (1991). "Inorganic fibres- A Literature Review". *Journal of the American Ceramic Society*. 74: 2959–2978. doi:10.1111/j1151-2916.1991.tb04289.x (inactive 2019-11-24).

12. K. Kumagawa; H. Yamaoka; M. Shibuysa; T. Ymamura (1998). Fabrication and mechanical properties of new improved Si-M-C-(O) Tyranno fibre. *Ceramic Engineering and Science Proceedings*. 19A. pp. 65–72.

13. N. Miriyala; J. Kimmel; J. Price; H. Eaton; G. Linsey; E. Sun (2002). "The Evaluation of CFCC Liners After Field Testing in a Gas Turbine — III" (PDF). Volume 4: Turbo Expo 2002, Parts A and B. pp. 109–118. doi:10.1115/GT2002-30585. ISBN 978-0-7918-3609-5. Archived from the original (PDF) on 2012-09-25. Retrieved 2011-07-01.

14. K.L. More; P.F. Tortorelli; L.R. Walker; J.B. Kimmel; N. Miriyala; J.R. Price; H.E. Eaton; E. Y. Sun; G.D. Linsey (2002). "Evaluating Environmental Barrier Coatings on Ceramic Matrix Composites After Engine and Laboratory Exposures" (PDF). Volume 4: Turbo Expo 2002, Parts A and B. pp. 155–162. doi:10.1115/GT2002-30630. ISBN 978-0-7918-3609-5. Archived from the original (PDF) on 2012-09-25. Retrieved 2011-07-01.

15. Norris, Guy, Hot blades, *Aviation Week & Space Technology*, April 27-May 10, 2015, p.55.

16. Stephen Trimble (30 May 2017). "After six years, 777X engine starts certification tests". *Flightglobal*.

17. "*c³harme*". www.c3harme.eu.

18. Sciti, Diletta; Silvestroni, Laura; Monteverde, Frédéric; Vinci, Antonio; Zoli, Luca (2018-10-17). "Introduction to H2020 project C3HARME – next

generation ceramic composites for combustion harsh environment and space". *Advances in Applied Ceramics*. 117 (sup1): s70–s75. doi:10.1080/17436753.2018.1509822. ISSN 1743-6753.

19. Sciti, D.; Zoli, L.; Silvestroni, L.; Cecere, A.; Martino, G.D. Di; Savino, R. (2016). "Design, fabrication and high velocity oxy-fuel torch tests of a Cf-ZrB₂ - fibre nozzle to evaluate its potential in rocket motors". *Materials & Design*. 109: 709–717. doi:10.1016/j.matdes.2016.07.090.

20. Mungiguerra, Stefano; Di Martino, Giuseppe D.; Savino, Raffaele; Zoli, Luca; Sciti, Diletta; Lagos, Miguel A. (2018-07-08). "Ultra-High-Temperature Ceramic Matrix Composites in Hybrid Rocket Propulsion Environment". 2018 International Energy Conversion Engineering Conference. Reston, Virginia: American Institute of Aeronautics and Astronautics. doi:10.2514/6.2018-4694. ISBN 9781624105715.

21. Szirczak, D.; Smith, H. (2016). "A review of design issues specific to hypersonic flight vehicles". *Progress in Aerospace Sciences*. 84: 1-28. doi:10.1016/j.paerosci.2016.04.001. hdl:1826/10119.

22. Vinci, Antonio; Zoli, Luca; Sciti, Diletta; Watts, Jeremy; Hilmas, Greg E.; Fahrenholtz, William G. (April 2019). "Mechanical behaviour of carbon fibre reinforced TaC/SiC and ZrC/SiC composites up to 2100 °C". *Journal of the European Ceramic Society*. 39 (4): 780–787. doi:10.1016/j.jeurceramsoc.2018.11.017. ISSN 0955-2219.

23. Mungiguerra, S.; Di Martino, G.D.; Cecere, A.; Savino, R.; Silvestroni, L.; Vinci, A.; Zoli, L.; Sciti, D. (April 2019). "Arc-jet wind tunnel characterization of ultra-high-temperature ceramic matrix composites". *Corrosion Science*. 149: 18–28. doi:10.1016/j.corsci.2018.12.039. ISSN 0010-938X.

24. Zoli, L.; Sciti, D. (2017). "Efficacy of a ZrB₂–SiC matrix in protecting C fibres from oxidation in novel UHTCMC materials". *Materials & Design*. 113: 207–213. doi:10.1016/j.matdes.2016.09.104.

25. Zoli, L.; Vinci, A.; Silvestroni, L.; Sciti, D.; Reece, M.; Grasso, S. (2017). "Rapid spark plasma sintering to produce dense UHTCs reinforced with

undamaged carbon fibres". *Materials & Design*. 130: 1-7. doi:10.1016/j.matdes.2017.05.029.

26. Galizia, Pietro; Failla, Simone; Zoli, Luca; Sciti, Diletta (2018). "Tough salami-inspired Cf/ZrB₂ UHTCMCs produced by electrophoretic deposition". *Journal of the European Ceramic Society*. 38 (2): 403–409. doi:10.1016/j.jeurceramsoc.2017.09.047.

27. Vinci, Antonio; Zoli, Luca; Sciti, Diletta; Melandri, Cesare; Guicciardi, Stefano (2018). "Understanding the mechanical properties of novel UHTCMCs through random forest and regression tree analysis". *Materials & Design*. 145: 97-107. doi:10.1016/j.matdes.2018.02.061.

28. Zoli, L.; Medri, V.; Melandri, C.; Sciti, D. (2015). "Continuous SiC fibres-ZrB₂composites". *Journal of the European Ceramic Society*. 35 (16): 4371-4376. doi:10.1016/j.jeurceramsoc.2015.08.008.

29. Sciti, D.; Murri, A. Natali; Medri, V.; Zoli, L. (2015). "Continuous C fibre composites with a porous ZrB₂ Matrix". *Materials & Design*. 85: 127–134. doi:10.1016/j.matdes.2015.06.136.

30. Sciti, D.; Pienti, L.; Murri, A. Natali; Landi, E.; Medri, V.; Zoli, L. (2014). "From random chopped to oriented continuous SiC fibres–ZrB₂ composites". *Materials & Design*. 63: 464–470. doi:10.1016/j.matdes.2014.06.037.

31. Vinci, Antonio; Zoli, Luca; Sciti, Diletta (September 2018). "Influence of SiC content on the oxidation of carbon fibre reinforced ZrB₂/SiC composites at 1500 and 1650 °C in air". *Journal of the European Ceramic Society*. 38 (11): 3767–3776. doi:10.1016/j.jeurceramsoc.2018.04.064. ISSN 0955-2219.

32. Failla, S.; Galizia, P.; Zoli, L.; Vinci, A.; Sciti, D. (March 2019). "Toughening effect of non-periodic fibre distribution on crack propagation energy of UHTC composites". *Journal of Alloys and Compounds*. 777: 612–618. doi:10.1016/j.jallcom.2018.11.043. ISSN 0925-8388.

33. Galizia, P.; Zoli, L.; Sciti, D. (December 2018). "Impact of residual stress on thermal damage accumulation, and Young's modulus of fibre-reinforced

ultra-high temperature ceramics". *Materials & Design*. 160: 803–809. doi:10.1016/j.matdes.2018.10.019. ISSN 0264-1275.

34. Zoli, Luca; Vinci, Antonio; Galizia, Pietro; Melandri, Cesare; Sciti, Diletta (2018-06-14). "On the thermal shock resistance and mechanical properties of novel unidirectional UHTCMCs for extreme environments". *Scientific Reports*. 8 (1). doi:10.1038/s41598-018-27328-x. ISSN 2045-2322.

35. Ененков В.Г., Буриченко Л.А. Охрана окружающей среды самолетов гражданской авиации.- М.: Транспорт, 1987. – 248 с.

36. O.S. Protoiereiskiy, O.I. Zaporozhets. Basics of labour precaution. Education manual – К: NAU, 2002 – 524 p.

37 Patent number; **US 6,932,571 B2**

Name of the invention; **MICROCIRCUIT COOLING FOR A TURBINE**

BLADE TIP Inventors: **Frank Cunha**, Avon, CT (US); **Bryan Dube**,

Columbia, CT (US)

38. Газотурбинный двигатель [Электронный ресурс] – Режим доступа:

<https://uk.wikipedia.org/wiki/%D0%93%D0%B0%D0%B7%D0%BE%D1>

<https://uk.wikipedia.org/wiki/%82%D1%83%D1%80%D0%B1%D1%96%D0%BD%D0%BD%D0%B8>

https://uk.wikipedia.org/wiki/%D0%B9_%D0%B4%D0%B2%D0%B8%D0%B3%D1%83%D0%BD

39. Кишалов Александр Евгеньевич, кандидат технических наук, доцент;

Кудоярова Вилина Маратовна, кандидат технических наук, доцент;

Маркина Ксения Васильевна, “Анализ нагрузок, действующих на элементы конструкции ГТД” (2012). Молодой учёный № 11 – 223 ст. ISSN 2072-0297

40. Л. А. Магеррамова. “Конструктивные мероприятия, направленные на увеличение расчетной долговечности лопаток высокотемпературных турбин”. ФГУП «Центральный институт авиационного моторостроения им.

П. И. Баранова», 2015. Т. 19, № 2 (68). С. 79–86 – Режим
доступу:

<https://cyberleninka.ru/article/n/konstruktivnyemeropriyatiya-napravlennye-na-uvelichenie-raschetnoy-dolgovechnostilopatok-vysokotemperaturnyh-turbin>

41. Patent number; **US 6,932,571 B2**

Name of the invention; **MICROCIRCUIT COOLING FOR A
TURBINE**

BLADE TIP Inventors: **Frank Cunha**, Avon, CT (US); **Bryan
Dube**, Columbia, CT (US)

42. **Patent number:** EP 2 589 753 A3

Filed: 01.11.2012

Date of Patent: 08.05.2013

Patent Publication Number: 12190939.4

Assignee: United Technologies Corporation Farmington, CT 06032
(US)

Inventor: • Wu, Charles C. Glastonbury, CT Connecticut 06033 (US) • McCusker,
Kevin N. West Hartford, CT Connecticut 06107 (US)

APPENDIX 1

TFE thermodynamic and gas-dynamic calculations

1.1 Determination of the parameters of the working body in the unperturbed flow to the engine. (Section a_m-a_m)

For altitude (H = 0_M) pressure and temperature equal p_{amb}=101325 Pa T_{amb}=288,15. Determine parameters of stop flow:

$$T_{amb}^* = T_{amb} + \frac{V^2}{2 \cdot \frac{k}{k-1} \cdot R} = 288$$

$$T_{amb}^* = 288 \text{ K}$$

$$P_{amb}^* = P_{amb} \cdot \left(\frac{T_{amb}^*}{T_{amb}} \right)^{\frac{k}{k-1}} = 101300 \text{ Pa}$$

A.1.2 Characterization of air at the fan inlet (Section B-B)

Temperature and pressure determined from:

$$T_{inlet}^* = T_{amb}^* = 288 \text{ K}$$

Total pressure recovery coefficient of the inlet device taken to be: $\sigma_{inlet} = 0.995$;

$$P_{inlet}^* = P_{amb}^* \cdot \sigma_{inlet} = 100.3 \text{ kPa}$$

A.1.3 Determine inlet parameters of the working body at fan discharge at secondary flow. (Section F_i-F_i)

Choosing the efficiency of the fan $\eta_{fan2}^* = 0.89$ and determine compression work in the secondary flow:

$$L_{fan2} = \frac{k}{k-1} \cdot R \cdot T_{inlet}^* \cdot \left(\pi_f^{\frac{k-1}{k}} - 1 \right) / \eta_{fan2}^*$$

$$L_{fan2} = 50.078 \frac{\text{kJ}}{\text{kg}}$$

Pressure and temperature after the fan:

$$P_{fan2}^* = P_{inlet}^* \cdot \pi_{fan1}^* \quad P_{fan2}^* = 165.5 \text{ kPa}$$

$$T_{fan2}^* = T_{inlet}^* + \frac{L_{fan2}}{k} \cdot \frac{R}{k-1}$$

$$T_{fan2}^* = 337.95 \text{ K}$$

Obtained results are used for next calculations.

1.4 Characterization of air at the discharge of the secondary flow nozzle (Section nII-nII)

Parameters in the air after the fan is equal to (at $\sigma_{II} = 0.99$):

$$T_{II}^* = T_{fan2}^* \quad T_{II}^* = 337.95 \text{ K}$$

$$P_{II}^* = P_{fan2}^* \cdot \sigma_{II} \quad P_{II}^* = 163.845 \text{ kPa}$$

Velocity of air from secondary flow nozzle determined by the formula for the full expansion (taking the speed coefficient of the secondary flow nozzle, its equal to $\phi_{cII} = 0.98$):

$$c_{nII} = \phi_{nII} \cdot \sqrt{2 \cdot \frac{k}{k-1} \cdot R \cdot T_{II}^* \cdot \left[1 - \left(\frac{P_{amb}}{P_{II}^*} \right)^{\frac{k-1}{k}} \right]} \quad c_{nII} = 289.4 \text{ m/s}$$

$$p_n = p_{amb}$$

$$p_n = 101.325 \text{ kPa}$$

$$T_n = T_{II}^* - \frac{k-1}{k} \cdot \frac{c_{nII}^2}{2 \cdot R}$$

$$T_n = 296.3 \text{ K}$$

A.1.5 Characterization of air at the compressor discharge (Section K-K):

Efficiency of the compressor is determined by the approximate formula, setting the efficiency of stage of the compressor $\eta_{st}^* = 0.91$.

$$\eta_c^* = \frac{\pi_{c\Sigma}^{\frac{k-1}{k}} - 1}{\pi_{c\Sigma}^{\frac{k-1}{k \cdot \eta_{st}^*}} - 1} = \frac{34^{\frac{1.4-1}{1.4}} - 1}{34^{1.4-0.91} - 1} \quad \eta_c^* = 0.835$$

Compression work of air in the compressor:

$$L_c = \frac{k}{k-1} \cdot R \cdot T_{inlet}^* \cdot \left(\pi_{c\Sigma}^{\frac{k-1}{k}} - 1 \right) / \eta_c \quad L_c = 494.1 \frac{\text{kJ}}{\text{kg}}$$

Temperature and pressure after the compressor:

$$T_{cd}^* = T_{inlet}^* + \frac{L_c}{k} \cdot \frac{R}{k-1} \quad T_{cd}^* = 337.95 \text{ K}$$

$$P_{cd}^* = P_{inlet}^* \cdot \pi_{c\Sigma}^* \quad P_{cd}^* = 2.226 \text{ MPa}$$

1.6 Determination of the parameters of the working body at the combustion chamber discharge (Section C_a-C_d):

Setting total pressure recovering coefficient in the combustion chamber ($\sigma_{cc}=0.98$) determine the pressure at the turbine:

$$P_{ti}^* = P_{cd}^* \cdot \sigma_{cc} \quad P_{ti}^* = 2.181 \text{ MPa}$$

The average heat capacity of gas in the combustion chamber:

$$\bar{c}_{p \text{ mean}} = (878 + 0.208) \cdot (T_{ti}^* + 0.48 T_{cd}^*) \quad \bar{c}_{p \text{ mean}} = 1.261 \frac{\text{kJ}}{\text{kg} \cdot \text{K}}$$

Set combustion efficiency $\eta_g=0.995$ and taking heat ability of fuel values: $H_u=43000000 \text{ J/kg}$, determine the relative fuel consumption:

$$g_f = \bar{c}_{p \text{ mean}} \cdot (T_{ti}^* - T_{cd}^*) / (\eta_g \cdot H_u) \quad g_f = 0.02$$

Air/fuel ratio coefficient in the combustion chamber $\left(\frac{\text{kg of air}}{\text{kg of fuel}} \right)$:

$$\alpha = 1 / (g_f \cdot l_0)$$

$$\alpha = 3.378$$

l_0 – amount of air required for complete combustion of 1 kg of fuel:

$$l_0 = 14.8 \left(\frac{\text{kg of air}}{\text{kg of fuel}} \right)$$

1.7 Determine the parameters of gas at the turbine discharge (Section T_a-T_d):

To determine the effective operation of all stages of the turbine take the following coefficient $g_{cool}=0.06$ – the relative amount of air for cooling of turbine parts;
 $\eta_M := 0.995$ – spending power to drive the turbine units and overcome friction in the bearings ;

$$L_T = \frac{m \cdot L_{fl} + L_K}{(1 + g_f) \cdot (1 - g_{cool}) \cdot n_m} = 780.4 \frac{\text{kJ}}{\text{kg}}$$

Taking the turbine efficiency, $\eta_t = 0.9$ determine the temperature and pressure at

$$\text{the turbine: } T_{td}^* = T_{ti}^* - \frac{L_T}{\frac{k_g}{k_g - 1} \cdot R_g} \quad T_{td}^* = 797.66 \text{ K}$$

$$p_{td}^* = p_{ti}^* \cdot \left(1 - \frac{T_{td}^* - T_{ti}^*}{T_{ti}^* \cdot \eta_t} \right)^{\frac{k_g}{k_g - 1}} \quad p_{td}^* = 124.9 \text{ kPa}$$

1.8 Characterization of gas parameters in the primary flow nozzle section discharge (Section n_I-n_I):

The gas temperature at the nozzle discharge is equal to the temperature at the turbine:

$$T_{nI}^* = T_{td}^* \quad T_{nI}^* = 797.66 \text{ K}$$

Taking the total pressure recovery coefficient from the turbine section to the output nozzle is, $\sigma_{cI} := 0.99$, so the pressure in the initial section of the nozzle is to be determined:

$$p_{nI}^* = p_{td}^* \quad p_{nI}^* = 123.56 \text{ kPa}$$

Determine the pressure drop in the primary flow jet nozzle and compare it with the critical difference:

$$\pi_{n,cr}^* = \left(\frac{k_g + 1}{2} \right)^{\frac{k_g}{k_g - 1}} = 1.87 \quad \pi_{n,cr}^* = 1.851$$

$$\pi_{nI}^* = \frac{p_{nI}^*}{p_{atm}} \quad \pi_{nI}^* = 1.2$$

because $\pi_{nI}^* < \pi_{n,cr}^*$, the expansion of gas is full ($p_{cs} = p_{atm}$) and the velocity of the gas from the primary flow nozzle is:

$$C_n = \varphi_n \cdot \sqrt{2 \cdot \frac{k_g}{k_g - 1} \cdot R_g \cdot T_g^* \cdot \left[1 - \left(\frac{P_{amb}^*}{P_{td}^*} \right)^{\frac{k_g - 1}{k_g}} \right]} \quad c_{nI} = 312 \text{ m/s}$$

$\phi_{nI} = 0.98$ is the nozzle speed coefficient.

Static gas temperature at the outlet/discharge of the primary flow nozzle:

$$T_n = T_g^* - \frac{C_n^2}{2 \frac{k_g}{k_g - 1} R_g} \quad T_{nI} = 758.9K$$

1.9 Determination of the main parameters of the engine and air flow rate:

Specific thrust is:

$$P_{spI} = c_{nI} (1 + g_f) \quad P_{spI} = 318.2 \frac{N \cdot s}{kg}$$

$$P_{spII} = c_{nII} \quad P_{spII} = 289.4 \frac{N \cdot s}{kg}$$

$$P_{sp\Sigma} = \frac{P_{spI} + P_{spII}}{1 + m} \quad P_{sp\Sigma} = 292.2 \frac{N \cdot s}{kg}$$

Specific fuel consumption:

$$C_{sp\Sigma} = 3600 \cdot g_f \cdot (1 - g_{cool}) / (P_{sp\Sigma} \cdot (1 + m)) \quad C_{sp\Sigma} = 0.0386 \frac{kg}{N \cdot h}$$

Air flow rate is determined as:

$$G_a = P / P_{sp\Sigma} \quad G_a = 253.4 \text{ kg/s;}$$

$$G_{a1} = G_a / (1 + m) \quad G_{a1} = 4A.13 \text{ kg/s;}$$

$$G_{a2} = m \cdot G_a / (1 + m) \quad G_{a2} = 211.17 \text{ kg/s.}$$

$$G_a = 253.4 \frac{kg}{s} \quad G_a = G_{a1} + G_{a2}$$

Internal engine efficiency:

$$\eta_{in} = \frac{(1 + m) P_{sp\Sigma}^2}{2 g_f H_u (1 - g_{cool})}$$

1.10 Gas-dynamic calculation of turbofan engine

The purpose of gas-dynamic calculation of aviation gas turbine engine is to determine the diametric dimension of typical air-gas channel cross-sections of the engine, the number and speed of rotor rotation, the number of stages of compressors and turbines in each spool and the distribution of compression (expansion) between them. The initial data for gas-dynamic calculation are the results of the thermodynamic calculation.

1.11 Determining the dimension at the inlet to the fan

Getting gas-dynamic calculation, we choose the value of the axial air velocity at the fan inlet $c_{1a} = 185 \text{ m/s}$ and the peripheral speed at the ends of the blades

$U_{1c} = 460 \text{ m/s}$ according to the recommendations, as well as the bushings ratio of the fan's first stage $\bar{d}_{1sleeve} = 0.35$

Reduced velocity of flow:

$$\lambda_{1a} = C_{1a} / (18.3 \cdot \sqrt{T_{inlet}^*})$$

$$\lambda_{1a} = 0.59$$

The general formula for determining the relative density of the flow is a function of the isentropic exponent and the reduced velocity of flow.

$$q(\lambda, k_i) := \left(\frac{k_i + 1}{2} \right)^{\frac{1}{k_i - 1}} \cdot \lambda \cdot \left(1 - \frac{k_i - 1}{k_i + 1} \cdot \lambda^2 \right)^{\frac{1}{k_i - 1}}$$

$$q(\lambda_{1a}, k) = 0.8$$

Cross-sectional area at the fan inlet:

$$F_{fi} = (G_a \cdot \sqrt{T_{inlet}^*}) / (m \cdot P_{inlet} \cdot q(\lambda_{1a}))$$

$$F_{fi} = 1.35 \text{ m}^2$$

where $m_a = 0.040348 \frac{\text{kg} \cdot \text{K}}{\text{J}}$

The diameter of rotor wheel at the periphery:

$$D_{1c} = \sqrt{\frac{4F_i}{\pi(1 - d_{1.resp}^2)}}$$

$$D_{1c} = 1.38 \text{ m}$$

Sleeve diameter:

$$D_{1sl} = \sqrt{D_{1c}^2 - \frac{4}{\pi} \cdot F_i}$$

$$D_{1sl} = 0.43 \text{ m}$$

Diameter of separating casing that separates the flows of first and second flows:

$$D_1 = \sqrt{D_{1c}^2 - \frac{4}{\pi} \cdot \frac{G_{a2}}{G_a} \cdot F_i}$$

$$D_1 = 0.686 \text{ m}$$

1.12 Determination of the number of LPC stages

Circumferential speed of blades at D_1 and sleeve diameters:

$$U_1 = (U_{1 \text{ tip}} \cdot D_1) / D_{1c}$$

$$U_1 = 228.7 \text{ m/s}$$

$$U_{1sl} = U_{1 \text{ tip}} \cdot (D_1 / D_{1c})$$

$$U_{1sl} = 143.3 \text{ m/s}$$

The lattice density at rotor wheel sleeve except $z_{\text{sleeve}}=1.8$ Calculate the lattice density at D_I diameter. Air twists air and the work being transferred to air by the fan blades at the diameter D_I :

$$z_I = z_{1 \text{ sleeve}} \cdot (D_1 / D_{1c})$$

$$z_I = 1.128$$

$$\Delta W_{uI} := c_{1a} \cdot \frac{1.55}{1 + 1.5 \cdot \frac{1}{z_I}}$$

$$\Delta W_{uI} = 123 \text{ m/s}$$

$$L_I = 28 \frac{\text{kJ}}{\text{kg}}$$

$$L_I := U_I \cdot \Delta W_{uI}$$

The air twist at the diameter $D_{1\text{sleeve}}$:

$$\Delta W_{u.sl} = c_{1a} \cdot \frac{1.55}{1 + 1.5 \cdot \frac{1}{z_{\text{sleeve}}}}$$

$$\Delta W_{u.sl} = 156.4 \text{ m/s}$$

The fan work in the area of the primary flow:

$$L_{u.sl} = U_{1.sl} \cdot \Delta W_{u.sl}$$

$$L_{u.sl} = 22.4 \frac{\text{kJ}}{\text{kg}}$$

$$L_{fI} = 0.5(L_{u.sl} + L_I)$$

$$L_{fI} = 25.2 \frac{\text{kJ}}{\text{kg}}$$

So finally accept single stage fan $z_f=1$, size at inlet:

$$D_{1c} = 1.38 \text{ M} \quad D_{1sl} = 0.43 \text{ M} \quad D_I = 0.686 \text{ M}$$

$$U_{1c} = 460 \frac{\text{M}}{\text{s}}$$

Work in the area of the secondary flow:

$$L_{fII} = 50.078 \frac{\text{kJ}}{\text{kg}}$$

in the area of the primary flow:

$$L_{fl} = 25.2 \frac{\text{kJ}}{\text{kg}}$$

1.13 Distribution of compression between the compressor and turbine spools of low, intermediate and high pressure and determination of the number of intermediate and high pressure turbine blades:

Distribution of compression between the compressor cascades performed with maximum load conditions each stage HPT:

$$L_c^* = L_c - L_{fl} - \left(20 \frac{\text{kJ}}{\text{kg}} \right)$$

$$L_c^* = 449 \frac{\text{kJ}}{\text{kg}}$$

$$z_{add}=1$$

Work of intermediate and high pressure turbines:

$$L_t = \frac{L_c^*}{(1 + g_t) \cdot (1 - g_{cool}) \cdot \eta_m} \frac{\text{kJ}}{\text{kg}}$$

$$L_t = 471 \frac{\text{kJ}}{\text{kg}}$$

Distribution of received spool work on IPC, HPC and IPT, HPT in such way that work of IPC and IPT is at 20 % lower work of HPC:

$$L_{IPC} = (0.8 \cdot L_c) / 1.8$$

$$L_{IPC} = 199.5 \frac{\text{kJ}}{\text{kg}}$$

$$L_{HPC} = L_c^* / 1.8$$

$$L_{HPC} = 249.4 \frac{\text{kJ}}{\text{kg}}$$

$$L_{IPT} = 0.8 L_t / 1.8$$

$$L_{MPT} = 209.4 \frac{\text{kJ}}{\text{kg}}$$

$$L_{HPT} = L_t / 1.8$$

$$L_{HPT} = 261.6 \frac{\text{kJ}}{\text{kg}}$$

$$z_{st.HPT}=1$$

$$U_{HPT.mean} = 460 \frac{\text{m}}{\text{s}}$$

$$Y^* = U_{mean} \cdot \sqrt{\frac{z \cdot \eta_{HPT}^*}{2 \cdot L_{HPT}}} \quad Y^* = 0.55$$

Load factor is in acceptable limits (0.45...0.55);

$$z_{st.IPT} = 1$$

$$U_{IPT,mean} = 400 \frac{M}{s}$$

$$Y^* = U_{HPTmean} \cdot \sqrt{\frac{z_{sl.IPT} \cdot \eta_t^*}{2 \cdot L_{IPT}}} \quad Y^* = 0.58$$

Load factor is in acceptable limits (0.53...0.58).

The compression work in the fan with attached stage:

$$L_{LPC} = L_{f1} + 20 \frac{kJ}{kg}$$

$$L_{LPC} = 45.2 \frac{kJ}{kg}$$

1.14 Determination of air parameters and diametric dimensions at the outlet of the fan and LPC:

The pressure ratio in the LPC:

$$\pi_{LPC}^* = \left[1 + \frac{L_{LPC} \cdot \eta_{fII}^*}{\frac{k}{k-1} \cdot R \cdot T_{inlet}^*} \right]^{\frac{k}{k-1}}$$

$$\pi_{LPC}^* = 1.576$$

Pressure and temperature at the exit/discharge of LPC :

$$p_{LPC}^* = p_{inlet} \cdot \pi_{LPC}^*$$

$$p_{LPC}^* = 158 \text{ kPa}$$

$$T_{LPC}^* = T_{fanI}^* + \left(\frac{((k-1) \cdot L_{LPC})}{k \cdot R} \right)$$

$$T_{LPC}^* = 333.1 \text{ K}$$

Diametric dimensions at the discharge of LPC are determined separately for the primary and secondary flows. In this case, take the axial velocity at the outlet/discharge of the fan:

- Secondary flow: $c_{a.fanII} = 175 \frac{M}{s}$;

- Primary flow: $c_{a.fanI} = 165 \frac{M}{s}$;

Reduced speeds and relative densities in both flows are calculated using equations:

$$\lambda_{a.fan1} = \frac{C_{a.fan1}}{18.3 \cdot \sqrt{T_{fan1}^*}}$$

$$\lambda_{a.fanI} = 0.49$$

$$\lambda_{a.fan2} = \frac{C_{a.fan2}}{18.3 \cdot \sqrt{T_{fan2}^*}}$$

$$\lambda_{a.fanII} = 0.52$$

$$q(\lambda_{a.fanI}^k) = 0.69$$

$$q(\lambda_{a.fanII}^k) = 0.73$$

Sectional area at the discharge of the fan in the secondary and primary flows:

$$F_{fan2} = \frac{G_{a2} \cdot \sqrt{T_{fan2}^*}}{m_a \cdot P_{fan2}^* \cdot q(\lambda_{afan2})}$$

$$F_{fanII} = 0.8 \text{ M}^2$$

$$F_{fan1} = \frac{G_{a1} \cdot \sqrt{T_{fan1}^*}}{m_a \cdot P_{fan1}^* \cdot q(\lambda_{afan1})}$$

$$F_{fanI} = 0.175 \text{ M}^2$$

We accept external diameter for the fan in the secondary flow to less than 2.2%, i.e.

$$D_{fanII} := 0.945 \cdot D_{1c}$$

$$D_{fanII} = 1.3 \text{ M}$$

Determination of the diameter of the dividing casing that divides the flow of primary and secondary flows:

$$D_{II} = \sqrt{D_{fan2}^2 - \frac{4}{\pi} F_{fan2}}$$

$$D_{II} = 0.82 \text{ m.}$$

We accept thickness of the wall that separates the two paths equal $\delta = 0.040 \text{ m}$, so the outer diameter of casing is equal to:

$$D_{fanI} = D_{II} - \delta$$

$$D_{II} = 0.87 \text{ m}$$

Then the diameter of the sleeve on the LPC discharge:

$$D_{slLPC} = \sqrt{D_{fan1}^2 - \frac{4}{\pi} F_{fan1}}$$

$$D_{sl.LPC} = 0.620 \text{ m}$$

1.15 The diameter of the sleeve at the IPC discharge

Parameters of air at inlet of IPC:

$$T_{inlet IPC}^* = T_{LPC}^*$$

$$T_{inlet IPC}^* = 333.1 \text{ K}$$

$$\lambda_{inlet IPC} = 0.5$$

Relative density of flow:

$$q(\lambda_{in IPC}, k) = 0.7$$

Sectional area at the inlet of the intermediate pressure compressor:

$$F_{inlet IPC} = \frac{G_{al} \cdot \sqrt{T_{inlet IPC}^*}}{m_a \cdot P_{inlet IPC}^* \cdot q(\lambda_{inlet IPC})}$$

$$F_{in IPC} = 0.175 \text{ m}^2$$

To determine the diametric dimensions IPC inlet, Calculate a relative diameter of the first stage IPC sleeve $\bar{d}_{lsleeve} = 0.645$

External diameter of rotor wheel at IPC inlet:

$$D_{1 IPC} = \sqrt{\frac{4F_{inlet IPC}}{\pi(1 - d_{sl}^2)}}$$

$$D_{1 IPC} = 0.62 \text{ m}$$

Diameter of rotor wheel sleeve IPC inlet:

$$D_{sl,IPC} := \sqrt{D_{1,IPC}^2 - \frac{4}{\pi} \cdot F_{in,IPC}}$$

$$D_{sl,IPC} = 0.4 \text{ M}$$

Length of airfoil part of the blade at rotor wheel of IPC inlet:

$$H_{1b} = (D_{1,IPC} - D_{in,sl,IPC}) / 2$$

$$h_{1b} = 0.11 \text{ M}$$

1.16 Determination diametric dimensions at the IPC discharge:

The temperature of the air at the IPC discharge:

$$T_{IPC}^* = T_{LPC,in}^* + \frac{L_{IPC}}{\left(\frac{k}{k-1}\right) \cdot R}$$

$$T_{IPC}^* = 531.5 \text{ K}$$

take:

$$\eta_{IPC}^* = 0.88$$

The air pressure ratio in IPC:

$$\pi_{IPC}^* = \left[1 + \frac{L_{IPC} \cdot \eta_{IPC}^*}{\frac{k}{k-1} \cdot R \cdot T_{in,IPC}^*} \right]^{\frac{k}{k-1}}$$

$$\pi_{IPC}^* = 4.37$$

$$P_{IPC}^* = P_{IPC,in}^* \cdot \pi_{IPC}^*$$

$$p'_{IPC} = 683.468 \text{ kPa}$$

Determine the reduced speed, relative density and cross-sectional area at the exit/discharge of IPC:

$$c_{2a,IPC} = 140 \frac{\text{M}}{\text{s}}$$

$$\lambda_{a,IPC} = \frac{c_{a,IPC}}{18.3 \cdot \sqrt{T_{IPC}^*}}$$

$$\lambda_{a,IPC} = 0.332$$

$$q(\lambda_{a,IPC}, k) = 0.5$$

Sectional area at the IPC discharge:

$$F_{IPC} = \frac{G_{aI} \cdot \sqrt{T_{IPC}^*}}{m_a \cdot p_{IPC}^* \cdot q(\lambda_{a,IPC}, k)}$$

$$F_{IPC} = 0.07 \text{ m}^2$$

Take the sleeve relative diameter at the IPC discharge $\bar{d}_{2,sleeve} = 0.8$, determine the diameter of the rotor wheel and length of blades airfoil at the sleeve of IPC discharge:

$$D_{2IPC} = \sqrt{\frac{4 \cdot F_{IPC}}{\pi \cdot (1 - d_{2,sleeve}^2)}}$$

$$D_{2,IPC} = 0.566 \text{ m}$$

$$D_{IPC,sleeve} = \sqrt{D_{2,IPC}^2 - \frac{4}{\pi} \cdot F_{IPC}}$$

$$D_{IPCsl} = 0.48 \text{ m}$$

$$H_{2b} = (D_{2,IPC} - D_{IPC.sl}) / 2$$

$$h_{2b} = 0.043 \text{ m}$$

1.17 Determination of diametric sectional dimensions at the high pressure compressor inlet

Parameters of air at the HPC inlet:

$$T_{inlet HPC}^* = T_{IPC}^*$$

$$T_{inlet.HPC}^* = 531.5 \text{ K}$$

$$P_{inlet HPC}^* = P_{LPC d}^* \cdot \sigma_{intermediate}$$

$$P_{inlet HPC}^* = 676.6 \text{ kPa}$$

where $\sigma_{nep.} = 0.99$ is the pressure recovery coefficient.

Take the transition axial velocity of air at HPC inlet:

$$c_{a HPC} = 150 \frac{\text{m}}{\text{s}}$$

Reduced speed:

$$\lambda_{HPC.in} = \frac{c_{HPC.i}}{18.3 \cdot \sqrt{T_{HPC}^*}}$$

$$\lambda_{,HPCin} = 0.355$$

Relative density of flow:

$$q(\lambda_{,HPin}, k) = 0.53$$

Cross-sectional area at the inlet of the high pressure compressor:

$$F_{HPC.in} = \frac{G_{al} \cdot \sqrt{T_{HPC.in}^*}}{m_a \cdot p_{HPC.in}^* \cdot q(\lambda_{HPC.in}, k)}$$

$$F_{HPC.in} = 0.067 \text{ m}^2$$

To determine the diametric dimensions at the inlet to the HPC, take the sleeve relative diameter at the first stage HPC $\bar{d}_{1sl} = 0.81$.

External diameter diameter of rotor wheel at HPC discharge:

$$D_{IHPC} = \sqrt{\frac{4 \cdot F_{HPC.in}}{\pi \cdot (1 - d_{1.sleeve}^2)}}$$

$$D_{1,HPC} = 0.498 \text{ M}$$

Sleeve diameter of rotor wheel at HPC inlet:

$$D_{HPCsleeve} = \sqrt{D_{1,IPC}^2 - \frac{4}{\pi} \cdot F_{IPC}}$$

$$D_{HPC.sl} = 0.4 \text{ M}$$

Length of rotor blade at the inlet of HPC:

$$H_{3b} = (D_{1,HPC} - D_{HPC.sl}) / 2$$

$$h_{3b} = 0.049 \text{ M}$$

1.18 Determination of diametric dimensions at the high pressure compression discharge:

The temperature of the air at the HPC discharge can be determined by the formula:

$$T_c^* = T_{IPC}^* + \frac{L_{HPC}}{k} \cdot \frac{R}{k-1}$$

$$T_c^* = 779.5 \text{ K}$$

$$\text{Take: } \eta_{HPC}^* = 0.88$$

The air pressure ratio in HPC:

$$\pi_{\text{HPC}}^* = \left[1 + \frac{L_{\text{HPC}} \cdot \eta_{\text{HPC}}^*}{\frac{k}{k-1} \cdot R \cdot T_{\text{in.HPC}}^*} \right]^{\frac{k}{k-1}}$$

$$\pi'_{\text{HPC}} = 3.334$$

$$P_{\text{HPC}}^* = P_{\text{HPC.in}}^* \pi_{\text{HPC}}^*$$

$$p'_{\text{CHP}} = 2.255 \text{ MPa}$$

Determine the reduced speed, relative density of flow and cross-sectional area at the exit/discharge of HPC, taking the axial air velocity at HPC discharge:

$$c_{\text{ac}} = 115 \frac{\text{m}}{\text{s}}$$

$$\lambda_{\text{ac}} = \frac{c_{\text{ac}}}{18.3 \cdot \sqrt{T_k^*}}$$

$$\lambda_{\text{ac}} = 0.225$$

$$q(\lambda_{\text{ak}}, k) = 0.347$$

Sectional area at the exit/discharge of HPC:

$$F_c = \frac{G_{\text{al}} \cdot \sqrt{T_c^*}}{m_a \cdot p_c^* \cdot q(\lambda_{\text{ak}}, k)}$$

$$F_c = 0.037 \text{ m}^2$$

Take sleeve relative diameter at the HPC discharge, $\bar{d}_{2\text{BT}} = 0.905$, and determine external diameter of the rotor wheel and length of the blade's airfoil at the HPC discharge:

$$D_{2\text{HPC}} = \sqrt{\frac{4 \cdot F_c}{\pi \cdot (1 - d_{2,\text{sleeve}}^2)}}$$

$$D_{2.HPC} = 0.51 \text{ M}$$

$$D_{HPCsleeve} = \sqrt{D_{2.HPC}^2 - \frac{4}{\pi} \cdot F_{HPC}}$$

$$D_{HPC.sl} = 0.461 \text{ M}$$

$$H_{4b} = (D_{2.HPC} - D_{HPC.sl}) / 2$$

$$h_{4b} = 0.024 \text{ M}$$

1.19 Determination of diametric dimension of high pressure turbine inlet

The angle of the gas flow at the exit from nozzle :

$$\alpha_1 = 20^\circ$$

Absolute speed at the first nozzle diaphragm discharge is determined from the Euler equation under the assumption of axial exit from the first high-pressure turbine rotor wheel:

$$c_1 = \frac{L_{HPT}}{U_{HPTmean} \cdot \cos \alpha_1}$$

$$c_1 = 605.6 \frac{\text{M}}{\text{s}}$$

Reduced speed:

$$\lambda_1 = \frac{c_1}{18.15 \cdot \sqrt{T_{t.in}^*}}$$

$$\lambda_1 = 0.87$$

Density of flow:

$$q(\lambda_1, k_g) = 0.98$$

Gas flow rate at the inlet of high pressure turbine taking $g_{cool1} = 1.03 g_{cool}$:

$$G_g = G_{a1} \cdot (1 + g_f) \cdot (1 - g_{cool})$$

$$G_g = 40.4 \frac{\text{kg}}{\text{s}}$$

Accepting total pressure recovery coefficient as $\sigma_{ca} := 0.98$, then the gas pressure at the outlet of the nozzle calculated by the formula:

$$P_{nd}^* = P_{cd}^* \cdot \sigma_{cc} \cdot \sigma_{nd} \quad P_{nd}^* = 2.165 \text{ MPa}$$

Sectional area at the nozzle vanes discharge:

$$F_{1nd} = \frac{G_g \cdot \sqrt{T_g^*}}{m_g \cdot p_{nd}^* \cdot q(\lambda_1, k_g) \cdot \sin \alpha_1}$$

$$F_{1nd} = 0.054 \text{ M}^2$$

where $m_g = 0.0396$

We take the average diameter HPT:

$$D_{hpt.in.me} = 0.57 \text{ M}$$

Length of vanes airfoil part is calculated by the formula:

$$h_{nd} := \frac{F_{1nd}}{\pi \cdot D_{hpt.in.me}}$$

$$h_{nd} = 0.03 \text{ M}$$

The length of the rotor wheel blade is accepted as: $h_{\text{л}} \approx h_{ca}$

$$h_b = 0.03 \text{ m}$$

The external diameter of turbine rotor wheel:

$$D_T := D_{B.TBT.cp} + h_{3\text{л}}$$

$$D_T = 0.6 \text{ M}$$

Diameter of high pressure turbine sleeve:

$$D_{t.sleeve} = \sqrt{D_t - \frac{4 \cdot F_{1nd}}{\pi}}$$

$$D_{t.sl} = 0.54 \text{ M}$$

Axial velocity of the gas at the Rotor wheel inlet:

$$c_{1aT} := c_1 \cdot \sin(\alpha_1)$$

$$c_{1aT} = 207.1 \frac{\text{M}}{\text{s}}$$

Tension in a dangerous section of the blade by centrifugal forces can be determined after setting the density of the material $\rho = 8.2 \cdot 10^3 \frac{\text{kg}}{\text{M}^3}$ and blades form

factor $k_\phi = 0.56$:

$$\sigma_{\text{tensile}} = 2 \cdot K_{sh} \cdot \rho \cdot U_{t \text{ mean}}^2 \cdot h_b \cdot 10^6 / D_{t \text{ mean}}$$

$$\sigma_{\text{tefl}} = 102.3 \text{ MPa}$$

Taking from table the long term strength of material strength of the high pressure turbine blades can be ensured if we use alloy ЖС6У in the making of the blade and intensive cooling of the blade to a temperature of 950K.

Under these conditions, limit safety factor of the material is equal to:

$$\sigma_{100} := 600 \text{ MPa}$$

and the long term strength safety factor coefficient is equal to:

$$n := \frac{\sigma_{100}}{\sigma_p} \quad n = 5,865$$

HPT rotor blades satisfy the conditions of safety factor.

1.20 Determination of diametric dimension at the high pressure turbine discharge:

Parameters of gas at the HPT discharge:

- temperature:

$$T_{HPT}^* = T_{ti}^* - \frac{L_{HPT}}{k_g - 1} R_g$$

$$T'_{HPT} = 1244.6 \text{ K}$$

- pressure:

$$p'_{HPT} = 1.016 \text{ MPa} \quad p'_{TBT} := p'_\Gamma \cdot \left(1 - \frac{T_\Gamma - T_{TBT}}{T_\Gamma \cdot 0.9} \right)^{\frac{k_\Gamma}{k_\Gamma - 1}}$$

Take the reduced speed: $\lambda_{2a} = 0.4$, corresponding to the axial component of the absolute velocity of the gas at the high pressure turbine discharge:

$$c_{2a} = \lambda_{2a} \frac{1}{18.15 \cdot \sqrt{T_{t.in}^*}}$$

$$c_{2a} = 256.1 \frac{\text{M}}{\text{s}}$$

Under these conditions, the density of flow is equal to:

$$q(\lambda_{2a}, k_\Gamma) = 0.59$$

In view of the fact that part of the air that cools the turbine is going in gas stream and will mix with it, accept $g_{cool2} = 0.97g_{cool1}$ and determine the gas flow rate at the high pressure turbine discharge:

$$G_g = G_{a1} \cdot (1 + g_f) \cdot (1 - g_{cool2})$$

$$G_g = 40.85 \frac{\text{kg}}{\text{s}}$$

Sectional area at the HPT discharge:

$$F_{HPTd} = \frac{G_g \sqrt{T_{HPT}^*}}{m_g P_{HPTd}^* q(\lambda_{2a})}$$

$$F_{HPT} = 0.06 \text{ m}^2$$

The average diameter at the high pressure turbine discharge:

$$D_{t, \text{mn}} := 0.585M$$

Length of HPT blade airfoil at the tip:

$$h_{6b} = F_{\text{HPT d}} / (\pi \cdot D_{t, \text{mean}})$$

$$h_{6b} = 0.033M$$

Diameters of cross-section at high pressure turbine discharge:

$$D_{\text{HPT d}} = D_{t, \text{mean}} + h_{6b}$$

$$D_{\text{hpt d}} = 0.618M$$

$$D_{\text{sl HPT}} = \sqrt{D_{\text{HPT d}}^2 \frac{4}{\pi} F_{\text{HPT}}}$$

$$D_{\text{sl.hpt}} = 0.552M$$

Relative diameter is:

$$\bar{d}_{\text{hpt}} = \frac{D_{\text{sl.hpt}}}{D_{\text{hpt d}}}$$

$$\bar{d}_{\text{hpt}} = 0.89$$

1.21 Determination of high-pressure compressor stages:

The work of HPC first-stage can be determined by taking the lattice density: $Z_1 = 1.8$

$$\Delta W_{u \text{ sl}} = C_{a\text{HPC}} \cdot \frac{1.55}{1 + 1.5 \frac{1}{Z_1}}$$

$$\Delta W_{u.B.} = 126.8 \frac{\text{M}}{\text{s}}$$

$$U_{1 \text{ sl}} = (U_{t, \text{mean}} \cdot D_{\text{HPC sl}}) / 0.625$$

$$U_{1 \text{ sl}} = 322.8 \frac{\text{M}}{\text{s}}$$

$$L_{\text{ST 1}} = U_{1 \text{ sl}} \cdot \Delta W_{u \text{ sl}}$$

$$L_{\text{STT}} = 40.9 \frac{\text{kJ}}{\text{kg}}$$

The work of the HPC last stage is calculated by taking the lattice density: $Z_2 = 1.4$

$$\Delta W_{u \text{ sl}} = C_{ac} \cdot \frac{1.55}{1 + 1.5 \frac{1}{Z_2}}$$

$$\Delta W_{u.sl} = 86 \frac{M}{s}$$

$$U_{sl.z} = (U_{hpt \text{ mean}} \cdot D_{sl \text{ hpc}}) / 0.625$$

$$N_{HPT} = G_g \cdot L_{HPT} \quad U_{sl.z} = 372 \frac{M}{s}$$

$$U_{l.s} = (U_{hpt \text{ mean}} \cdot D_{l \text{ hpc}}) / 0.625$$

$$U_{1k} = 401.9 \frac{M}{c}$$

$$L_{ST z} = U_{sl} \cdot \Delta W_{u \text{ sl}}$$

$$L_{ST z} = 32 \frac{kJ}{kg}$$

The average work at the stage:

$$L_{\text{mean}} = (L_{ST z} + L_{ST1}) / 2$$

$$L_{\text{mean}} = 36.45 \frac{kJ}{kg}$$

$$z = L_{HPC} / L_{\text{mean}}$$

$$z_{HPC} = 6.84$$

$$L_{HPC} = 249.4 \frac{kJ}{kg} - \text{work of HPC.}$$

Number of HPC stages equal $z_{HPC} = 7$.

Distribution of HPC stages work:

The balance of HPC and HPT powers is checked by the formulae:

$$N_{HPC} = G_{al} \cdot L_{HPC}$$

$$N_{HPC} = 10532.16 \text{ kW}$$

$$N_{HPT} = G_g \cdot L_{HPT}$$

$$N_{hpt} = 10568.64 \text{ kW}$$

Mechanical efficiency

$$\eta_m = N_{HPC} / N_{HPT}$$

$$\eta_m = 0.996$$

High pressure rotor speed is determined separately for the compressor and turbine:

$$n_{HPC} = 60 \cdot U_{1c \text{ tip}} / (\pi \cdot D_{c \text{ tip}})$$

$$n_{HPC} = 15420.9 \text{ min}^{-1}$$

$$n_{HPT} = 60 \cdot U_{t \text{ mean}} / (\pi \cdot 0.625)$$

$$n_{hpt} = 15420.9 \text{ min}^{-1}$$

1.22 Determination of diametric dimension at the intermediate pressure turbine inlet:

$$T_{B.TCT} := T_{TB1}$$

$$T_{ipt} = 1244.6 \text{ K}$$

Absolute speed at the first turbine nozzle vanes discharge:

$$c_1 = 524.3 \frac{\text{M}}{\text{s}}$$

$$h_{7nd} = 0.063 \text{ M}$$

Take the length of the rotor blade: $h_{7nd} = h_{7b}$

$$h_{7b} = 0.063 \text{ M}$$

The external diameter of the turbine rotor wheel:

$$D_t = D_{IPT.i \text{ mean}} + h_{7b}$$

$$D_t = 0.743 \text{ M}$$

Determine the internal diameter of the turbine:

$$D_{IPT.sl} := \sqrt{D_{IPT}^2 - \frac{4}{\pi} \cdot F_{IPT}}$$

$$D_{IPT.sl} = 0.617 \text{ M}$$

Axial velocity of the gas at the rotor wheel:

$$C_{1aIPT} = C_1 \cdot \sin \alpha_1$$

$$c_{1a.IPT} = 162 \frac{\text{M}}{\text{s}}$$

Tension in a dangerous section of the blade by centrifugal forces is determined after setting the density of the material and blades form factor (0.5...0.6)

$$k_f = 0.55, \rho = 8.1 \cdot 10^3 \frac{\text{kg}}{\text{M}^3};$$

$$\sigma_{ten} = 2 \cdot K_f \cdot \rho \cdot U_{IPT \text{ mean}}^2 \cdot U_{IPT \text{ mean}} \cdot 10^6 / D_{IPT.i \text{ mean}}$$

$$\sigma_{ten} = 145,6 \text{ MPa}$$

From the table we take the long term strength of a blade materials and the strength of intermediate pressure turbine can be achieved if we use for the manufacturing of blades ЖС6К and its intensive cooling up to a temperature of 1150K.

Under these conditions, long term strength of the material is equal to:
 $\sigma_{500} := 250 \text{ MPa}$

and the safety factor coefficient is equal to:

$$n = \frac{\sigma_{500}}{\sigma_{ten}}$$

$$n = 1.71$$

IPT blades satisfy the conditions of safety factor.

1.23 Determination of diametric dimension at the intermediate pressure turbine discharge:

Parameters of gas at the exit of IPT:

- temperature:

$$T_{IPT}^* = T_{HPT}^* - \frac{L_{IPT}}{\left(\frac{k_g}{k_g - 1}\right) \cdot R}$$

$$T_{IPT}^* = 1064.2 \text{ K}$$

- pressure:

$$p_{IPT}^* = p_{HPT}^* \cdot \left(1 - \frac{T_{HPT}^* - T_{IPT}^*}{T_{HPT}^* \cdot 0.87}\right)^{\frac{k_g}{k_g - 1}} \quad p'_{IPT} = 477.7 \text{ kPa}$$

We set the reduced speed: $\lambda_{2a} = 0.35$, and corresponding axial component of the absolute speed of the gas at the intermediate pressure turbine discharge:

$$c_{2a} = \lambda_{2a} \frac{1}{18.15 \cdot \sqrt{T_{IPT}^*}}$$

1.24 Determination of levels and distribution of work on low-pressure turbine stages:

Taking into account that the LPT inlet temperature is less than 1200K ($T_{TCT} = 1064.2 \text{ K}$) we do not need to cool the nozzle diaphragm and drive rotor blades of the first stage. We accept the amount of air required for cooling equal to $g_{cool LPT} = 0$. So:

- gas flow rate through LPT:

$$G_{g,LPT} = G_{al} \cdot (1 + g_f) \cdot (1 - g_{cool LPT})$$

$$G_g = 43 \frac{\text{kg}}{\text{s}}$$

- LPT work due to the balance of powers:

$$L_{LPT} = \frac{m \cdot L_{fII} + L_{LPC}}{(1 + g_f) \cdot n_m}$$

$$L_{LPT} = 291.25 \frac{\text{kJ}}{\text{kg}}$$

accept:

$$D_{LPT.mn} := 0.7M$$

$$U_{LPTmean} = U_{1c} \cdot (D_{LPTmean} / D_{1c})$$

$$U_{LPTmean} = 243.5 \frac{\text{M}}{\text{s}}$$

The parameter determining the load when the number of stages $Z_{THT} := 3$ and efficiency of LPT is less than the efficiency of the whole turbine $\eta'_{THT} := 0.95\eta'_T$, (must be equal to 0.55...0.6):

$$Y = U_{LPTmean} \cdot \frac{D_{LPTmean}}{D_{1c}}$$

$$Y = 0.562$$

Distribute the LPT work by stages so that the work of each next stage is was Work on the stages will equals:

$$L_{st1} = 116.5 \frac{\text{kJ}}{\text{kg}}$$

1.26 Determination of diametric dimension at the LTP first nozzle diaphragm discharge:

Take the total pressure recovery coefficient as $\sigma_{nd}=0.98$, then the gas pressure at the nozzle vanes discharge will be calculated by the formula:

$$P_{LPTi}^* = P_{IPT}^* \cdot \sigma_{nd}$$

$$p'_{LPT} = 470.5 \text{ kPa}$$

Critical gas velocity at the LPT nozzle vanes discharge is determined by the formula:

$$c_{cr} = 18.15 \cdot \sqrt{T_{IPT}^*}$$

$$c_{cr} = 592 \frac{\text{M}}{\text{s}}$$

Taking angle $\alpha = 20.5^0$ (20...25), determine the velocity of the gas at the nozzle vanes discharge:

$$c_{1LPT} = \frac{L_{LPT1}}{U_{LPTmean} \cdot \cos(\alpha_{1nd})}$$

$$c_{1LPT} = 511.1 \frac{M}{s}$$

axial speed:

$$c_{1a} = c_{1LPT} \cdot \sin(\alpha_{1nd})$$

$$c_{1a} = 178.9 \frac{M}{s}$$

Reduced speed and relative density of flow determined from the formulae:

$$\lambda_{1LPT} = \frac{c_{1LPT}}{c_{cr}}$$

$$\lambda_{1LPT} = 0.863$$

$$q(\lambda_{1LPT}, k_T) = 0.978$$

Sectional area at the LPT nozzle vanes is determined by the formula:

$$F_{1ndLPT} = \frac{G_{gLPT} \cdot \sqrt{T_{IPT}^*}}{m_g \cdot p_{IPT}^* \cdot \sigma_{tension} \cdot \sigma_{nd} q(\lambda_{1LPT}, k_g) \cdot \sin \alpha_{1nd}}$$

$$F_{1ndLPT} = 0.22 \text{ m}^2$$

Length of blade airfoil part:

$$h_{9b} := \frac{F_{1nd.LPT}}{\pi \cdot D_{LPT.mean}}$$

$$h_{9b} = 0.1 \text{ m}$$

Then the external diameter of the LPT nozzle vanes:

$$D_{nd.LPT} = D_{LPT.mean} + h_{9b}$$

$$D_{nd.LPT} = 0.8 \text{ m}$$

Sleeve diameter:

$$D_{LPTsleeve} = \sqrt{D_{nd.LPT}^2 - \frac{4}{\pi} \cdot F_{1nd.LPT}}$$

$$D_{LPTsleeve} = 0.6 \text{ m}$$

1.27 Determination diametric dimension at the low pressure turbine discharge:

Parameters of gas at the LPT discharge is determined by the formula:

$$T_t^* = T_{IPT}^* - \frac{L_{LPT}}{\left(\frac{k_g}{k_g - 1}\right) \cdot R}$$

$$T_T = 813.3 \text{ K}$$

$$p_t^* = p_{IPT}^* \cdot \sigma_{transition} \cdot \left(1 - \frac{T_{IPT}^* - T_t^*}{T_{IPT}^* \cdot 0.87}\right)^{\frac{k_g}{k_g - 1}}$$

$$p_t' = 132 \text{ kPa}$$

We set reduced speed at the exit/discharge of LPT: $\lambda_{at} = 0.55$ and corresponding axial component

$$c_{1LPT} = \lambda_{at} \cdot 18.15 \cdot \sqrt{T_t^*}$$

$$c_{1,LPT} = 284.7 \frac{\text{M}}{\text{s}}$$

The relative density of flow is equal to:

$$q(\lambda_{at}, k_g) = 0.765$$

Cross-sectional area at the LPT discharge is calculated by the formula:

$$F_t = \frac{G_{gLPT} \cdot \sqrt{T_t^*}}{m_g \cdot p_t^* \cdot q(\lambda_{at}, k_g)}$$

$$F_t = 0.370 \text{ M}^2$$

Sleeve diameter at the LPT discharge:

$$D_{t,sl} := 0.58 \text{ M}$$

Then the external diameter equals:

$$D_{LPT} = \sqrt{D_{t,sl}^2 - \frac{4}{\pi} \cdot F_t}$$

$$D_{LPT} = 0.9 \text{ M}$$

The length of blade aerofoil:

$$h_{10b} = (D_{LPT} - D_{t,sleeve})$$

$$h_{10II} = 0.16 \text{ м}$$

Determine the stress caused by the action of centrifugal forces in a dangerous section of the LPT blades last stage ($\rho = 8.5 \cdot 10^3 \frac{\text{kg}}{\text{m}^3}$);

$$K_f = 0.58 :$$

$$\sigma_{\text{ten}} = 2 \cdot K_f \cdot \rho \cdot U_{\text{LPT mean}}^2 \cdot U_{\text{IPT mean}} \cdot 10^6 \cdot (h_{10b} / D_{\text{LPT mean}})$$

$$\sigma_{\text{ten}} = 133.6 \text{ MPa}$$

We find that the LPT blades can be made from the alloy ЭИ-920 at the temperature of the last stage blades which is equal to about 812 K ($\sigma_{500} = 180 \text{ MPa}$).

Safety Factor coefficient is equal to:

$$n = \frac{\sigma_{500}}{\sigma_{\text{ten}}}$$

$$n = 1.347 .$$

Balance of turbine and fan power is checked by the following equations:

$$N_{\text{LPT}} = G_{g, \text{LPT}} \cdot L_{\text{LPT}}$$

$$N_{\text{LPT}} = 1252.375 \text{ kW}$$

$$N_{\text{fanI}} = G_{aI} \cdot L_{\text{LPC}}$$

$$N_{\text{fanI}} = 1908.8 \text{ kW}$$

$$N_{\text{fanII}} = G_{aII} \cdot L_{fII}$$

$$N_{\text{fanII}} = 10575 \text{ kW}$$

$$N_{\text{fan}} = N_{\text{fanI}} + N_{\text{fanII}}$$

$$N_{\text{fan}} = 12483.8 \text{ CHP}$$

$$\eta_m = N_{\text{fan}} / N_{\text{LPT}}$$

$$\eta_m = 0.976$$

Low pressure rotor speed is determined separately for the fan and turbine:

$$\begin{aligned}n_{LPC} &= U_{1c} / (\pi \cdot D_{1c}) \\n_{LPC} &= 6369.4 \text{ min}^{-1} \\n_{LPT} &= U_{LPT \text{ mean}} / (\pi \cdot D_{LPT \text{ mean}}) \\n_{LPT} &= 6369.4 \text{ min}^{-1}\end{aligned}$$

1.28 Determination of diameter

Pressure drop in the nozzle ($\sigma_{cl} = 0.99$):

$$\pi_c^* = \frac{p_t^* \cdot \sigma_{nl}}{p_{amb}^*}$$

$$\pi'_c = 1.29$$

because $\pi'_{kp} > \pi'_c$, the exhaust from the nozzle of primary flow is subcritical at full expansion.

Exhaust velocity from the nozzle is determined by the formula:

$$c_{nl} = \phi_{nl} \cdot \sqrt{2 \cdot \frac{k_g}{k_g - 1} \cdot R_g \cdot T_t^* \cdot \left[1 - \left(\frac{P_{amb}^*}{P_t^* \cdot \sigma_{nl}} \right)^{\frac{k_g - 1}{k_g}} \right]}$$

$$c_{nl} = 326.5 \frac{\text{m}}{\text{s}}$$

$$\lambda_{nl} = \frac{c_{nl}}{18.3 \cdot \sqrt{T_t^*}}$$

$$\lambda_{nl} = 0.63$$

$$q(\lambda_{nl}, k_g) = 0.84$$

The area of the nozzle is determined from the equation:

$$\begin{aligned}F_{nl} &= \frac{G_{gLPT} \cdot \sqrt{T_t^*}}{m_g \cdot p_t^* \cdot \sigma_{nl} \cdot q(\lambda_{c1}, k_g)} \\F_{nl} &= 0.285 \text{ m}^2\end{aligned}$$

We set the internal diameter of the primary flow nozzle $D_{cl.BH} := 0.02 \text{ m}$

$$D_{nl} = \sqrt{D_{nl.internal}^2 - \frac{4}{\pi} \cdot F_{cl}}$$

$$D_{nI} = 0.6 \text{ m}$$

Exhaust velocity from the secondary flow nozzle is determined in the thermodynamic calculation, the reduced speed is determined by the formula:

$$\lambda_{n2} = \frac{c_{n2}}{18.3 \cdot \sqrt{T_{fan2}^*}}$$

$$\lambda_{n2} = 0.86$$

$$q(\lambda_{n2}, k_g) = 0.976$$

Sectional area of the secondary flow nozzle is determined by the equation

$$F_{n2} = \frac{\sigma_{II} \cdot G_{aII} \cdot \sqrt{T_{fan2}^*}}{m_g \cdot p_{t_{fan2}^*} \cdot \sigma_{II} \cdot q(\lambda_{n2}, k_g)}$$

$$F_{n2} = 0.6 \text{ m}^2$$

The internal diameter of the secondary flow nozzle according to the drawings of design set $D_{cII_{BH}} = 0.96$:

$$D_{nII} = \sqrt{D_{nII.internal}^2 - \frac{4}{\pi} \cdot F_{nII}}$$

$$D_{nII} = 1.298 \text{ m}$$

1.29 Refinement/correction of engine parameters:

According to the gas-dynamic calculation the corrected parameters of the designed turbofan engine:

Specific thrust:

$$P_{spI} = (1 + g_f) \cdot C$$

$$P_{spI} = 326.5 \frac{\text{N} \cdot \text{s}}{\text{kg}}$$

$$P_{sp2} := c_{cII}$$

$$P_{sp2} = 289.4 \frac{\text{N} \cdot \text{s}}{\text{kg}}$$

$$P_{sp\Sigma} = (P_{spI} + P_{spII}) / (1 + m)$$

Engine thrust: $P_{sp\Sigma} = 295.6 \frac{\text{N}\cdot\text{s}}{\text{kg}}$

$$P_{\Sigma} = P_{sp\Sigma} \cdot G_a$$

$$P_{\Sigma} = 74.9 \text{ N}$$

The results obtained in calculations gas dynamic parameters of the gas flow is used in strength calculations of main loaded engine elements of engine and its main functional systems.